INFORMATION TO USERS

This dissertation was produced from a microfilm copy of the original document. While the most advanced technological means to photograph and reproduce this document have been used, the quality is heavily dependent upon the quality of the original submitted.

The following explanation of techniques is provided to help you understand markings or patterns which may appear on this reproduction.

1. The sign or "target" for pages apparently lacking from the document photographed is "Missing Page(s)". If it was possible to obtain the missing page(s) or section, they are spliced into the film along with adjacent pages. This may have necessitated cutting thru an image and duplicating adjacent pages to insure you complete continuity.

2. When an image on the film is obliterated with a large round black mark, it is an indication that the photographer suspected that the copy may have moved during exposure and thus cause a blurred image. You will find a good image of the page in the adjacent frame.

3. When a map, drawing or chart, etc., was part of the material being photographed the photographer followed a definite method in "sectioning" the material. It is customary to begin photoing at the upper left hand corner of a large sheet and to continue photoing from left to right in equal sections with a small overlap. If necessary, sectioning is continued again — beginning below the first row and continuing on until complete.

4. The majority of users indicate that the textual content is of greatest value, however, a somewhat higher quality reproduction could be made from "photographs" if essential to the understanding of the dissertation. Silver prints of "photographs" may be ordered at additional charge by writing the Order Department, giving the catalog number, title, author and specific pages you wish reproduced.

University Microfilms

300 North Zeeb Road
Ann Arbor, Michigan 48106

A Xerox Education Company

THE UNIVERSITY OF OKLAHOMA

GRADUATE COLLEGE

LIFETIME MEASUREMENTS OF EXCITED ELECTRONIC STATES IN ATOMIC HELIUM AND THE MOLECULAR HYDROGEN CONTINUUM

A DISSERTATION

SUBMITTED TO THE GRADUATE FACULTY

in partial fulfillment of the requirements for the

degree of

DOCTOR OF PHILOSOPHY

By

RICHARD T. THOMPSON, JR.

Norman, Oklahoma

1972

LIFETIME MEASUREMENTS OF EXCITED ELECTRONIC STATES IN

ATOMIC HELIUM AND THE MOLECULAR HYDROGEN CONTINUUM

A DISSERTATION

APPROVED FOR THE DEPARTMENT OF PHYSICS

By Richard S. Fowler

Robert M. St. John

P Day

Stanley B. Ellison

Dennis Slaff

ACKNOWLEDGEMENT

I am deeply indebted to Dr. R. G. Fowler for his direction in the completion of this project. Without his very able pushing when necessary and injection of extremely valuable suggestions this project would never have been completed.

I am indebted to those who have worked in this laboratory before me, aiding the development of the technique applied here.

I am grateful to Roger A. Mickish for our frequent rap sessions. I am grateful to the many acquaintances I have made while studying here which resulting friendships gave moral support when needed.

TABLE OF CONTENTS

TABLE OF CONTENTS (continued)

LIST OF TABLES

LIST OF FIGURES

LIST OF FIGURES (continued)

LIFETIME MEASUREMENTS OF EXCITED ELECTRONIC STATES IN ATOMIC HELIUM AND THE MOLECULAR HYDROGEN CONTINUUM

CHAPTER I

INTRODUCTION

Lifetime measurements of excited electronic states of atoms, ions and molecules provide information directly useful in the fields of plasma physics, astrophysics, and spectroscopy. Utilizing a knowledge of lifetimes and cross sections it is possible to ascertain electron temperatures[1] in a plasma by measuring the relative intensity of two transitions. A knowledge of lifetimes aids in discovery of situations wherein population inversions can be maintained thus contributing to laser development. Astrophysicists utilize this information to determine temperatures for extraterrestrial objects.

The probability of spontaneous transition from state j to state i is given by

$$A_{ji} = \frac{64\pi^4 e^2 \nu_{ji}^3}{3hc^2} |\chi_{ji}|^2 \qquad j>i$$

where $|\chi_{ji}|^2$ is the dipole moment matrix element of the transition from E_j to E_i. The frequency ν_{ji} is that associated with the energy loss $E_j - E_i = h\nu_{ji}$. The dipole transitions are required to follow the

selection rules of $\Delta\ell = \pm 1$ where ℓ is the angular momentum quantum number.

The lifetime τ_j of a state j is given by the relation $\tau_j = 1/\sum_i A_{ji}$. It is often true that $\tau_j \simeq 1/A_{jk}$ where k is the lowest state to which state j can radiate under a dipole transition. This is due primarily to the importance of the ν_{jk}^3 factor.

Since excitation cross sections fall off approximately as n^3 (where n is the principal quantum number) and since branching falls even more dramatically, and since in addition lifetimes of higher n states are in general longer ($\propto n^3$), we would expect it to be possible to observe the decay of an excited state with the technique described herein. At most we could expect to see some relatively weak longer exponentials in addition which when subtracted should yield a representative value of the observed state lifetime. It will be shown, however, that this is not the case. It is apparent that there is a faster lifetime than cascade would provide interacting with nearly every state reported here. The result of an interaction between two states of sufficiently close (within a factor of two) lifetimes and populations allows an erroneous lifetime to be determined because of an inability to separate them in the intensity decay data. This is not a defect of the data or the analysis technique but a limitation in resolution inherent in multiple exponential data. Consequently the original goal of measuring the lifetimes of all levels of helium has been altered to one of investigating the subsidiary processes which affect the validity of the lifetime measurements, especially in helium.

Application of these lifetime methods to the hydrogen molecular continuum were very successful and support the model of excitation presented. Some insight to radiation from low pressure discharges can be obtained from Handbuch der Physik.[2] A useful source on experimental techniques for lifetime measurements is contained in Advances in Electronics and Electron Physics.[3] Other general sources of great value to the researcher are the National Bureau of Standards publications by Wiese et al.[4-6] The foundation upon which this research has developed was built by Holzberlein,[7] Johnson,[8] Copeland,[9] Schaefer,[10] Mickish,[11] and Skwerski.[12] It is to these sources that the reader is referred for further details of lifetime measurement and analysis by delayed coincidence using the invertron or the cold cathode developed by Copeland.

In the following chapters we discuss methods of analysing the data obtained, present a brief description including changes and improvements of the apparatus used, examine the experimental results of lifetime measurements in atomic helium, and the experimental results of lifetime measurements in molecular hydrogen and conclude with a general discussion of the results.

CHAPTER II

ANALYTICAL DISCUSSION OF THE DATA INTERPRETATION

In general the time variation of population density N_k of state k can be expressed as

$$\dot{N}_k = -N_k \sum_i A_{ki} + \sum_\ell N_\ell A_{\ell k} - N_k \sum_\ell B_{k\ell} U(\nu) + \sum_i N_i B_{ik} U(\nu)$$

$$- N_k \sum_i B_{ki} U(\nu) + \sum_\ell N_\ell B_{\ell k} U(\nu) - N_o V N_k \sum_i \sigma_{ki}$$

$$+ N_o V \sum_\ell \sigma_{k\ell} N_\ell + n_e N_o \sigma'_k V_e + n_e V_e \sum_i \sigma'_{ki} N_i$$

$$+ D_k \nabla^2 N_k \qquad (1)$$

where states ℓ lie energetically above state k and states i lie below state k. The parameters B_{mn} represent the Einstein transition probability of absorption (m<n) or induced emission (m>n), $U(\nu_{mn})$ is the radiation field density of photons of frequency ν_{mn}, A_{mn} is the Einstein probability per second of spontaneous transition from state m to state n, σ_{mn} is the cross section for a radiationless collisional transfer from state m to state n, $n_e V_e$ is the excitation electron current density, D_k is the diffusion coefficient for state k and ∇^2 is the Laplacian. Transition probabilities A_{ki} are related to lifetimes τ_k by the relationship given earlier. For simplification A_k will be

used to replace $\sum_i A_{ki}$. The electron excitation cross section is denoted by σ'_k. The electron excitation cross section from other excited states, such as metastable states, is denoted by σ'_{ik}.

Because of the complexity of Eq. (1) it is generally warranted to consider only certain mechanisms, dropping those terms expected to be negligibly small.

Holzberlein[7] has solved many of these special cases and his solutions are presented here for completeness. Including terms of direct decay, electron excitation and collisional depopulation (first, ninth and seventh terms of Eq. (1)) he obtains

$$N_k(t') = N_{ko}\, e^{-(A_k+N_o V\sigma_k)t'} + \frac{n_e N\sigma'_k V_e}{A_k+NV\sigma_k}\left(1 - e^{-(A_k+NV\sigma_k)t'}\right) \qquad (2)$$

where we assume the only other loss mechanism of consequence is collision with neutrals (where $\sigma_k = \sum_i \sigma_{ki}$). If time zero is chosen as the onset of the excitation pulse then $N_{ko} = 0$ and after time t'_o, N_k has a population

$$N_k(t'_o) = \frac{n_e N_o \sigma'_k V_e}{A_k+N_o V\sigma_k}\left(1 - e^{-(A_k+NV\sigma_k)t'_o}\right) \qquad (3)$$

which for large t_o approaches the constant value

$$N_k(\infty) = \frac{n_e N\sigma'_k V_e}{A_k+N_o V\sigma_k}$$

If the excitation source is removed at t'_o, $N_{ko} \equiv N_k(t'_o)$ and $t = t'-t'_o$ then at $t'>t'_o$

$$N_k(t) = \frac{n_e NV_e\sigma'_k}{A_k+NV\sigma_k}\left(1 - e^{-(A_k+NV\sigma_k)t'_o}\right)e^{-(A_k+NV\sigma_k)t} . \qquad (4)$$

For simplicity we assume the excitation pulse width t_o' to be large so that $e^{-(A_k+NV\sigma_k)t_o'}$ terms are $\simeq 0$. The $NV\sigma_k$ term is expected to be pressure and temperature dependent.

When the above problem is expanded to two stages of cascading, Holzberlein[7] obtains after rearranging:

$$N_k(t') = \left\{N_{ko} + \sum_\ell \left[-\frac{A_{\ell k}N_{\ell o}}{A_k'-A_\ell'} + A_{\ell k}\sum_m \frac{A_{m\ell}N_{mo}}{(A_k'-A_m')(A_k'-A_\ell')}\right]\right\}e^{-A_k't'}$$

$$+ \sum_\ell \left\{\frac{A_{\ell k}N_{\ell o}}{A_k'-A_\ell'} - A_{\ell k}\sum_m \frac{A_{m\ell}N_{mo}}{(A_\ell'-A_m')(A_k'-A_\ell')}\right\}e^{-A_\ell't'}$$

$$+ \sum_\ell A_{\ell k}\sum_m \frac{A_{m\ell}N_{mo}}{(A_\ell'-A_m')(A_k'-A_m')}\, e^{-A_m't'} + n_eV_eN\left\{\frac{\sigma_k'}{A_k'} + \sum_\ell \left[-\frac{A_{\ell k}\sigma_\ell'}{A_k'(A_k'-A_\ell')}\right.\right.$$

$$\left.\left. + A_{\ell k}\sum_m \frac{A_{m\ell}\sigma_m'}{A_k'(A_k'-A_\ell')(A_k'-A_m')}\right]\right\}\left(1 - e^{-A_k't'}\right) + n_eV_eN\sum_\ell \left\{\frac{A_{\ell k}\sigma_\ell'}{A_\ell'(A_k'-A_\ell')}\right.$$

$$\left. + A_{\ell k}\sum_m \frac{A_{m\ell}\sigma_m'}{A_\ell'(A_k'-A_\ell')(A_\ell'-A_m')}\right\}\left(1 - e^{-A_\ell't'}\right)$$

$$+ n_eV_eN\sum_\ell A_{\ell k}\sum_m \frac{A_{m\ell}\sigma_m'}{A_m'(A_\ell'-A_m')(A_k'-A_m')}\left(1 - e^{-A_m't'}\right) \qquad (5)$$

where $A_i' = A_i + NV\sigma_i$. From this expression we can determine N_{ko}, $N_{\ell o}$ and N_{mo} at t_o by matching the solutions before and after cutoff so as to obtain a solution at $t = t'-t_o$

$$N_k(t) = \left[N_{ko} - \sum_\ell \frac{A_{\ell k}N_{\ell o}}{A_k'-A_\ell'} + \sum_{\ell m}\frac{A_{\ell k}A_{m\ell}N_{mo}}{(A_k'-A_m')(A_k'-A_\ell')}\right]e^{-A_k't}$$

$$+ \sum_\ell \left[\frac{A_{\ell k}}{A_k'-A_\ell'}N_{\ell o} - \sum_m \frac{A_{\ell k}A_{m\ell}N_{mo}}{(A_\ell'-A_m')(A_k'-A_\ell')}\right]e^{-A_\ell't}$$

$$+ \sum_{\ell m}\frac{A_{\ell k}A_{m\ell}N_{mo}}{(A_\ell'-A_m')(A_k'-A_m')}\, e^{-A_m't} \qquad (6)$$

We can readily see that for a simple one-stage cascade with a single cascading state ℓ Eq. (5) becomes

$$N_k = \left(\frac{\sigma_k N V_e n_e}{A_k} - \frac{A_{\ell k}\sigma_\ell N V_e n_e}{A_k(A_k - A_\ell)}\right) e^{-A_k t} + \frac{A_{\ell k}\sigma_\ell N V_e n_e}{A_\ell(A_k - A_\ell)}\, e^{-A_\ell t} \qquad (7)$$

where t=0 at termination of the excitation pulse. The excitation pulse is assumed long with respect to the lifetime of the states involved (i.e., reciprocal of A_ℓ for state ℓ if ℓ is the longest lived state).

R. G. Fowler has considered the problem of radiation excitation from a hot cathode such as might be expected for $2^3S \rightarrow 2^3P$ including diffusion terms and finds such an argument tends to indicate an observed lifetime that is shorter than the actual lifetime. The differential equations of the two states are

$$\dot{N}_k = -A_k N_k - \Lambda^2 N_k + B_m N_m + p_k$$

$$\dot{N}_m = -B_m N_m - \Lambda^2 N_m + A_k N_k + p_m$$

where N_k is the population density of 2^3P states, N_m is the population density of 2^3S states, A_k is the transition probability for the $2^3P \rightarrow 2^3S$ transition, B_m is elatation rate ($2^3S \rightarrow 2^3P$) due to photon flux from the cathode and represents a product of radiation field density and Einstein probability of absorption, $\Lambda^2 = \left(\frac{2.405}{R}\right)^2 D$ comes from the spatial solution of the complete diffusion equation for an infinite cylinder of radius R. p_k and p_m are production rates by all other processes and are assumed to be zero after cutoff of the electron current.

After Kaplan[13] (p. 471) we have the solutions

$$N_k = c_1 e^{-\Lambda^2 t} + c_2 e^{-(A_k+B_m+\Lambda^2)t}$$

$$+ \frac{p_k+p_m}{\left(1+\frac{A_k}{B_m}\right)\Lambda^2}\left(1 - e^{-\Lambda^2 t}\right) + \frac{p_k - \frac{B_m}{A_k} p_m}{\left(1+\frac{B_m}{A_k}\right)(A_k+B_m+\Lambda^2)}\left(1 - e^{-(A_k+B_m+\Lambda^2)t}\right) \quad (9)$$

and

$$N_m = c_1 \frac{A_k}{B_m} e^{-\Lambda^2 t} - c_2 e^{-(A_k+B_m+\Lambda^2)t} + \frac{p_k+p_m}{\left(1+\frac{B_m}{A_k}\right)\Lambda^2}\left(1 - e^{-\Lambda^2 t}\right)$$

$$- \frac{p_k - \frac{B_m}{A_k} p_m}{\left(1+\frac{B_m}{A_k}\right)(A_k+B_m+\Lambda^2)}\left(1 - e^{-(A_k+B_m+\Lambda^2)t}\right) . \quad (10)$$

If we require $N_k=N_m=0$ at $t=0$ then $c_1=c_2=0$ then at some $t=t_o$ we can redefine c_1 and c_2 by setting $p_k=p_m=0$ and match the equation before and after cutoff to get

$$c_1+c_2 = \frac{p_k+p_m}{\left(1+\frac{A_k}{B_m}\right)\Lambda^2}\left(1 - e^{-\Lambda^2 t_o}\right) + \frac{p_k - \frac{B_m}{A_k} p_m}{\left(1+\frac{B_m}{A_k}\right)(A_k+B_m+\Lambda^2)}\left(1 - e^{-(A_k+B_m+\Lambda^2)t_o}\right)$$

and

$$c_1 \frac{A_k}{B_m} - c_2 = \frac{p_k+p_m}{\left(1+\frac{B_m}{A_k}\right)\Lambda^2}\left(1 - e^{-\Lambda^2 t_o}\right) - \frac{p_k - \frac{B_m}{A_k} p_m}{\left(1+\frac{B_m}{A_k}\right)(A_k+B_m+\Lambda^2)}\left(1 - e^{-(A_k+B_m+\Lambda^2)t_o}\right)$$

or

$$c_1 = \frac{p_k+p_m}{\left(1+\frac{A_k}{B_m}\right)\Lambda^2}\left(1 - e^{-\Lambda^2 t_o}\right)$$

and

$$c_2 = \frac{p_k - \frac{B_m}{A_k} p_m}{\left(1 + \frac{B_m}{A_k}\right)(A_k + B_m + \Lambda^2)} \left(1 - e^{-(A_k + B_m + \Lambda)t_o}\right) .$$

The final solution for population of $2\,^3P$ at time t after cutoff at time t_o is given by:

$$N_k = \frac{p_k + p_m}{\left(1 + \frac{A_k}{B_m}\right)\Lambda^2} \left(1 - {}^{-\Lambda^2 t_o}\right) e^{-\Lambda^2 t} +$$

$$+ \frac{p_k - \frac{B_m}{A_k} p_m}{\left(1 + \frac{B_m}{A_k}\right)(A_k + B_m + \Lambda^2)} \left(1 - e^{-(A_k + B_m + \Lambda^2)t_o}\right) e^{-(A_k + B_m + \Lambda^2)t} . \quad (11)$$

This result indicates that if a diffusion effect exists of consequence we should see two exponentials. If diffusion is very important the last exponential would correspond to the diffusion plus absorption plus natural lifetime and the diffusion "lifetime" would enter as a longer exponential. If stimulated emission were included as well one could expect the observed lifetime to be even shorter since its effect would be to add to A_k.

The collisional transfer of excitation from the $n\,^1P$ states to $n^{1,3}F$ states which then decays to an $m^{1,3}D$ state can be described analytically by solving the following set of simultaneous differential equations:

$$\dot{W} = -(B_o - D_w \nabla^2)W \qquad A_{Po} P \quad (12)$$

$$\dot{P} = B_o W - (A_P + NV\sigma_{PF} - \nabla^2 D_P)P + NV\sigma_{FP} F + p_P \quad (13)$$

$$\dot{F} = NV\sigma_{PF} P - (A_F + NV\sigma_{FP})F + p_F \quad (14)$$

where P, W and F represent the population density of the singlet P states, the photon flux due to $n\,^1P \rightarrow 1\,^1S$ transitions and the total ^1F and ^3F states involved in the process of mixing respectively. The total transition probabilities from the P and F states are designated by A_P and A_F which include any linear pressure dependent pure quenching effects if present. The neutral ground state helium density is designated by N and is assumed to be constant. Direct production by electron excitation is designated by p_P and p_F. The mean atomic velocities are expressed by V and are obtained from cavity temperature by the expression $V = \sqrt{3kT/m}$. The transfer cross-sections $n\,^1P \rightarrow n^{1,3}F$ and $n^{1,3}F \rightarrow n\,^1P$ are expressed by σ_{PF} and σ_{FP} respectively and are required to fulfill the conditions of detailed balance. The probability of transition $n\,^1P \rightarrow 1\,^1S$ is expressed by A_{Po} and the photon capture probability B_o is obtained from integrating the Einstein B coefficient multiplied by the Planck radiation formula over the line profile to obtain the expression

$$B_o = \frac{c^4 g_i A_{Po} p}{4\pi^2 \sqrt{2}\, \nu^3 g_o V} \tag{15}$$

in which c is the velocity of light, p the pressure, ν the radiation frequency, g the appropriate statistical weight and V is the mean atomic velocity. The diffusion terms $\nabla^2 D_p$ and $\nabla^2 D_W$ account for diffusion losses of excited P states and photons respectively. They can be solved independently since they are spatial only and have the solutions in cylindrical geometry of

$$\Lambda_P = -D_P \nabla^2 = D_P \left| \left(\frac{\pi}{\ell}\right)^2 + \left(\frac{2.405}{a}\right)^2 \right|$$

$$\Lambda_W = -D_W \nabla^2 = D_W \left[\left(\frac{\pi}{\ell}\right)^2 + \left(\frac{2.405}{a}\right)^2 \right] \tag{16}$$

where ℓ is the length of the cylinder and a its radius. D_P and D_W are given by $\frac{v\lambda}{3}$ for the particles under consideration where λ is the mean free path (mfp). Due to the restriction of the surface of the cylinder it is necessary to impose a limitation on mfp as expressed below.

$$\frac{1}{\lambda_c} = \frac{1}{\lambda_g} + \frac{1}{a}$$

where λ_c is the corrected mfp and λ_g is the mfp of the gas. For He ions[14] D = 380 cm^2/sec at 1 mm-Hg and 300°K. Temperature and pressure corrections are made as follows

$$D = \frac{D_o P_o}{P} \left(\frac{T}{T_o}\right)^{\frac{3}{2}} = \frac{1}{3} v\lambda_g$$

Values of D for atoms in their own gas indicate $D_{ions} < D$ by a factor of 4 or 5.[14]

This yields a mfp for helium at 1175°K and p μ-Hg of $\lambda_g = .765/P$ cm. Similarly for λ_W the mfp for the photon gas we use $\lambda_W = \frac{C}{B}$ (i.e., velocity over collision frequency). Since $B_o \propto P$ we note that λ_P and λ_W are both $\propto \frac{1}{P}$ so that $\lambda_C \to a$ as $p \to 0$ for both cases.

Equation (14) actually consists of a sum of the two equations

$$\frac{d^3F_3}{dt} = NV\sigma_{P\,^3F_3} P - (A_{^3F_3} + NV\sigma_{FP})\,^3F_3$$

and

$$\frac{d^1F_3}{dt} = NV\sigma_{P\,^1F_3} P - (A_{^1F_3} + NV\sigma_{FP})\,^1F_3$$

so that upon adding

$$\frac{dF}{dt} = NVP(\sigma_{P\,^3F_3} + \sigma_{P\,^1F_3}) - (A_{F_3} + NV\sigma_{FP})F$$

where $A_{^1F_3} \sim A_{^3F_3}$, $\sigma_{^3F_3P} \sim \sigma_{^1F_3P}$ and $F = {}^3F_3 + {}^1F_3$. The principle of detail balance requires that

$$g_P\sigma_{P\,^3F_3} = g_{^3F_3}\sigma_{^3F_3P} = g_{^1F_3}\sigma_{^1F_3P} = g_P\sigma_{P\,^1F_3}$$

if we assume that the singlet and triplet states are not mixed. If they are somewhat mixed as anticipated theoretically by R. K. van der Eynde et al,[15] there would still be a symmetric and an antisymmetric state which would be expected to fulfill similar conditions of detail balance. The statistical weights to use for the above relation are

$$g_P = 3;\ g_{^3F_3} = g_{^1F_3} = 7\ .$$

Now the constant of Eq.'s (12), (13) and (14) have all been defined and we seek the form of the solutions. Applying the standard technique of assuming solutions of the form $P = Ae^{-\lambda t}$, $W = Be^{-\lambda t}$ and $F = Ce^{-\lambda t}$ and substituting back we find it necessary to solve the following secular determinant:

$$\begin{vmatrix} \lambda - (\Lambda_W + B_o) & A_{Po} & \\ B_o & \lambda - (A_P + NV\sigma_{PF} + \Lambda_P) & NV\sigma_{FP} \\ & NV\sigma_{PF} & \lambda - (A_F + NV\sigma_{FP}) \end{vmatrix} = 0$$

which is third degree in λ. For convenience we solve it numerically for each level from n=4 to n=10 using transfer cross-sections of St. John and Nee[16] and transition probabilities of N.B.S.[4] and Jobe and St. John[17] the solutions have been obtained at several values of pressure. Form of the solution is

$$W = A_1e^{-\lambda_1 t} + B_1e^{-\lambda_2 t} + C_1e^{-\lambda_3 t} \qquad (17)$$

$$P = A_2 e^{-\lambda_1 t} + B_2 e^{-\lambda_2 t} + C_2 e^{-\lambda_3 t} \tag{18}$$

$$F = A_3 e^{-\lambda_1 t} + B_3 e^{-\lambda_2 t} + C_3 e^{-\lambda_3 t} \tag{19}$$

The solutions for λ_2 and λ_3 are plotted in Figures 1 and 2 for the pressure range from 0 to 200 microns of Hg. A transfer cross section σ_{PF} of $7.5 \times 10^{-16} n^2$ where n is the principal quantum number, was used to obtain the results shown.

Since the fast lifetime λ_1 represents the photon state's equilibriating process and takes place in the order of picoseconds it will not normally be observed in experimental data. A plot of the ratio of B_2 to C_2 and B_3 to C_3 versus pressure for each n value is shown in Figures 3 and 4 for the P state and F state density expressions respectively. The expressions for A_2, B_2, C_2, A_3, B_3 and C_3 are

$$A_2 = \left[\frac{P_F (A_F + NV\sigma_{FP} - \lambda_3)(A_F + NV\sigma_{FP} - \lambda_2)}{\sigma_{PF} NV (A_F + NV\sigma_{FP} - \Lambda_W - B_o)} - P_P \right]$$

$$\times \left[\frac{(A_F + NV\sigma_{FP} - \lambda_1)(\Lambda_W + B_o - \lambda_1)}{(\lambda_3 - \lambda_1)(\lambda_1 - \lambda_2)} \right] \frac{(1 - e^{-\lambda_1 t_o})}{\lambda_1} ,$$

$$B_2 = \left[P_P \frac{(\lambda_2 - \Lambda_W - B_o)}{(\lambda_2 - \lambda_3)} + A_2 \frac{(\lambda_3 - \lambda_1)}{(\lambda_2 - \lambda_3)} \frac{(\Lambda_W + B_o - \lambda_2)\lambda_1}{(\Lambda_W + B_o - \lambda_1)\lambda_2 (1 - e^{-\lambda_1 t_o})} \right]$$

$$\times \frac{(1 - e^{-\lambda_2 t_o})}{\lambda_2} ,$$

$$C_2 = \left[P_P - \frac{A_2 \lambda_1}{1 - e^{-\lambda_1 t_o}} - \frac{B_2 \lambda_2}{(1 - e^{-\lambda_1 t_o})} \right] \frac{(1 - e^{-\lambda_3 t_o})}{\lambda_3} ,$$

$$A_3 = \frac{A_2 \sigma_{PF} NV}{A_F + (\sigma_{FP} + \sigma_P) NV} ,$$

$$B_3 = \frac{B_2 \sigma_{PF} NV}{A_F + (\sigma_{FP} + \sigma_P) NV} ,$$

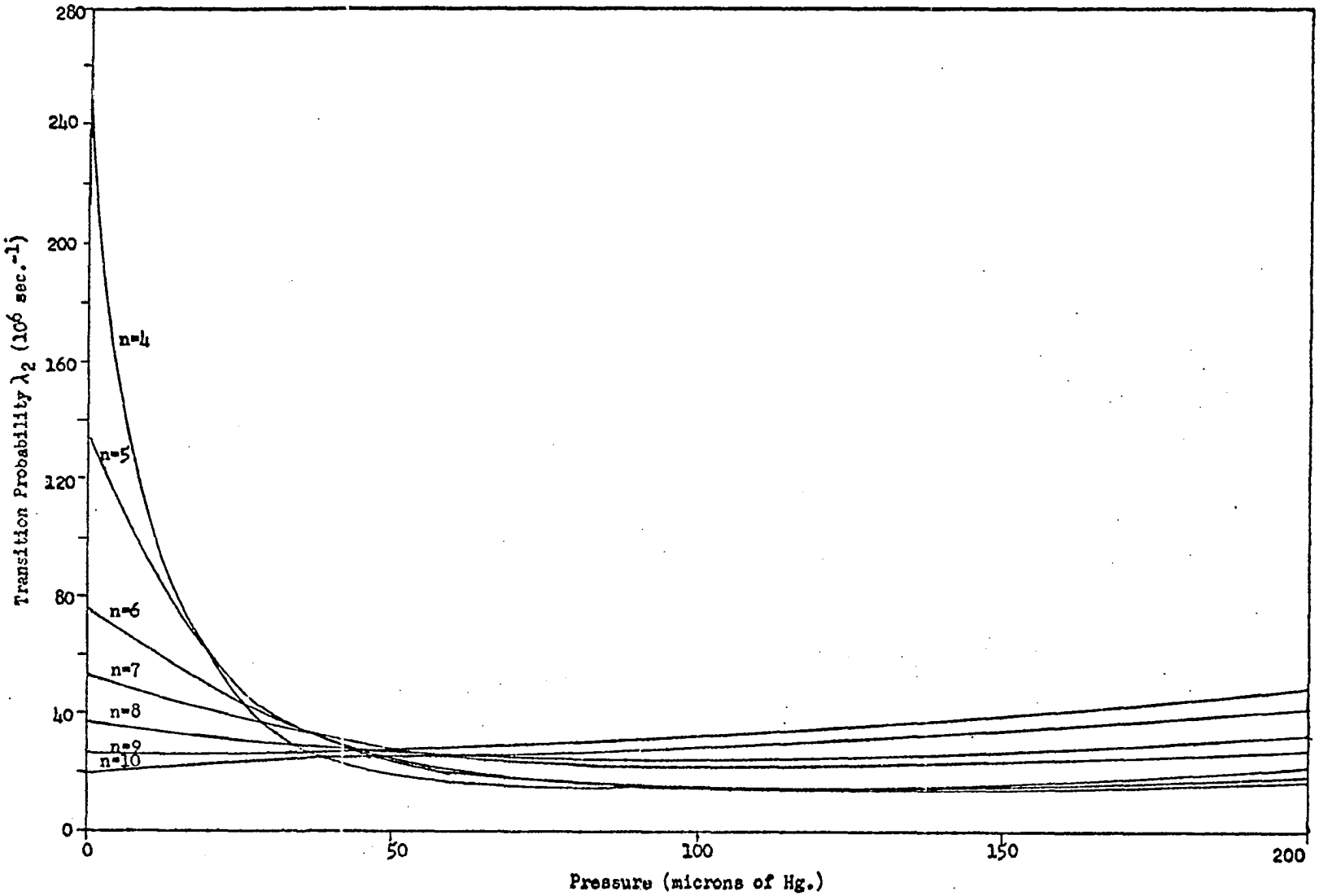

Figure 1. Solutions for λ_2 of Eq.'s (17,18,19) Showing the Pressure Dependence of the Calculated Fast Lifetime.

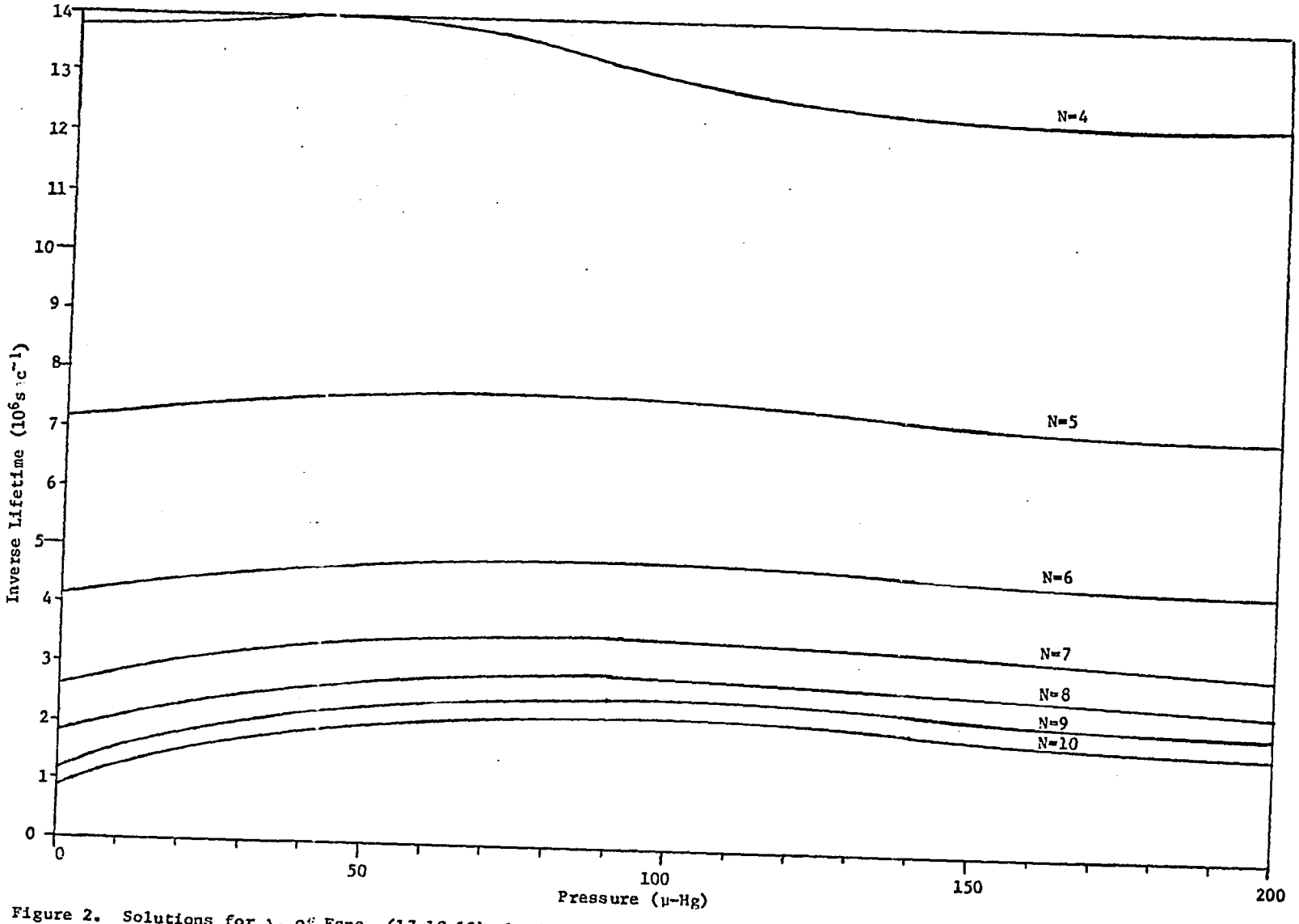

Figure 2. Solutions for λ_3 of Eqns. (17,18,19) showing the calculated pressure dependence of the inverse apparent lifetime.

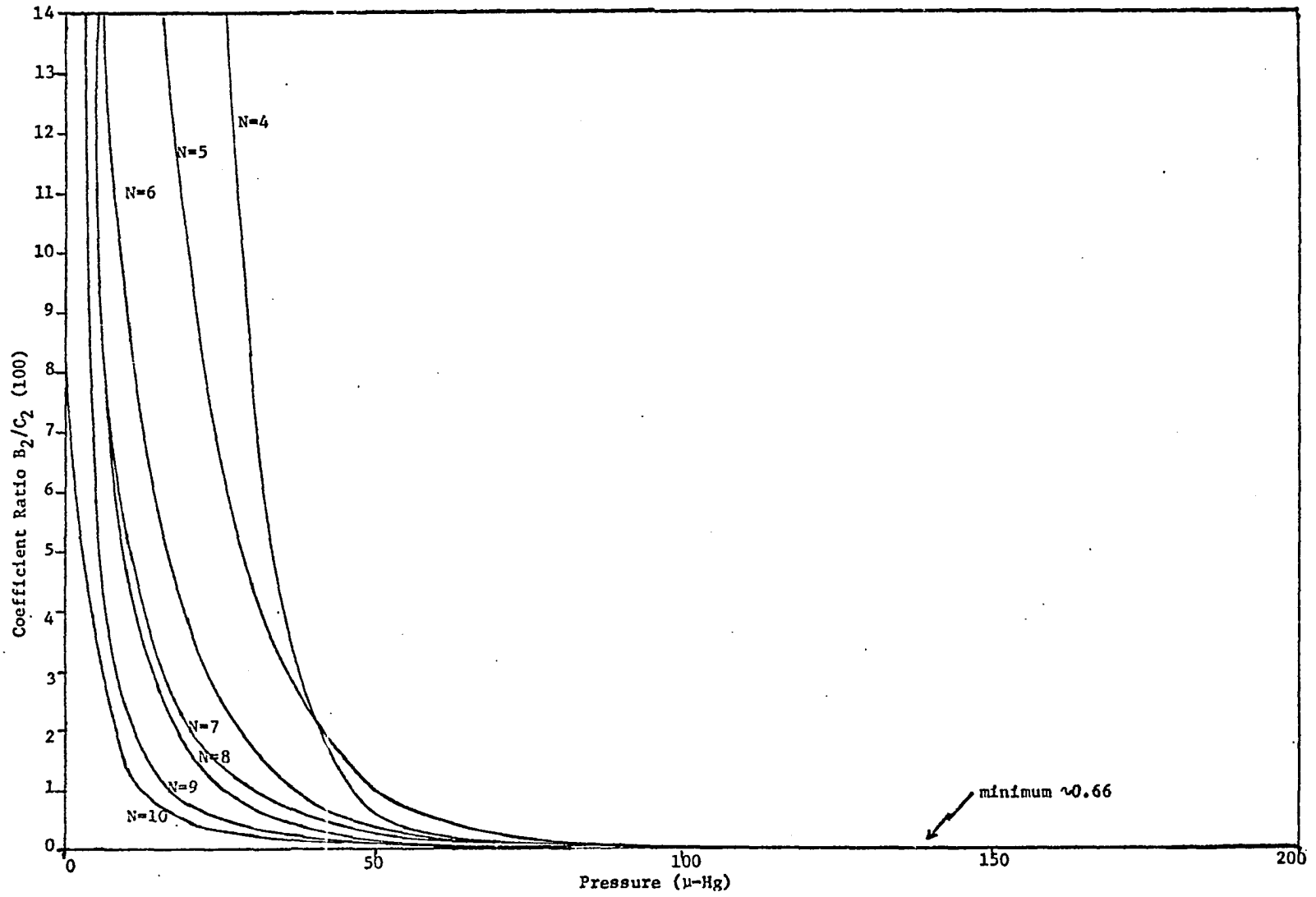

Figure 3. Ratio of calculated apparent time zero populations B_2 and C_2 for Eqn. (18) vs. pressure.

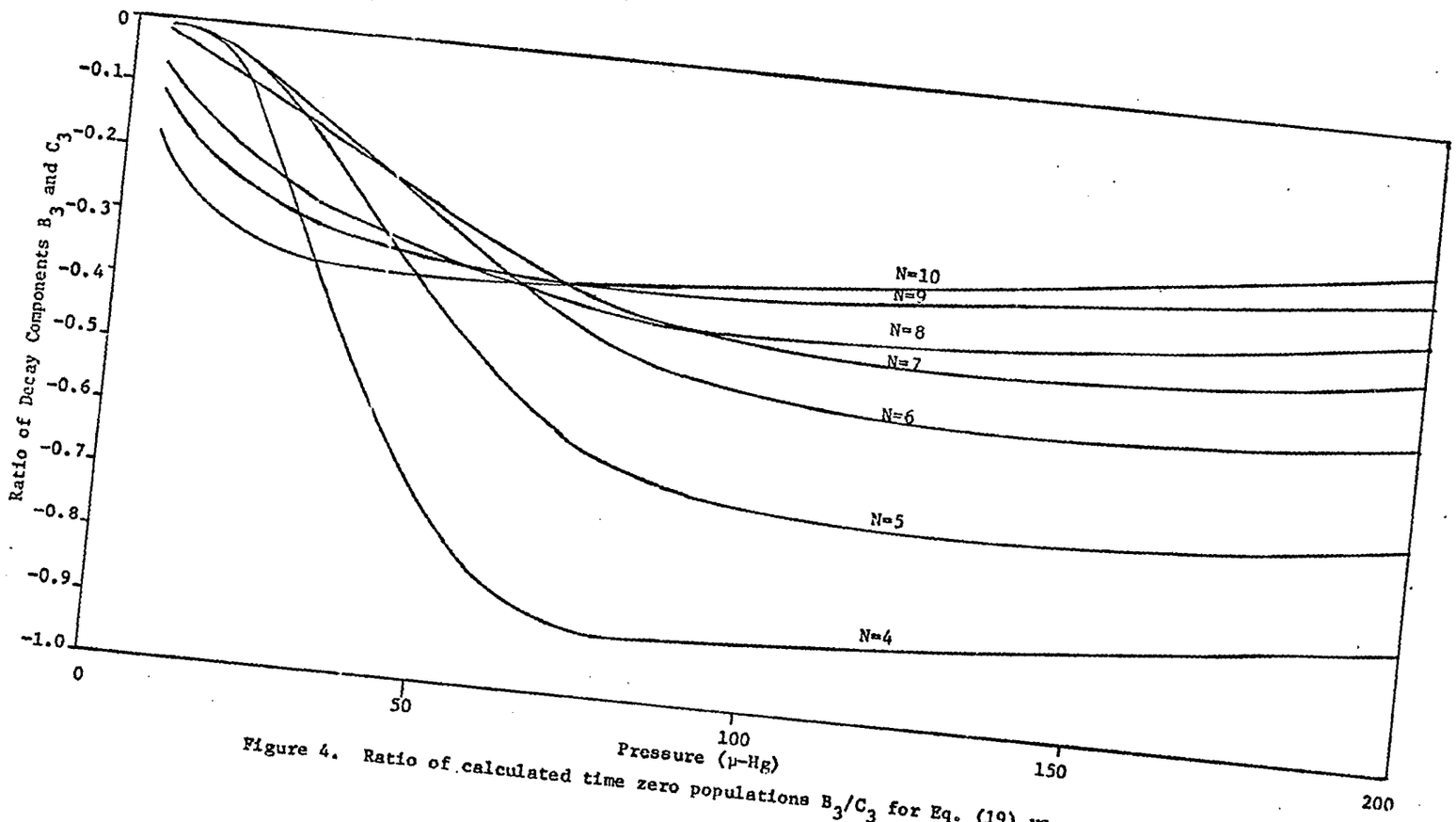

Figure 4. Ratio of calculated time zero populations B_3/C_3 for Eq. (19) vs. pressure.

and

$$C3 = \frac{C2\sigma_{PF}NV}{A_F+(\sigma_{FP}+\sigma_P)NV}$$

where t_o is the time length of the excitation pulse.

It is now possible to compute the anticipated cascade contributions to $n^{1,3}D$ states due to $n^{1,3}F$ state decay by solving the differential equation

$$\dot{D} = -(A_D + \sigma_D NV)D + A_{FD}F + P_D \tag{20}$$

where F is obtained from Eq. (19) using the results after cutoff. Then Eq. (20) has the solution

$$D = D_o e^{-\alpha t} + A_{FD}\left[\frac{A_3 e^{-\lambda_1 t}}{(A_D+\sigma_D NV-\lambda_1)} + \frac{B_3 e^{-\lambda_2 t}}{(A_D+\sigma_D NV-\lambda_2)} + \frac{C_3 e^{-\lambda_3 t}}{(A_D+\sigma_D NV-\lambda_3)}\right]$$

where

$$D_o = \left[P_D - \frac{A_{FD}A_3\lambda_1}{(\alpha-\lambda_1)(1-e^{-\lambda_1 t_o})} - \frac{A_{FD}B_3\lambda_2}{(\alpha-\lambda_2)(1-e^{-\lambda_2 t_o})} - \frac{A_{FD}C_3\lambda_3}{(\alpha-\lambda_3)(1-e^{-\lambda_3 t_o})}\right]$$

$$x \frac{(1-e^{-\alpha t_o})}{\alpha}$$

where

$$\alpha = A_D + \sigma_D NV$$

From these expressions it is possible to predict the components of the $n^{1,3}D$ decay function provided the model, cross-sections and transition probabilities are correct.

CHAPTER III

COMPUTER PROGRAMS DEVELOPED FOR LIFETIME DATA ANALYSIS

Introduction

In pursuit of improved data analysis methods, four computer programs have been coded at the University of Oklahoma. The technique employs direct readout of data froma 256 channel analyzer onto punched paper tape through a 33ASR Teletype. The resulting paper tape is loaded into disc storage peripheral to the computer employing the same teletype and a standard telephone line. The data is then reduced to obtain the desired lifetime using the aforementioned programs.

The first three programs are written in such a manner that each of them employs the same data input subroutine (named INPAK). This subroutine accepts multichannel analyzer data from the previously constructed disc file (named INPUT), stores the data in core for computations, and prints the appropriate heading and date information with each execution. Because of the on line nature of the time sharing system, a question and answer format has been employed to enter the remaining parameters needed in the analysis.

The fourth program is used to generate data simulations for the purpose of testing reliability of the data analysis programs.

A block diagram describing the experimental arrangement is given in Fig. 5. A brief description of each of the four computer programs (FPLOT, RICH, LASL and JERK1) is given in the following four sections. A brief analysis of program limitations and check-out methods is also presented below, followed by a complete listing of the four programs and their associated subroutines in Appendix A. As an additional aid in describing the computations involved, a sample execution of each program is given in Appendix B.

FPLOT, a Semi-Logarithmic Plotting Routine

This program employs only the INPAK subroutine. The purpose of this program is to plot the logarithm of intensity at the appropriate channel location. It is from this plot that a judgment is made as to data quality, complexity (e.g. how many exponential components) and usability (i.e., what section of the data set can be used). The number of channels (points) to be considered for the plot is determined from an entry in the file INPUT. The following steps are performed in the program:

a. Search all data for maximum and minimum (excluding zeros) intensity values.

b. Request plot density from user (e.g. 1 means plot every point, 2 every other point, etc.).

c. Inform user as to maximum and minimum values and accept any changes given.

d. Compute a scaling factor from maximum and minimum intensity

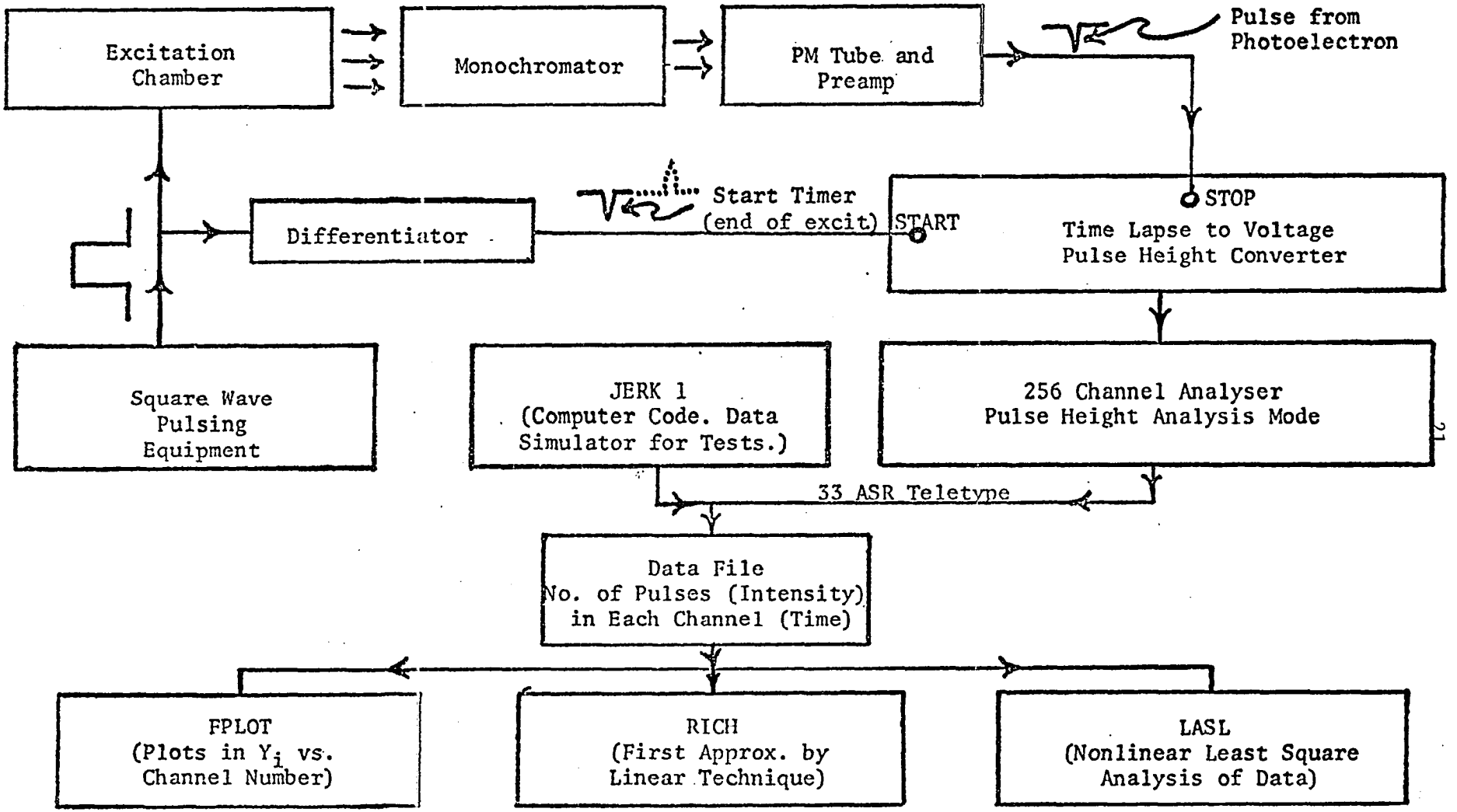

Figure 5. Functional flow chart for excited state electron lifetime data.

values and the number of print columns (e.g. 64 on Teletype printer) available for plotting.

e. Compute and print a symbol (+) in the printer column determined by $(\text{Log}_e Y_i - \text{Log}_e S)/S_f$ where S is the minimum, S_f the scaling factor, and Y_i the intensity recorded in the $i^{\underline{th}}$ channel.

Further clarification may be obtained by inspecting the sample problem in Appendix B and the program listing in Appendix A.

RICH, a Linear Technique for a First Approximation

This program employs the subroutines INPAK, RGRES and DSPAK. The primary function of this program is to obtain a first approximation for the lifetime and coefficient of each exponential and the constant corresponding to a noise or background level. The block diagram given in Fig. 6 shows the general solution procedure of this program.

Subroutine INPAK is used to perform the first function shown in Fig. 6. The next step requests from the user whether or not each step of the linear regressions results of the exponential unpeeling procedure is to be printed (normally suppressed), whether or not a tabulation of the data is desired, number of exponential parameters (including the constant) to be anticipated, first point of useful data, last point of useful data, excitation pulse repetition rate (pulses/second) and a break point in the curve if it was detected visually from the plot but not by the program in a previous attempt. At this point a check is made on the multichannel analyzer calibration data to determine if the calibration (ns/chan) is known (a negative calibration coefficient for the first entry in the third

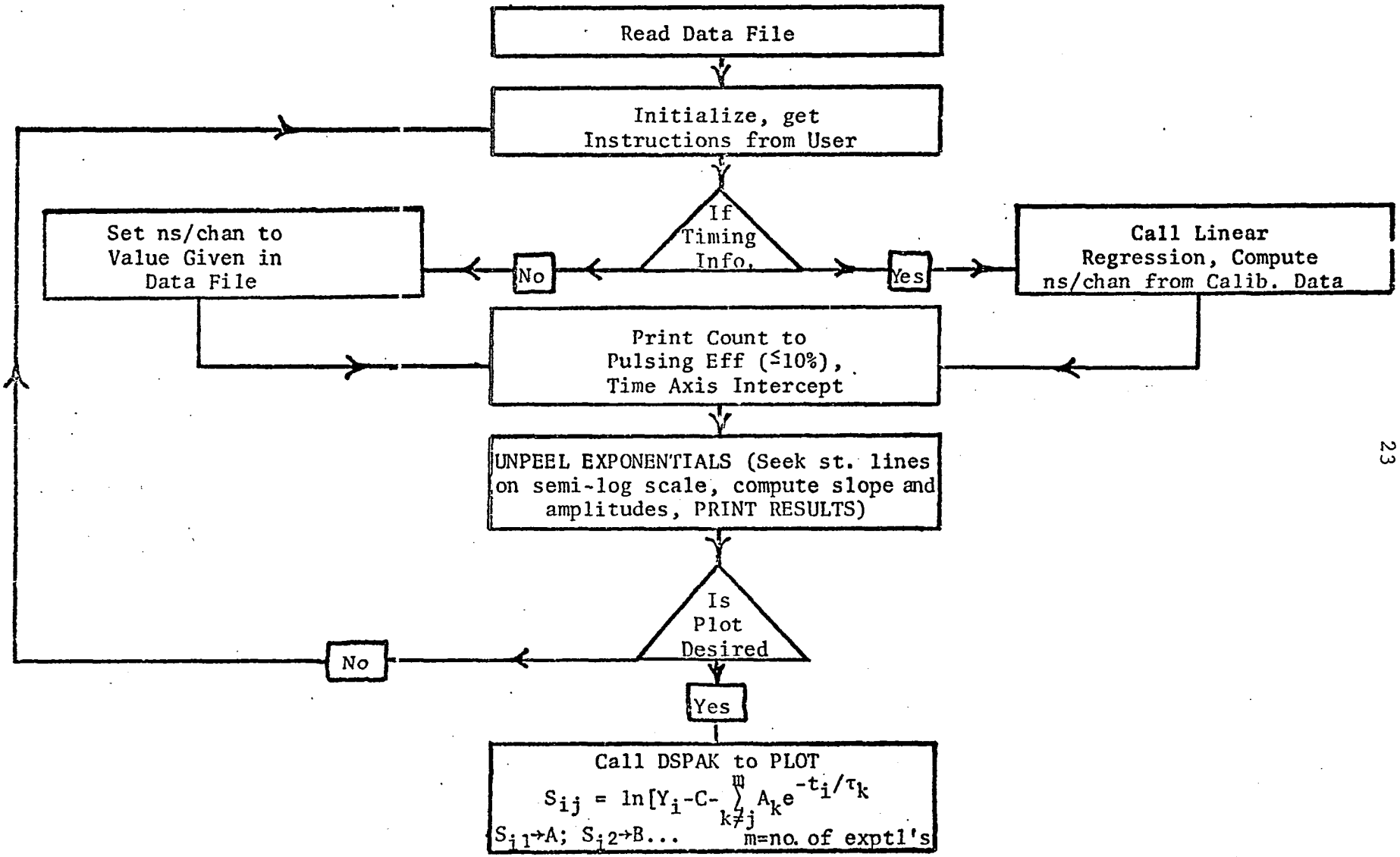

Figure 6. Flow chart for program RICH--to obtain first approximation.

line of INPUT) or must be computed from channel numbers and corresponding time increments obtained from lines 2 and 3 (all positive in value) of the data file INPUT. Next, the percentage of count rate to excitation pulse repetition rate is printed. This value should be held to less than 10% (see Chapter IV) to obtain acceptable data.

The procedure for unpeeling exponentials begins by performing a linear regression on the natural logarithm of the last 50 data points of the designated set of data. Pertinent equations used in the regression calculations are:

$$A = \frac{1}{n}\left[\sum_i^n V_i - \frac{n\sum_i^n V_i t_i - \left(\sum_i^n t_i\right)\left(\sum_i^n V_i\right)}{n\sum_i^n t_i^2 - \left(\sum_i^n t_i\right)^2}\sum_i^n t_i\right],$$

$$B = \frac{n\sum_i^n V_i t_i - \left(\sum_i^n t_i\right)\left(\sum_i^n V_i\right)}{n\sum_i^n t_i^2 - \left(\sum_i^n t_i\right)^2},$$

$$R_2 = \frac{\left[n\sum_i^n V_i t_i - \left(\sum_i^n t_i\right)\left(\sum_i^n V_i\right)\right]}{\left[n\sum_i^n t_i^2 - \left(\sum_i^n t_i\right)^2\right]\left[n\sum_i^n V_i^2 - \left(\sum_i^n V_i\right)^2\right]},$$

where t is the independent variable (time, V is the dependent variable (Log_e intensity) and A and B are the best fit parameters for the equation $V = A+Bt$. The value of R_2 is used to monitor linearity of the set of n points. This value is 1.0 for a straight line and decreases in value as the nonlinearity of the n points increases. The procedure for unpeeling exponentials continues by performing successive

regression on the last 70 points, then 90 points, etc., monitoring R_2 each time. A decrease in R_2 is taken as an indication that a second exponential is entering the data. When this decrease in R_2 occurs the values of A and B for the previous R_2 are stored. At this point a constant is subtracted from the data used to calculate A and B. The regression is applied again. The value of the constant is varied to three significant figures until the highest value of R_2 is reached. At this point the new values of A and B are converted to the form of the coefficients and the lifetime of the long exponentials and the constant is stored as a background level. Successive regression calculations are made on the remaining data set progressing toward the first data point (while monitoring R_2) with the long exponential and the constant subtracted off seeking parameters of the remaining exponentials. As each additional exponential is detected, its parameters are recorded and it is subtracted from each of the remaining data points.

Having obtained all exponential components recognizable through this unpeeling procedure and having printed out the function parameters, one can now request a plot to evaluate the quality of this first approximation. Normally a plot of every third or fourth point is sufficient. The magnitude of the $i^{\underline{th}}$ point to be plotted is determined by the expression:

$$S_{ij} = \frac{\mathrm{Log}_e\left(Y_i - C - \sum_{k\neq j}^{m} A_k e^{-t_i/\tau_k}\right)}{S_f}$$

where Y_i is the actual data point, C is the constant level, A_k is the coefficient of the $k^{\underline{th}}$ exponential component, τ_k is the lifetime of

the k^{th} exponential, m is the number of exponentials discovered, t_i is the time corresponding to the i^{th} data point and S_f is the scale factor appropriate to the printer used. The plots of each j are denoted by different letters of the alphabet with S_{i1} (the fastest component) plotted as the letter A, S_{i2} as B, and on with S_{im+1} (illustrating the noise or background level) represented by the highest letter used. This curve represents deviations of the data points about the approximated solution.

Further clarification of the capability of this program may be obtained by inspecting the sample solution given in Appendix B and the program listing in Appendix A.

LASL, Nonlinear Least Square Parameter Adjustment for Best Fit

This program employs subroutines INPAK, ISPAK, QSPAK, LAMBDA, RSPAK, YPS, RGRES and DSPAK in addition to the two subroutines MINV and GMPRD from the Scientific Subroutines package. The objective of this program is to adjust the exponential parameters given as a first approximation until the best fit of the analytical curve is obtained. A rough outline of the computational procedure is given in Fig. 7.

Program LASL first calls ISPAK which loads all data and identification through subroutine INPAK then requests from the user the:

a. number of parameters to fit the curve to (e.g. two times the number of exponential components plus 1 for the constant term),

b. first location of the data set containing useful data,

c. last location of the data set containing useful data,

d. power (x) to which a weighting function

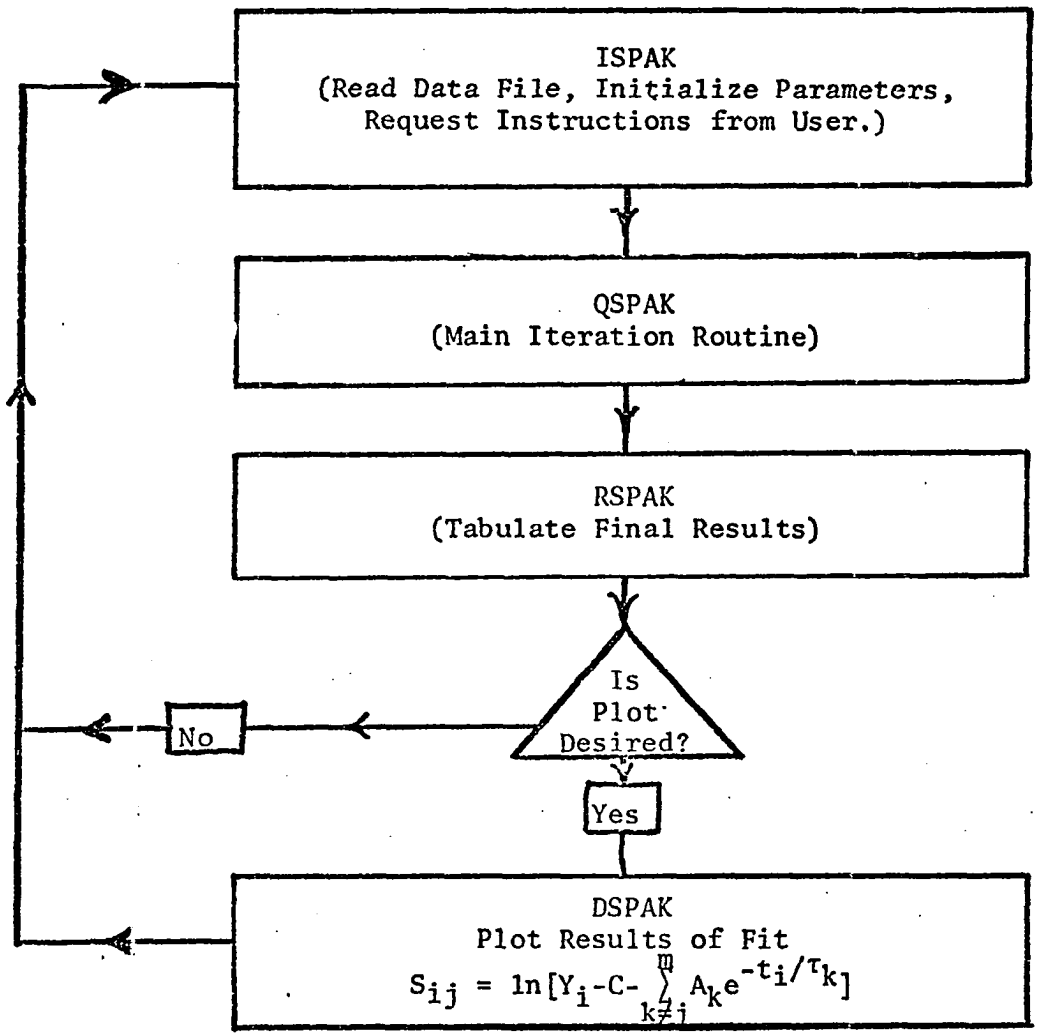

Figure 7. Flow chart for nonlinear least squares program--LASL.

$$W_i = \left[N \left(\sum_j^m A_j e^{-t_i/\tau_j} + C \right) \right]^x$$

is raised for use in least squares calculations,

e. printer control (normally 0) which can be set to 1, 2, or 3 for increasing amounts of debugging information if problems arise in execution,

f. desirability of holding the constant term fixed (1 no, 2 yes),

g. initial values of lifetimes coefficients and constant to be used.

The exponential power on the weighting function allows one to put more emphasis on one end of the curve. Since the noise observed in most of the data tends to vary with the square root of intensity a weighting power of -0.5 will tend to remove this effect. The weighting factors are calculated using the initial parameters and remain fixed throughout the least square procedure. This program was initially obtained from Los Alamos Scientific Laboratory[18] but has undergone major alterations in being adapted to our application.

The least squares technique used is that of Gauss-Newton modified to give a steeper path of descent. The technique is described briefly below with proofs left to other sources.[19,20,21]

First compute a $\hat{Y}_i$ determined from the initial parameters P_k of the m exponential components,

$$\hat{Y}_i = \sum_{j=2}^{2m} P_{j-1} e^{-t_i/P_j} + P_{2m+1} \qquad j=2,4,\ldots 2m \tag{21}$$

then compute a difference between the calculated value and the true

data

$$\Delta Y_i = \hat{Y}_i - Y_i \ . \tag{22}$$

Compute the following 2m+1 by 2m+1 matrix:

$$a_{ik} = \sum^{n} \frac{\partial \hat{Y}_\ell}{\partial P_i} \frac{\partial \hat{Y}_\ell}{\partial P_k} W_\ell \qquad i,k=1,2,\ldots 2m+1 \tag{23}$$

where W_ℓ is the weight to be attributed to this data point. Compute the column vector,

$$b_i = \sum^{n} \frac{\partial \hat{Y}_\ell}{\partial P_i} \Delta Y_\ell \ W_\ell \ . \tag{24}$$

Application of the A and B matrices defined in Eqs. (23) and (24) is described by the following development. One can argue by means of a Taylor series, truncated to the first order, that:

$$\Delta Y_i = \sum_{\ell}^{2m+1} \frac{\partial \hat{Y}_i}{\partial P_\ell} \Delta P_\ell \tag{25}$$

multiply through by

$$\frac{\partial \hat{Y}_i}{\partial P_k} W_i$$

then sum over i to get the 2m+1 equations:

$$\sum_{i}^{n} \Delta Y_i \frac{\partial \hat{Y}_i}{\partial P_k} W_i = \sum_{i}^{n} \sum_{\ell}^{2m+1} \frac{\partial \hat{Y}_i}{\partial P_\ell} \frac{\partial \hat{Y}_i}{\partial P_k} W_i \ \Delta P_\ell \tag{26}$$

which can be written in the following matrix form:

$$B = A\Delta P \quad \text{or} \quad b_i = a_{ij} p_j \tag{27}$$

Perform a normalization of A such that:

$$a^*_{ij} = \frac{a_{ij}}{\sqrt{a_{ii} a_{jj}}} \tag{28}$$

Then

$$b^*_i = a^*_{ij} p^*_j \tag{29}$$

if

$$b_i^* = \frac{b_i}{\sqrt{a_{ii}}} \quad \text{and} \quad p_j = \frac{p_j^*}{\sqrt{a_{jj}}} \quad . \tag{30}$$

It has been shown[22] that addition of a constant matrix λI to A* has the effect of rotating the B* and ΔP^* vectors in configuration space so as to attain a more definite convergence.

Hence the procedure is to solve the expression

$$B^* = (A^* + \lambda I)\Delta P^* \tag{31}$$

for the ΔP^* vector which can be converted to ΔP_i's by equation (30) to obtain the next set of P_i's for an iteration.

Normal procedure is to monitor

$$\Phi \equiv \sum_i^n \Delta Y_i^2 \, W_i$$

for each iteration. As long as Φ decreases from one iteration to the next λ is left small and the Gauss-Newton method works normally.

On any given iteration if Φ increases from its previous value, the value of λ is increased until (1) Φ no longer is larger than it was on the previous iteration or (2)

$$\cos \lambda \equiv \frac{B^* \Delta P^{*\dagger}}{|B^*| \; |\Delta P^*|} > \cos 45^\circ$$

Condition (1) is the normal condition and has caused convergence for cases that otherwise would not have converged. If Condition (2) arises a correction of the form $\Delta P_j = H\Delta P_j$ where H<1 is applied until Φ satisfies the requirement that it not increase in size. A converged solution is accepted when

$$\left|\frac{\Delta P_i}{P_i}\right| < 10^{-5} \text{ for all i.}$$

Other output information includes

$$\text{The weighted variance} = \frac{\sum_{i}^{n} \Delta Y_i^2 W_i}{n-2m-1} \quad ,$$

$$\text{The unweighted sigma} = \sqrt{\frac{\sum_{i}^{n} \Delta Y_i^2}{n-2m-1}} \quad ,$$

$$\text{The unweighted sum of squares of the devs.} = \sum_{i}^{n} \Delta Y_i^2$$

and

$$\text{Standard deviation} \equiv \sigma_{p_j} = \sqrt{A_{jj}^{-1} \sum \frac{W_i \Delta Y_i^2}{n-2m-1}} \quad .$$

Exact least squares equations:

$$\text{Fitted function } U_j = \sum_{i}^{n} W_i \hat{Y}_i \frac{\partial \hat{Y}_i}{\partial P_j} \quad ,$$

$$\text{Input data } V_j = \sum_{i}^{n} W_i Y_i \frac{\partial \hat{Y}_i}{\partial P_j} \quad .$$

At this point one can choose to plot out the results of the solution to make a visual check. The method of the plotting routine is described earlier in this chapter. Further clarification of LASL may be obtained by inspection of the sample execution in Appendix B and the listing in Appendix A.

JERK1, A Data Set Simulation Program

Program JERK1 uses no subroutines other than a systems supplied random number generator RANDU. This vital program simulates data with known lifetimes, coefficients and a constant. In addition an adjusta-

ble fraction of random noise is added to each data point in a manner proportional to the square root of each point so as to more nearly simulate actual data.

This program generated the cases discussed in the next section to determine some limitations of the analysis programs. It is kept available so that if a true data run looks suspicious it can be simulated then checked for repeatability.

The inputs required by this program are:

a. READ ID TAPE, for which 12 spaces are available for a name, 9 spaces for the data, 2 spaces (I2) for a data run number, 6 spaces for a run identification, 5 spaces (F5.0) for a wavelength and 5 spaces (F5.1) for pressure in microns.

b. ENTER NUMBER OF CHANNELS (N), CALIBRATION (NS/CHAN), MULTIPLIER FOR NOISE, requests the user to enter the number of data points in the simulation (e.g. 255), the calibration factor for the independent variable and a factor U to adjust the amount of noise to be added onto each analytical data value.

c. NUMBER OF EXPTL. PARAMS., $1^{\underline{st}}$ COEF., $1^{\underline{st}}$ LIFETIME, $2^{\underline{nd}}$ COEF., ..., CONSTANT, requests entry of the parameters representing the data set that is to be simulated.

The principal equations used in JERK1 are:

$$y_i = \left[\sum_{j=1}^{m} A_j \, e^{-\chi_i/\tau_j} \right] + \sigma_i \quad ,$$

$$\sigma = \sqrt{\frac{\sum_{i=1}^{n} \sigma_i^2}{n-2m-1}} \quad ,$$

and

$$\sigma_i = U(R_i - 0.5)\left(\sum_{j=1}^{m} A_j\, e^{-\chi_i/\tau_j} + C\right)^{\frac{1}{2}}$$

where y_i is the simulated intensity of the $i^{\underline{th}}$ time point, A_j the coefficient of the $j^{\underline{th}}$ exponential component, τ_j the lifetime of the $j^{\underline{th}}$ exponential component, m the number of exponential components, C the constant background level, U the multiplier (normally a number between 0 and 10) to determine the amount of noise to add to the curve and R_i is a random number between 0 and 1.0.

Further clarification of this program is available by inspecting the listing given in Appendix A and the example given in Appendix B.

Analysis of Program Limitations

A complete analysis of limitations of programs RICH and LASL would be extremely voluminous and will not be considered here. However, an indication of problems that might arise is obtainable from Tables 1, 2 and 3. It is necessary for each user of the programs to become familiar with their operating characteristics in order to properly assign uncertainties to any parameters thusly arrived at.

An examination of Table 3 would indicate that, as one might expect, more reliable results are obtained for smaller values of sigma. It is also apparent that, even when poor results are obtained, the value of sigma is very close to the sigma imposed on the original simulations. In general, as Table 3 indicates, one can expect a large value in standard deviation to indicate rather poor results as it should. However, as certain runs of case #8 indicate, poor results are not always accompanied with large statistical standard deviations.

The problem of analysis of case #8 is due to τ_1 and τ_2 differing only by a factor of 2, having equal exponential amplitudes and most important a large error superimposed on the true curve as previously indicated. It should be noted that for the same set of parameters but with decreasing levels of random noise (see runs #5, #6 and #7) the reliabilities of the solutions become much greater.

Rather than construct a set of tables to cover all eventualities, which could lull the user into convincing himself that his problem falls within the limits of a certain table, another procedure is recommended. The procedure is that upon running a case that falls outside the region of prior experience one uses these results in JERK1 to simulate the case introducing sufficient error to give a sigma comparable to case in question. If this simulation and one or two others with slightly adjusted exponential parameters give favorable results, then one could assume equally favorable results were obtained in the original case.

The LASL results listed in Table 3 were computed prior to inclusion of the LAMBDA routine to give a steeper path of descent. Since this modification case #8 with weight option-3 has been rerun and was successful in converging to a meaningful result.

TABLE 1. DESCRIPTION OF TEST CASES GENERATED IN JERK1.
(Time scale was set at 1.0 in units of ns/channel.)

Case No.	Noise Level Multiplier	τ_1 ns.	τ_2 ns.	A_1 counts in 1000's	A_2 counts in 1000's	C counts in 1000's	σ counts
1	5	10	100	10	10	1.0	103.0
2	5	10	50	10	10	1.0	82.4
3	5	5	50	5	10	0.5	71.8
4	5	5	50	2	10	0.5	71.2
5	5	35	70	10	10	1.0	103.0
6	2.5	35	70	10	10	1.0	51.3
7	0	35	70	10	10	1.0	0.0
8	10	35	70	10	10	1.0	205.0

TABLE 2. FIRST APPROXIMATIONS FOR TEST CASES GIVEN IN TABLE 1 AS DETERMINED BY RICH.

Case No.	Error in parameters calculated				
	τ_1 ns.	τ_2 ns.	A_1 counts	A_2 counts	C counts
1	+ 0.25	+ 3.1	+ 194.0	- 70.0	- 74.4
2	+13.0	+ 23.2	+ 841.0	-4635.0	- 149.0
3	+ 6.1	+ 6.2	- 88.9	-1388.0	- 58.8
4	---	+ 4.4	---	- 714.0	- 51.9
4(a)	+ 2.82	+ 5.3	+1141.0	-1035.0	- 55.7
5	- 9.4	- 2.5	-2318.0	+3054.0	- 58.8
6	- 7.6	- 2.4	-1479.0	+2291.0	- 25.0
7	- 9.5	- 7.2	-3493.0	+3964.0	+ 28.0
8	---	- 7.4	---	+6406.0	- 83.8
8(b)	+ 3.8	+150.0	8201.0	-6057.0	-1000.0

(a) First search failed to locate fast component so a break point of 10 was given.

(b) First search failed. Break point of 180 was given.

TABLE 3. QUALITY OF BEST FIT TO TEST CASES LISTED IN TABLE 1 AS DETERMINED BY LASL USING INITIAL VALUES FROM RICH.

Case No.	Weight Option	Error in parameters calculated: τ_1 (a) ns.	τ_1 (b) ns.	τ_2 (a) ns.	τ_2 (b) ns.	A_1 (a) counts	A_1 (b) counts	A (a) counts	A (b) counts	C (a) counts	C (b) counts	Sigma $\sqrt{\frac{\sum\|Y_i-f_i(t)\|^2}{250}}$ counts
1	0	- 0.20	0.16	- 2.02	1.59	- 22	85	+ 70	53	+ 43	43.0	102.0
1	1	- 0.29	0.14	- 3.19	1.97	- 60	81	+ 90	53	+ 74	62.0	103.0
1	-1	- 0.07	0.24	- 0.95	1.54	0	128	+ 40	64	+ 17	37.0	103.0
2	0	- 0.32	0.18	- 0.90	0.58	- 142	126	+ 230	126	+ 9	12.0	81.8
2	-1	- 0.20	0.27	- 0.56	0.57	- 76	158	+ 150	149	+ 4	9.0	81.9
2	-3	+ 0.55	1.25	+ 0.37	0.97	- 28	913	- 141	339	- 38	87.0	87.5
3	-1	- 0.22	0.23	- 0.30	0.32	+ 48	135	+ 70	64	2	6.0	71.3
3	+1	- 0.16	0.10	- 0.09	0.48	+ 60	55	+ 50	45	- 4	22.0	71.3
4	-1	- 0.51	0.53	- 0.30	0.31	42	131	70	61	2	6.0	70.7
4	+1	- 0.36	0.23	- 0.10	0.45	53	53	50	42	- 4	21.0	70.8
5	-1	3.66	3.62	10.91	16.58	3070	3100	-3000	3065	- 56	81.0	102.0
5	+1	- 6.15	5.91	-10.49	5.78	-4465	3105	4430	3051	96	79.0	103.0
5	-3	- 2.55	9.05	- 2.24	9.99	- 944	4175	1150	4451	4	53.0	106.0
5	-0.5	3.24	3.50	9.09	15.50	2700	3126	-2633	3076	- 47	83.0	102.0
6	1	- 2.40	2.8	- 5.5	4.9	2039	2132	2020	2094	46	51.0	50.8
6	0	0.80	2.0	1.4	5.3	580	1698	- 569	1674	- 6	37.0	50.9
6	-3	- 1.40	4.4	- 1.3	5.7	564	2354	670	2491	2	29.0	53.3
6	-0.5	- 1.10	1.9	3.8	5.6	1300	1593	-1280	1576	- 20	34.0	50.9

TABLE 3 (continued)

Case No.	Weight Option	τ_1 (a) ns.	τ_1 (b) ns.	τ_2 (a) ns.	τ_2 (b) ns.	A_1 (a) counts	A_1 (b) counts	A_2 (a) counts	A_2 (b) counts	C (a) counts	C (b) counts	Sigma counts
6(c)	0	2.00	---	- 2.0	---	2800	---	1000	---	100	---	---
7	0	0	0.01	0	0.03	0	9	-1	9	0	0.2	2.86
7	-3	- 0.03	0.04	- 0.1	0.06	- 22	24	20	24	0	0.3	3.03
8	0	3.96	7.0	11.3	37.8	3300	6744	-3196	6585	-52	214.0	204.0
8	-3	18.30	39.0	3.7	13.2	5970	10790	-6012	11690	15	65.0	565.0
8(d)	-3	DIVERGED, NO SOLUTION							4684			
8	-0.5	+64.1	60.4	-28.7	5.3	-5283	4465	5450	4684	7622	288.0	204.0
8	+1	17.1	1.95	-55.6	6.0	8490	760	-8544	7880	219	78.0	207.0
8	-0.2	5.3	6.0	19.8	48.5	4550	5643	-4413	5452	-95	250.0	204.0
8	0.5	25.5	10.3	-39.9	10.2	3890	5707	-3880	5775	86	116.0	204.0
8(e)	0.5	- 4.7	10.2	- 9.3	11.0	3732	6087	3740	6010	84	120.0	204.0

(a) This column gives the error in the calculated value from the true value.

(b) This column gives the calculated standard deviation for the parameter.

(c) This run was made to check final result against initial values. Result is identical to previous 0 weight option case but initial parameter values were deviated from the JERK1 parameters by the amount listed here.

(d) This case ran the maximum of 26 iterations and diverged way beyond meaningful interpretation.

(e) As an additional check this case was initialized with the true values as given in Table 1.

CHAPTER IV

LABORATORY EQUIPMENT AND PROCEDURES

Many facets that should be presented in this section have been treated in detail elsewhere. Taking advantage of this we discuss most items briefly, note sources of more detail and expound on recent changes that have developed.

First we shall consider the source chamber (invertron) and its vacuum system. Second we shall discuss the electronics associated with pulsing the invertron. Third we look at the method of detecting a monochromatic signal and recording the information needed for analysis as discussed in Chapter III.

The system shown schematically in Fig. 8 is used to measure lifetimes in the range of 2000 Å to 7800 Å. Components of the photon detection and counting system must be replaced for measurement above 7800 Å as mentioned below.

Source Chamber and Vacuum System

The components of the system are capable of attaining a base pressure of 10^{-6} torr and had a vacuum integrity capable of holding to 10^{-3} torr per seven days. The source chamber (designated invertron for its inverted diode configuration) was originated by Holzberlein,[23]

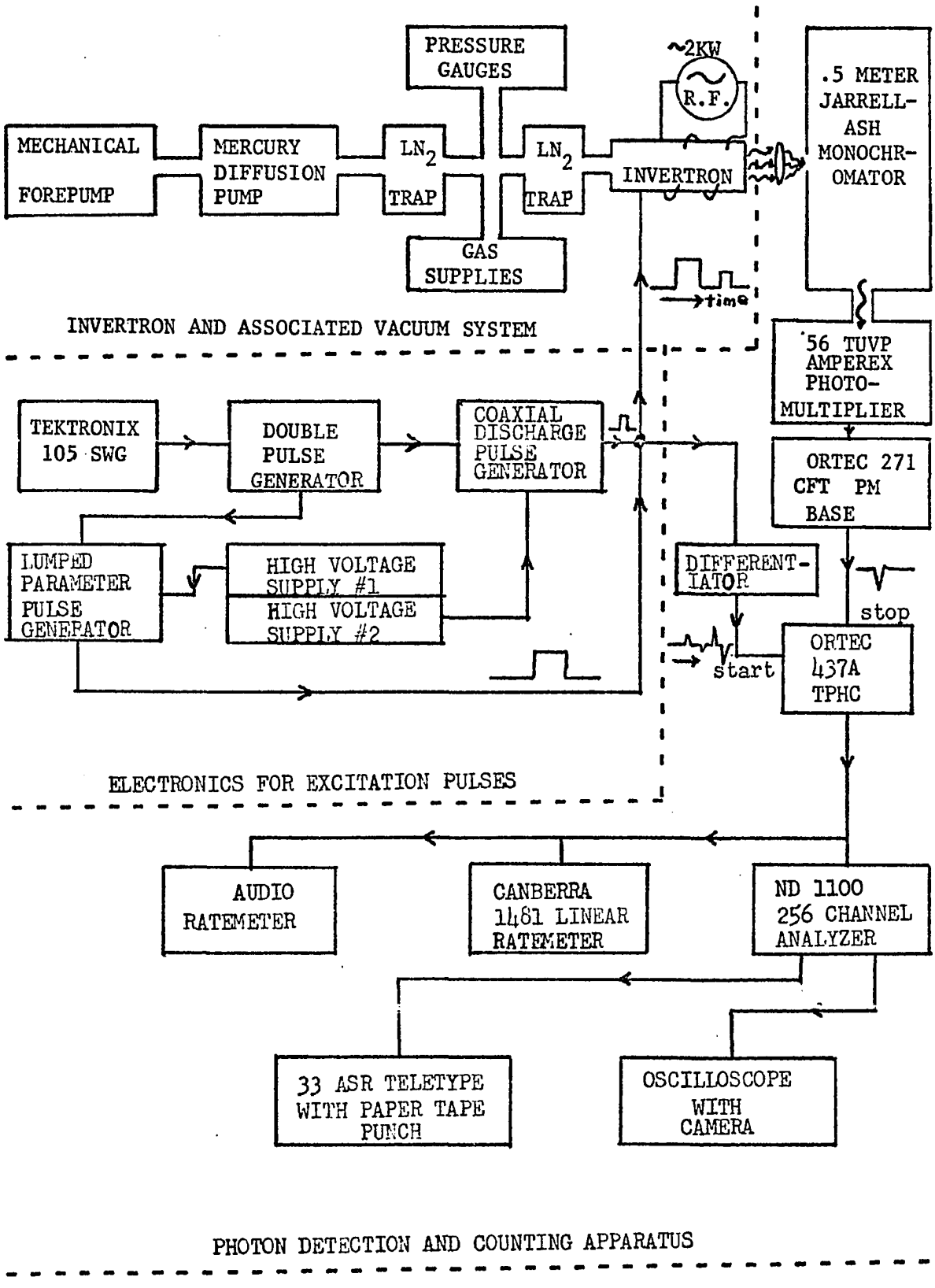

Figure 8. Schematic of System used for Lifetime Measurements in the 2000Å to 7800Å Range.

analyzed mathematically for breakdown by Russell[24] and modified slightly by Johnson[8] to the design currently in use. The hollow nickel cathode is coated with mixed carbonates of barium, calcium and strontium, air dried, then heated inductively at or slightly above operating temperature for a full day under continuous pumping for outgassing.

Electronics for Source Activation

The source excitation rate is controlled by a Tektronix 105 Square Wave Generator in place of the less versatile neon bulb relaxation oscillator. Because of the high voltages applied to the 2D21 thyratrons used for switching the source voltage, the frequency must be adjusted to find a stable firing rate. The activation pulses of interest here are either single pulse per cycle from discharging a length of coaxial cable through the invertron (this method bypasses the double pulse generator), or two pulses per cycle in which the first square pulse is obtained by discharging a lumped parameter delay line (artificial coaxial cable) of one-half to five microseconds duration and the second pulse is the same as that used when single pulsing. Lengths of pulses available from the coaxial cable arrangements are 10, 88, 93, 126, 512 and 760 nanoseconds or various combinations thereof. The delay between pulses out of the double pulse timer is continuously variable over a range of 0 to 50 microseconds. The double pulse generator is similar to the "timer" of Johnson[8] (p. 140). Because of the extensive modifications incorporated, a recent schematic of the double pulse generator is shown in Fig. 9. The

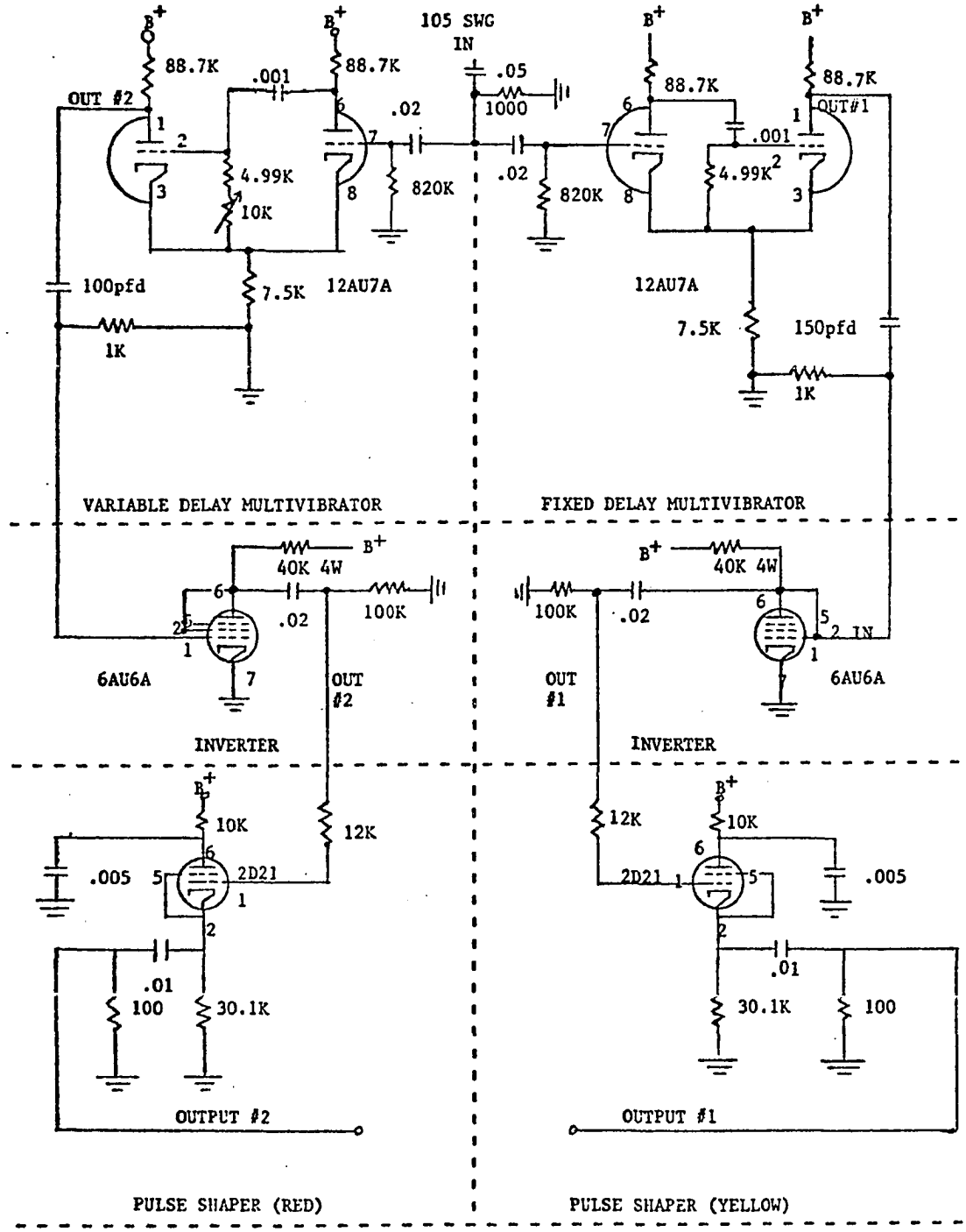

UNITS: RESISTANCE-OHMS; CAPACITANCE-MICROFARADS; B^+=460 VOLTS.

Figure 9. Double Pulse Generator Circuits.

voltage applied to the invertron is monitored via a high speed (2.3 ns rise time) oscilloscope.

Detecting and Recording Data

Using a quartz lens, light from the invertron is focussed onto the entrance slit of a ½-meter Jarrel-Ash monochromator. The selected line is monitored by a 56TUVP Amperex photomultiplier. The photomultiplier output is amplified by an Ortec 271 Constant Fraction Timing (CFT) base which can be biased with the Ortec 403A Time Pickoff Control (TPC) to discriminate against low level (i.e. non-cathode originated) pulses. This pulse is applied to the stop gate of the Ortec 437A Time to Pulse Height Converter (TPHC) which was previously turned on by a negative pulse obtained by differentiation of the square wave applied to the invertron. The differentiator consists of a series variable resistor and variable capacitor so as to allow adjustment of the differentiated signal until the first negative pulse is too small to trigger the TPHC, yet the second negative pulse (which is much sharper) is large enough to provide a stable trigger point. The voltage pulse out of the TPHC, which is proportional to the time between start and stop signals, is recorded in a multichannel analyzer operating in a pulse height analysis (PHA) mode.

Accumulation of data proceeds for 45 to 75 minutes until a satisfactorily smooth curve is obtained. Degree of smoothness required depends upon the number of exponential components anticipated to be present in the data and the precision required of each parameter. The resulting data when displayed on an oscilloscope has the shape of

an exponential decay (assuming no abnormal effects in the discharge) as expected from an intensity (number of counts in a channel) versus time (channel number) acquisition. The acquired data is printed through a 33ASR teletype and simultaneously punched on paper tape. This paper tape in turn can be loaded onto a computer data file for analysis as described in Chapter III.

A very important factor in the accuracy of measurements made by coincidence counting is the ratio of acquisition rate to the source pulsation rate. This problem arises from the fact that only the first photon observed from each excitation is recorded with all others ignored. It is then necessary to require a negligible probability of multiple photon detection by the photomultiplier. Johnson[8] (pp. 19-25) has considered this problem analytically and has arrived at a correction formula for each data point. It appears, however, that a negligible effect on lifetime is expected when the acquisition rate is held to less than 10% of the source pulse repetition rate. This contention was upheld by an experiment in which an incandescent light was placed before the monochromator and its intensity profile was found to be flat (within a normal statistical distribution). This experiment also served to certify the linearity of the multichannel analyzer and proper adjustment of its controls. Perhaps a more conclusive demonstration of this effect would be to choose an apparently cascade-free transition such as the N_2^+ 3914 band and determine lifetime at 80%, 50%, 10% and 1% acquisition-to-pulsation ratio.

Tunnel-Diode Monostable Multivibrator Preamp

In order to extend our capability into the S-1 spectral response range of the infrared spectrum an astable multivibrator circuit utilizing a low capacitance tunnel-diode has been built.

Construction of this circuit was based on a design described in the tunnel-diode handbook.[25] The tunnel diode circuit, which is shown in Fig. 10(a) is encased in a 1 cm × 1 cm × 3 cm metal box for shielding. Input and output attachments are made with BNC connectors. Operation of the preamp requires a DC bias to a level just below the 120 ma peak in the tunnel diode characteristic curve shown in Fig. 10(b). Under such a condition the diode is caused to switch at constant current to 600 mv upon receiving the 5 ns Gaussian pulse from the PMT. Exact adjustment of the bias level is determined experimentally so as to cause switching only when a photon strikes the PMT cathode. It is the constant current tendency of the inductance that maintains the tunnel-diode current during its switching operation.

The output pulse from the circuit has the form shown in Fig. 10(c) when terminated into 50Ω. This output pulse fulfills the stop signal requirements of the time-to-pulse height converter used for delayed coincidence techniques.

A check of feasibility was undertaken by exposing an S-1 response photomultiplier to a constant level light source (a hot cathode) stopped down with an iris until a count rate of 10 per cent of the start signal repetition rate was observed. Counting at this level produced the expected data set consisting of equal counts in all channels within the normal error distribution, i.e., error varying

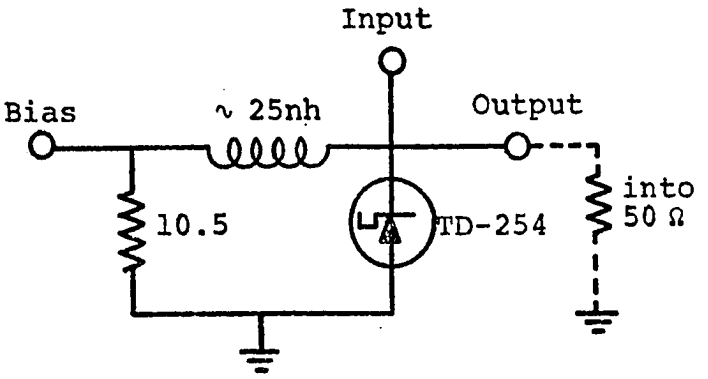

(a) Tunnel-diode circuit.

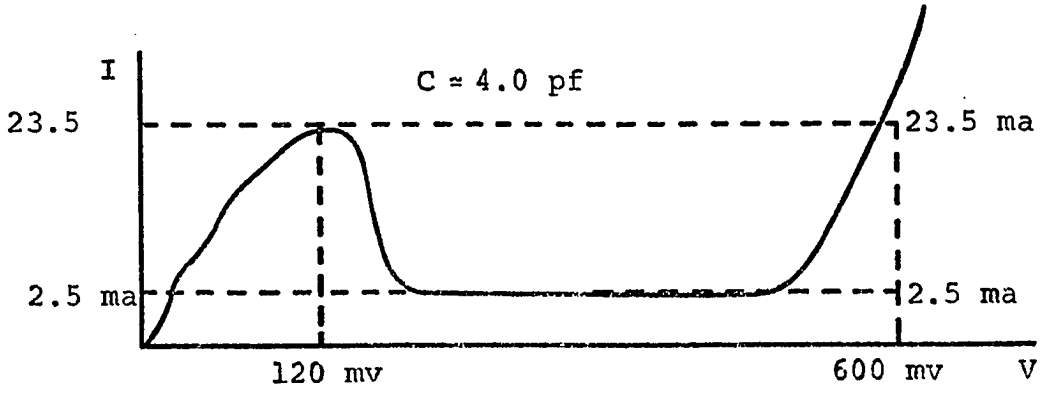

(b) Tunnel-diode characteristics.

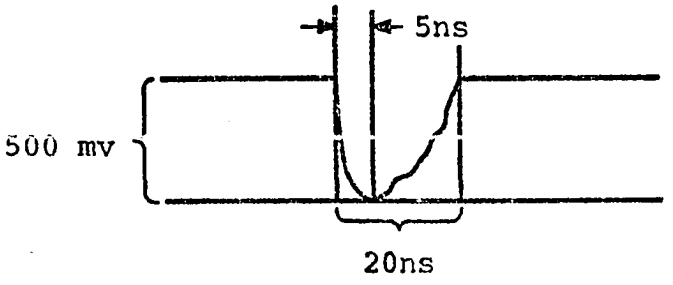

(c) Waveform observed from preamp into 50Ω.

Figure 10. Photomultiplier pulse preamplifier.

inversely with the square root of the number of counts accumulated in each channel. For best results the photomultiplier voltage was set at its maximum allowable value and cooled to liquid nitrogen temperature.

CHAPTER V

EXCITED STATE LIFETIME MEASUREMENTS IN ATOMIC HELIUM

In this chapter we shall inspect the new data obtained, compare it to results of others and attempt to analyze its meaning. For all cases the intensity vs. time data was analyzed by digital computer using the programs discussed in Chapter IV. Where a sufficiently large sampling of observed lifetime as a function of pressure was available the data was fitted to a straight line using a linear regression with appropriate weighting to convert to reciprocal lifetimes for the fit. Statistical weights for the points were the uncertainties developed by the non-linear least squares fit of the data to exponential functions. The most probable results indicated by 199 individual measurements of lifetime are shown graphically in Figs. 11 through 17. In most cases, above n=5, the data exhibited two exponential components, the faster component being more characteristic of ^1P state lifetimes than of the state observed. When this occurred the "cascade", second, or slower lifetime was identified with the state observed. The uncertainties quoted for calculated or NBS derived results are those set by the NBS authors.

Analysis of He n^1S Transitions (n=3-9)

(Results are shown in Fig. 11.)

From six pressure measurements the lifetime of He 3^1S has been determined to be 55.9±2 ns. The data obtained had no discernable cascade contribution. For comparison the lifetime derived from NBS[4] transition probabilities is 53.2±1.5 ns. That of Osherovich and Verolainen[26] is 60±3 ns, whereas Bennett, Kindlemann and Mercer[27] measured 55 ns.

The lifetime for 4^1S of 89±3 ns was reported by Johnson and Fowler.[28] In comparison to this a value of 89.8±3 is obtained from NBS[4] transition probabilities, 84 ns is reported by Bennett et al[27] and 75±4 ns was reported by Osherovich and Verolainen.[26]

The lifetime of 5^1S was determined to be 160±3 ns from determinations at 5 pressures. This state exhibited no secondary or cascade lifetime in any measurements. This value can be compared to the NBS-derived[4] value of 151±15 ns, the Pendleton and Hughes[29] measured value of 144±3 ns, the Osherovich and Verolainen[26] measured value of 115±5 ns, Allen et al[30] measured 118±8 ns, Kindlemann and Bennett[31] measured 333±18 ns, and Bennett et al[27] measured 141 ns.

A lifetime of 210±4 ns was determined for 6^1S from data at seven different pressures, each case exhibiting two exponentials. The shorter component lifetimes fell between the non-blockaded 6^1P lifetime of 12.9 ns and the blockaded value of 269 ns and exhibited the characteristic trend of a blockaded state, which is to increase with pressure, rather than to decrease as with normal quenching. For comparison one can calculate a value of 240±12 ns from NBS[4] transition probabilities.

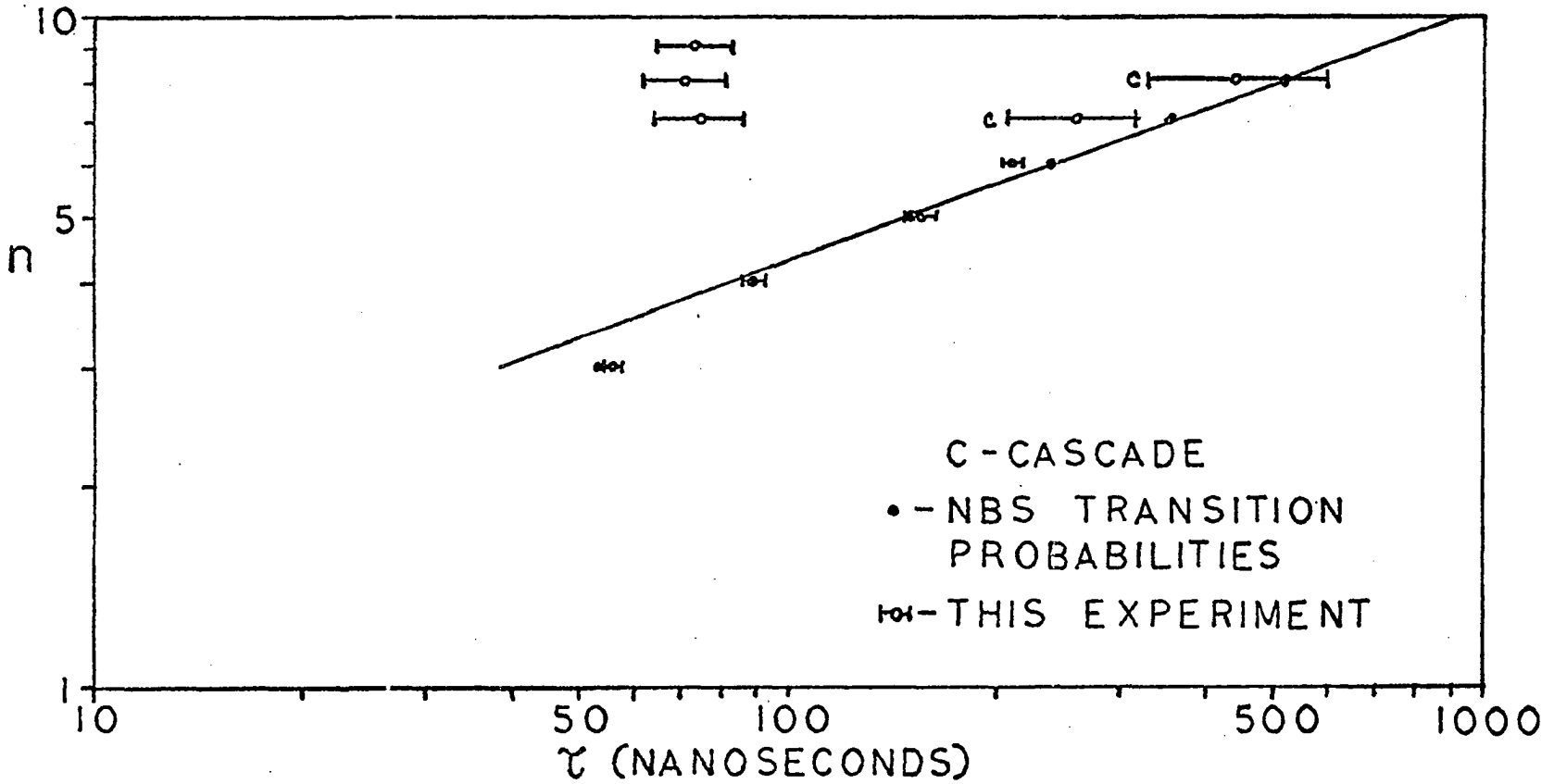

Figure 11. Lifetime vs. Principal Quantum Number for Helium n^1S.

For 7^1S only one pressure was used. This measurement exhibited two components of 44±4 ns and 192±24 ns at 140 microns of Hg. Assuming a quenching cross section of $7\times10^{-15}cm^2$ for this level, the slow component could yield a lifetime near the 356±35 ns calculated from NBS[4] and Gabriel and Heddle[32] transition probabilities. Such a cross section is not incompatible with that observed for other states where a pressure dependence was obtained. The exponential amplitudes of the two components were of approximately equal magnitude but since this represents intensity rather than population each must be multiplied by the corresponding lifetime to obtain representative time zero (end of excitation) population densities. This would indicate a population due to direct excitation of approximately four times that due to the alternate process. The process causing the 44 ns lifetime could not be due to cascade, for the rate equations would require its coefficient to be negative which was not the case. In addition an independent measurement of 7^1P at 150 μ-Hg yields a lifetime of 49 ns which was comparable to the fast component of the 7^1S decay.

For 8^1S four measurements of lifetime were obtained, each of which indicated at least two components and the two highest pressure measurements at 140 μ-Hg indicated three components the fastest of which (11 ns) was quite possibly due to barium which has a very strong line at the same wavelength. The other two measurements at 76 μ-Hg and 110 μ-Hg appeared as two exponentials, the fast components of which at 55 and 59 ns are very similar to that observed for 8^1P. The longer lived components at 431±27 and 550±200 ns, although statistically very uncertain due to an insufficient supply of data, do compare

favorably to a calculated value of 521±52 ns at zero pressure. The ratio of coefficients of these two components indicated that about 1/3 of the decayed states came through the faster process.

For 9^1S one measurement was made at 145 μ-Hg and appeared to be a single exponential having a lifetime of 47±1 ns. This is most likely due to the inadequacy of the time scale used to resolve a lifetime on the order of 700 ns as expected from the 9^1S state. The value observed here is larger than but on the order of the 36 ns observed for 9^1P at 140 μ-Hg.

He n^1P Transitions (n=5-10)

(See Fig. 12.)

It was not originally proposed to measure these transitions because of the nonlinear effects of "blockading" due to resonance absorption; however, several were measured in the course of the experiment for comparison to anomalies found in other states. It should be possible eventually to place these results on the lifetime curves given in Fig. 1 when the true constants of the equations and the complete set of equations have been found and solved for the transfer processes. The data measured for ^1P states is given in Table 4.

TABLE 4. MEASURED LIFETIMES OF n^1P TRANSITIONS.

Level	Pressure μ-Hg	fast lifetime (ns)	slow lifetime (ns)
5^1P	100	27.9±0.3	114 ±4
	140	23.1±0.4	108 ±4
6^1P	40	33.8±0.6	293±25
---	120	23.4±0.4	200 ±7
---	35	20.2±0.2	153 ±5
---	200	18.0±0.3	214 ±4
---	300	17.7±0.5	196 ±4

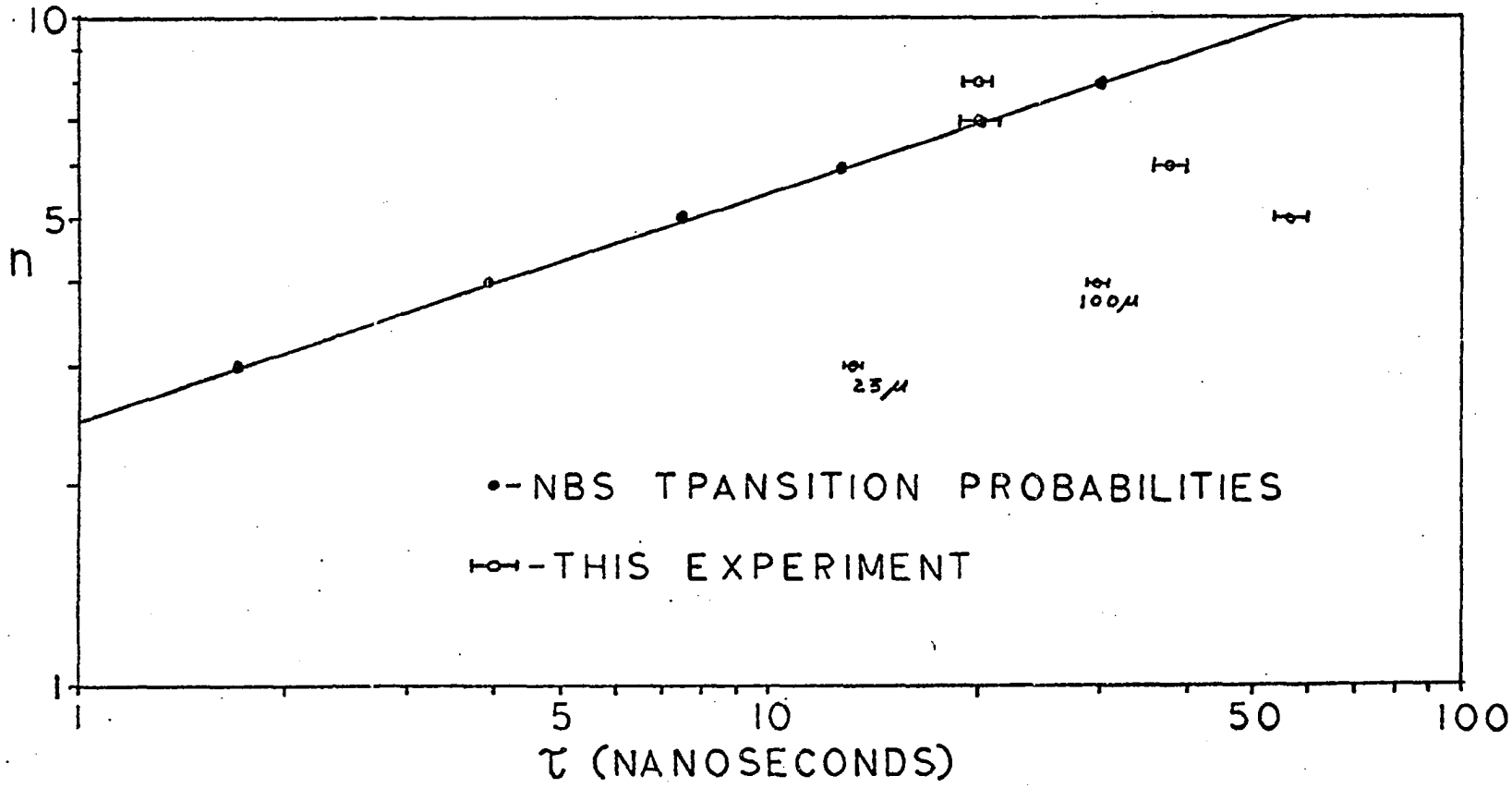

Figure 12. Lifetime vs. Principal Quantum Number for Helium n^1P.

TABLE 4 (continued)

Level	Pressure μ-Hg	fast lifetime (ns)	slow lifetime (ns)
7^1P	125	16.8±0.3	146 ±3
---	150	49.0±2.0	355±40
---	150	24.0±1.0	280±24
8^1P	78	30.0±2.0	153 ±4
---	120	17.4±0.5	356±33
---	145	67.0±3.0	
---	145	42.0±1.0	
---	150	46.0±1.0	
---	500	15.0±1.0	120±11
9^1P	140	36.0±2.0	259 ±7
10^1P	130	38.0±2.0	255±10

Analysis of n^1D Transitions (n=3-9)

(See results in Fig. 13.)

From three measurements the zero pressure lifetime of the 3^1D state was determined to be 20±1 ns. This result compares to 15.4±0.5 ns calculated from NBS[4], 16±1 ns as measured by Osherovich and Verolainen,[26] 15.5±1.5 ns measured by Allen et al,[30] 18±5 ns measured earlier by Fowler et al,[33] 16±4 ns measured by Kindlemann and Bennett[31] and 22 ns measured earlier by Bennett et al.[27] The three data points at 26, 58 and 90 μ-Hg fit a stright line, exhibiting a quenching cross section of $3.7\times10^{-14}cm^2$. These results compare quite favorably with that of Drtil[34], who measured a lifetime of 20.5±0.9 ns and a "depolarization" cross section of $6.0\times10^{-14}cm^2$ using the Hanle technique. The data all exhibited two exponential characteristics, the longer of which is surmised to be from one or more ^1F states. The longer component lifetimes did not appear to fit a straight line as well as did the short component. It appeared, however, that an extrapolation of the second component would fall in a range from 400 ns to 1100 ns

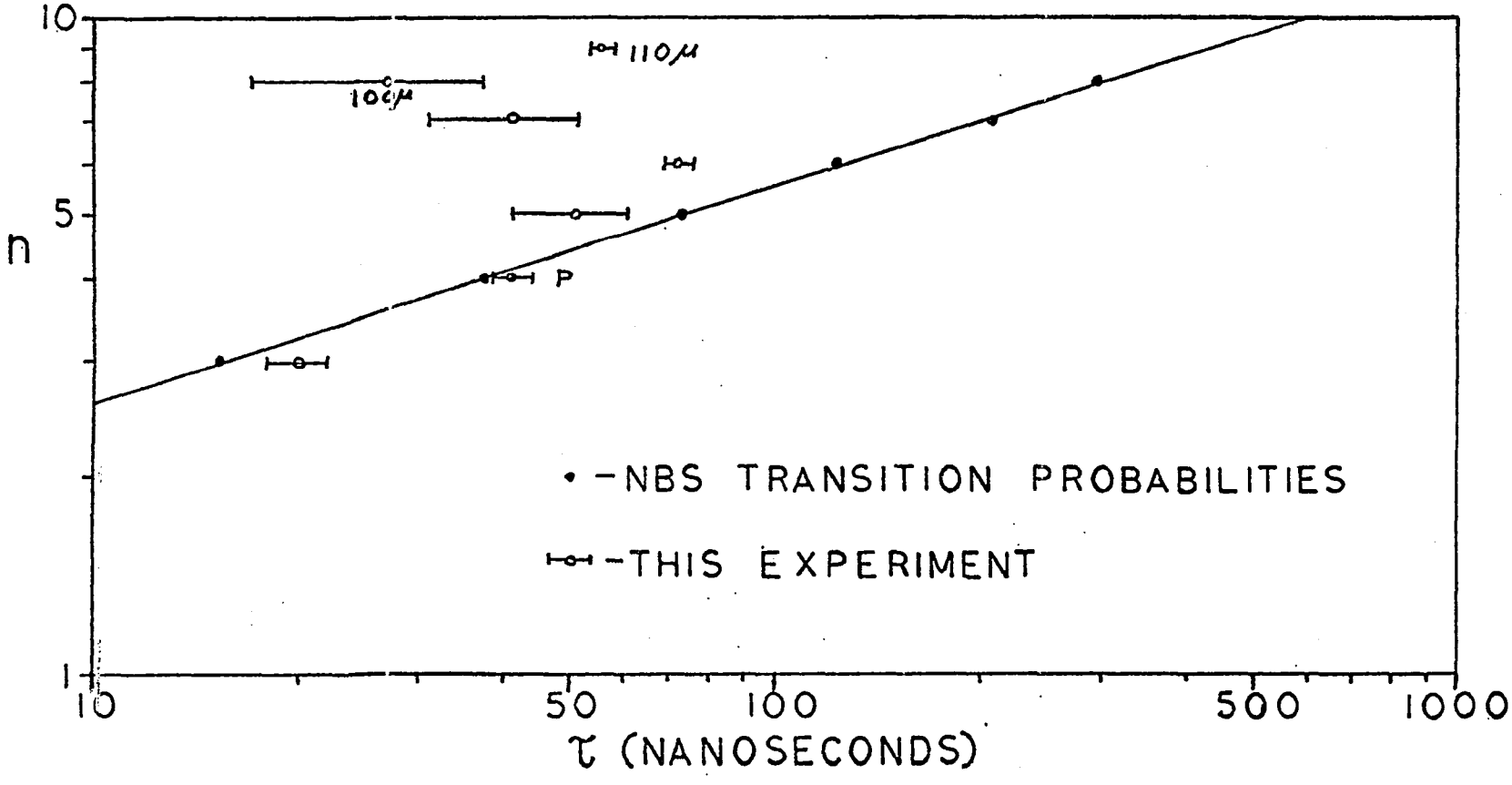

Figure 13. Lifetime vs. Principal Quantum Number for Helium n^1D.

which is the range for 7, 8, 9 and 10 ^{1}F.

Measurements by this method of 4^{1}D were reported earlier by Johnson and Fowler[28] to be 41±3 ns. This result compares to the NBS[4] derived value of 37.8±1.2 ns, Osherovich and Verolainen's[26] measured value of 30±2 ns, Pendleton and Hughes[29] measured value of 47±5 ns, Allen et al[30] measured 38±5 ns. Fowler et al[33] in an earlier measurement reported 35±4 ns, Kindlemann and Bennett[31] measured it at 33±6 ns, Chin-Bing and Head[35] measured 44±5 ns and Bennett et al[27] measured 34 ns.

The 5^{1}D line was measured at two pressures and extrapolated to 56 ns. However, because of the lack of data to establish the line more definitely a large error of ±10 ns is assigned to the value. These lifetimes also exhibited two exponential characteristics, the longer of which is thought to belong to a higher ^{1}F state. Due to uncertainties in the measured slower decay constant and the lack of sufficient pressure statistics they cannot reliably be extrapolated to zero pressure. It is however within range of what one might expect for the free atom lifetimes of 7, 8, 9 or 10 ^{1}F. For comparison the value obtained from NBS transition probabilities is 72.7±3 ns whereas Osherovich and Verolainen[26] observed 46±3ns and Bennett et al[27] measured 59 ns. The 6^{1}D lifetimes measured at five pressures exhibited two exponential behavior; however, the fast component appeared well-behaved (quite linear) with pressure and extrapolated to 72±3 ns. In comparison the value calculated from NBS[4] data obtains 123±12 ns. The cascade or slower component also fits a straight line quite well and extrapolates to 380±30 ns which compares quite well to that expec-

ted for 7^1F of 370 ns as calculated from transition probabilities computed by Jobe and St. John.[17]

For 7^1D a set of four lifetimes was measured, each member of which exhibited double exponentials. The first component indicated a zero pressure lifetime of 65±20 ns; the second, a value on the order of 800±200 ns. Neither value agrees with the calculated[4] value of 207±40 for this level. The value of 800 ns compares quite well however with the calculated value for 9^1F. It is probable that both collisional transfer direct to 7^1D and through 8^1F and 9^1F were present and masked the true F state lifetime. Such a presence would yield a three-exponential decay and might be observed with better statistics using a longer acquisition time at each pressure.

For 8^1D only two measurements were made yielding short component lifetimes of 26.6±0.4 ns and 33±1 ns at 100 and 110 μ-Hg respectively. The longer-lived components were 286±2 ns and 577±13 ns respectively. Again none of these compare favorably to the calculated[4] value of 297±9 ns. It is apparent that the true lifetime at this level is again masked by other processes. The short component lifetime is notably similar to that expected of 8^1P lifetimes suggesting that a direct transfer is now beginning to set in at this large value of n.

For 9^1D only one measurement was obtained at 110 μ-Hg yielding lifetimes of 56±1 ns and 298±6 ns. A plot of residuals (data minus the two exponentials) indicated the possible presence of a third exponential but it was not extractable. Neither value agrees with the calculated[4] value of 420±50 ns, and it is again apparent that the short component exhibits characteristics similar to that observed in

9^1P, indicating a direct transfer mechanism.

Analysis of n^3S results (n=3-9)

(See Fig. 14.)

The 3^3S level was measured at eleven pressures and did not appear to contain more than one exponential. Results of the data suggests a free atom lifetime of 57±1 ns. This compares to an NBS[4] derived value of 36.4±1 ns and a value of 47±3 ns as measured by Osherovich and Verolainen.[26]

The 4^3S value of 62±3 ns was reported by Johnson and Fowler.[28] This compares to 64±6 ns obtained from NBS[4] transition probabilities and measured values of 69±3 ns by Osherovich and Verolainen,[26] 68±1 ns by Pendleton and Hughes,[29] 59±6 ns by Holzberlein,[23] 65±4 ns by Kindlemann and Bennett,[31] 65±3 ns by Nichols and Wilson,[36] 67.5±1 ns by Heron et al,[37] 77.5±4 ns by Bennett and Dalby,[38] 44 ns by Bennett et al,[27] 64.5±1 ns by Allen et al,[30] 59±6 ns by Fowler et al,[33] and 52±5 ns by Chin-Bing and Head.[35]

For 5^3S two measurements at different pressures were obtained having lifetimes of 58±0.6 ns and 108.5±1 ns at 170 and 35 μ-Hg respectively. These apparently single exponential results extrapolate to 140±20 ns at zero pressure with a cross-section of $2.5\times10^{-14}cm^2$ which is in general agreement with other quenching cross-sections observed in this experiment. The calculated[4] value is 110±11 ns, whereas Osherovich and Verolainen[26] have measured 106±5 and Bennett et al[27] have measured 65 ns.

The lifetimes measured for 6^3S showed two exponentials. The reciprocal lifetime did not appear very linear with pressure for

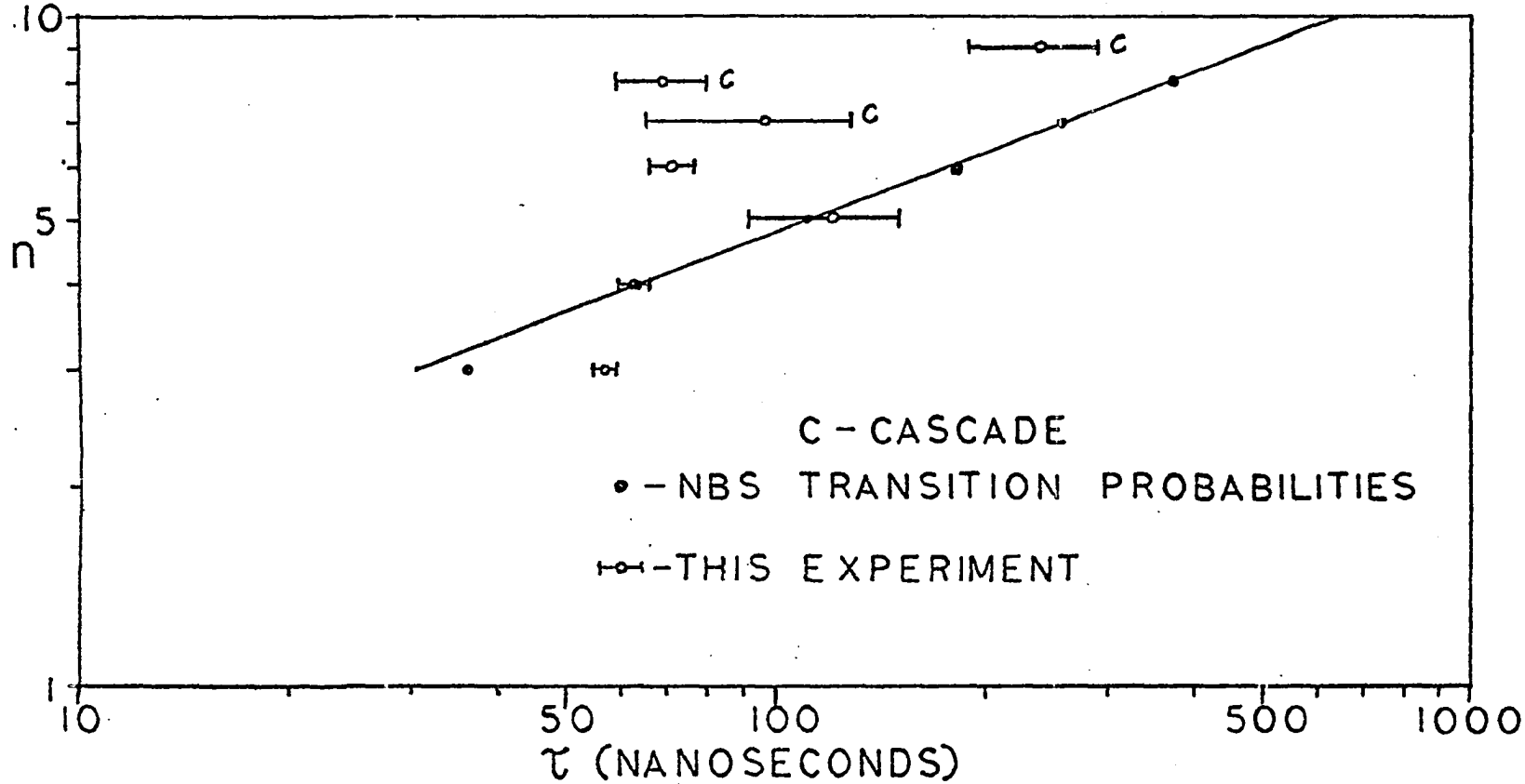

Figure 14. Lifetime vs. Principal Quantum Number for Helium n^3S.

the fast component and suggested a value of 75±20 ns whereas the longer-lived components indicate a zero pressure lifetime of 400±100. By comparison the calculated[4] value is 183±18 ns.

For 7^3S four measurements gave fast components between 63 and 129 ns which are longer than those observed at 7^1P but shorter than calculated[4] for 7^3S at 260 ns. The longer lifetimes measured ranged from 356 ns to 602 ns. All samples exhibited two exponential components.

For 8^3S four measurements, three analyzed as two exponentials, yielded fast component lifetimes ranging from 50 to 87 ns and slow components ranging from 203 to 577 ns. These compare to a calculated value of 360 ns. From Table 4 we see that the fast component is on the order of the 8^1P measured transitions. Two measurements at 9^3S yielded two exponentials each, the shorter of which were 26 and 36 ns (comparable to 9^1P results). The longer components were 171 and 238 ns which is much shorter than the calculated[4] value of 500 ns for this level.

We can conclude that in the case of the n^3S states, the small cross section for direct excitation causes the direct transfer from n^1P which becomes increasingly important with n to blend two exponentials into a combination which was not successfully resolved. Otherwise we must assume shortcomings in the theory of these states.

Results of n^3P Lifetime Measurements (n=2-9)

(See Fig. 15.)

A total of 21 data runs were accumulated on the 2^3P state at various pressures and excitation voltages using the special infrared

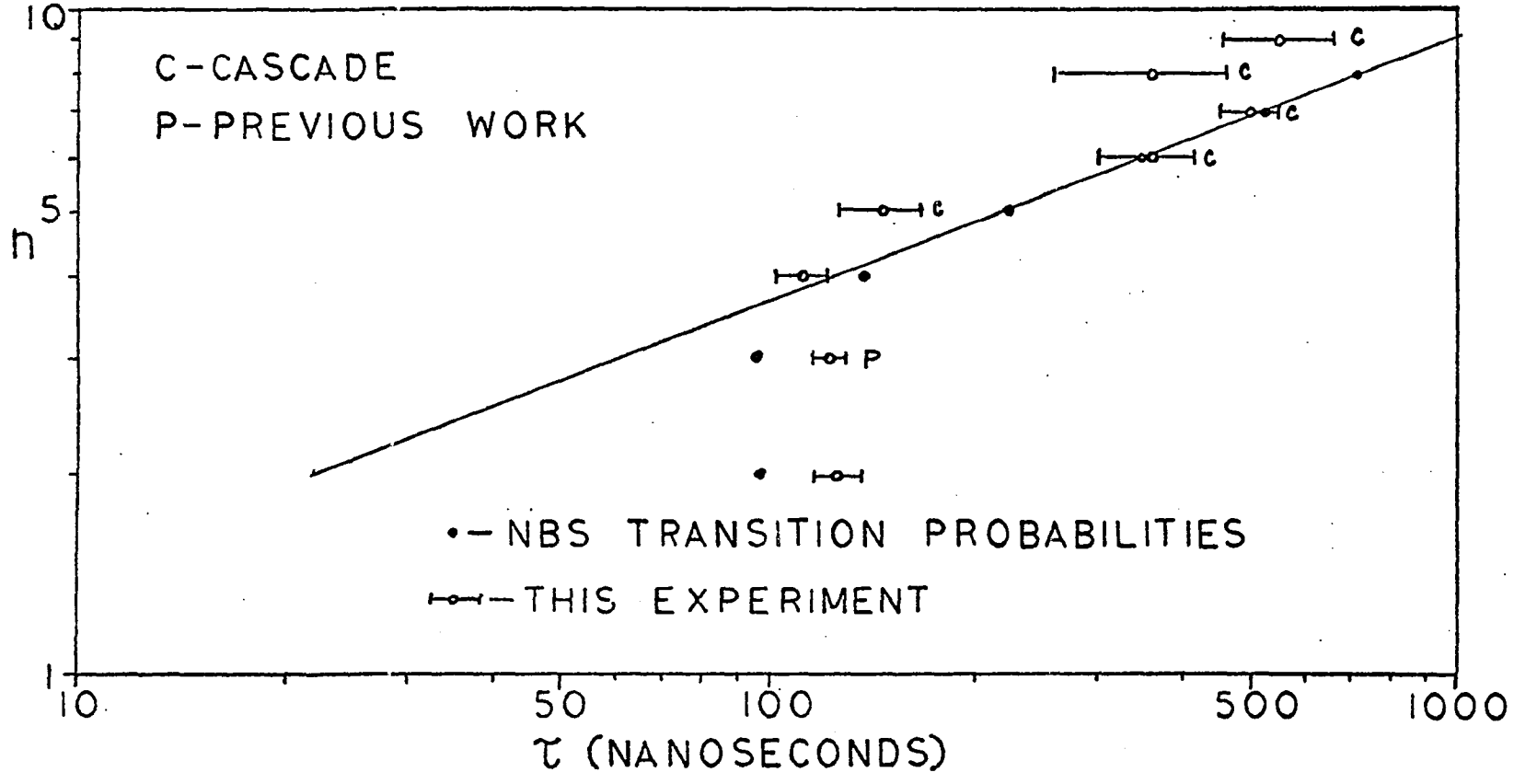

Figure 15. Lifetime vs. Principal Quantum Number for Helium n^3P.

detection equipment previously described. In addition to varying pressure and excitation voltages two different excitation methods were used. The first method employed two excitation pulses, the first of which ionized the gas so as to allow the second pulse to penetrate more quickly. The second pulse was required to realize a sharp cut-off. The first pulse was of 5 microseconds duration, whereas the second pulse, which started immediately after the first pulse stopped, was 0.5 microseconds long. The voltages of the two pulses were set independently so as to give a suitably intense signal at the PMT.

The second method, which was found to yield comparable results, used only a single 0.5 microsecond pulse. The repetition rate of the excitation pulses was 1100 pps for the two-pulse method and approximately 12,000 pps for the single pulse method.

There was no well-defined trend observed in the lifetime with pressure, with excitation method or with excitation voltage. The simple average value of lifetime is 130 ns with a standard deviation of 7 ns. Since we expect that there are no damping mechanics for this state, while there may be weak enhancing mechanics such as radiation blockading, it can be argued that the lower values should be favored and that a better value would be 125 ns. Further arguments for this value are that inclusion of data before the inflection point (see below) in the analysis or delay of the excitation shut-off or both could only have the effect of extending the lifetime. This result is somewhat higher than the theoretical value of 98 ns computed from the transition probability,[4] but we see no systematic cause of the discrepancy, and favor our observed value, especially since both

TABLE 5. HELIUM 2^3P-2^3S LIFETIME VARIATION WITH OPERATING CONDITIONS

Case No.	Case Identification	τ (ns)	First Pulse Voltage (Volts)	Second Pulse Voltage (Volts)	Pressure (Torr)
1	6/20/#2	120	41	28	.150
2	2/27/#1(b)	122	36	24	.330
3	2/27/#1(a)	123	36	24	.330
4	2/28/#2	123	40	22	.043
5	6/20/#4	123	33	26	.625
6	9/13/#5	124	--	110	.500
7	2/25/#3	124	50	22	.074
8	1/6 /#1	125	--	100	.092
9	9/13/#6	126	--	95	.060
10	9/13/#1	130	--	90	.115
11	9/11/#4	132	--	135	.115
12	6/20/#1	132	44	26	.150
13	2/25/#1	133	53	30	.100
14	9/13/#4	133	--	120	.115
15	2/27/#3(b)	134	46	30	.033
16	2/25/#2	135	51	30	.100
17	2/27/#3(a)	136	46	30	.033
18	1/13/#3	136	--	150	.115
19	1/11/#2	138	--	90	.115
20	2/25/#4	142	38	26	.074
21	6/20/#3	145	40	30	.025

theory and our experiment agree that the values of 3^3P and 2^3P will be the same.

A semi-log plot of the data from a typical case is shown in Fig. 16 and serves to illustrate the scatter in the data. In order to eliminate transient effects caused by cascades from n^3S and n^3D levels, each of which has a shorter lifetime, it is necessary to analyze only the data accumulated in the channels beyond the inflection point of the curve. The data obtained in a 256 channel analyzer was curve-fitted by a digital computer using conventional non-linear least square techniques. The second curve shown in Fig. 16 is a plot of the data minus the least squares fit to a single exponential decay and a constant background level. Although presence of a second exponential in the decay could shorten the decay constant of the first exponential, our program permits us to use an arbitrary number of exponentials, and best fit was always obtained with the choice shown. For the case in Fig. 16 the value of the background was 1000 counts per channel and resulted primarily from light from the hot cathode.

The lifetime of 3^3P was reported by Johnson and Fowler[28] as 122±5 ns. Other values include the NBS[4] derived result of 96.6±1 ns and the measured values 115±5 ns of Osherovich and Verolainen,[26] 100±8 ns by Osherovich and Savich,[39] 115±5 ns by Heron et al,[37] 106±5 ns by Bennett and Dalby,[38] 105 ns by Bennett et al,[27] 91±8 ns by Fowler et al,[33] and 108±15 ns by Chin-Bing and Head.[35]

For 4^3P lifetimes were measured at two different pressures which extrapolated to 125±20 ns. The higher pressure measurement at 200 μ-Hg exhibited two components with the slow component appearing much weaker

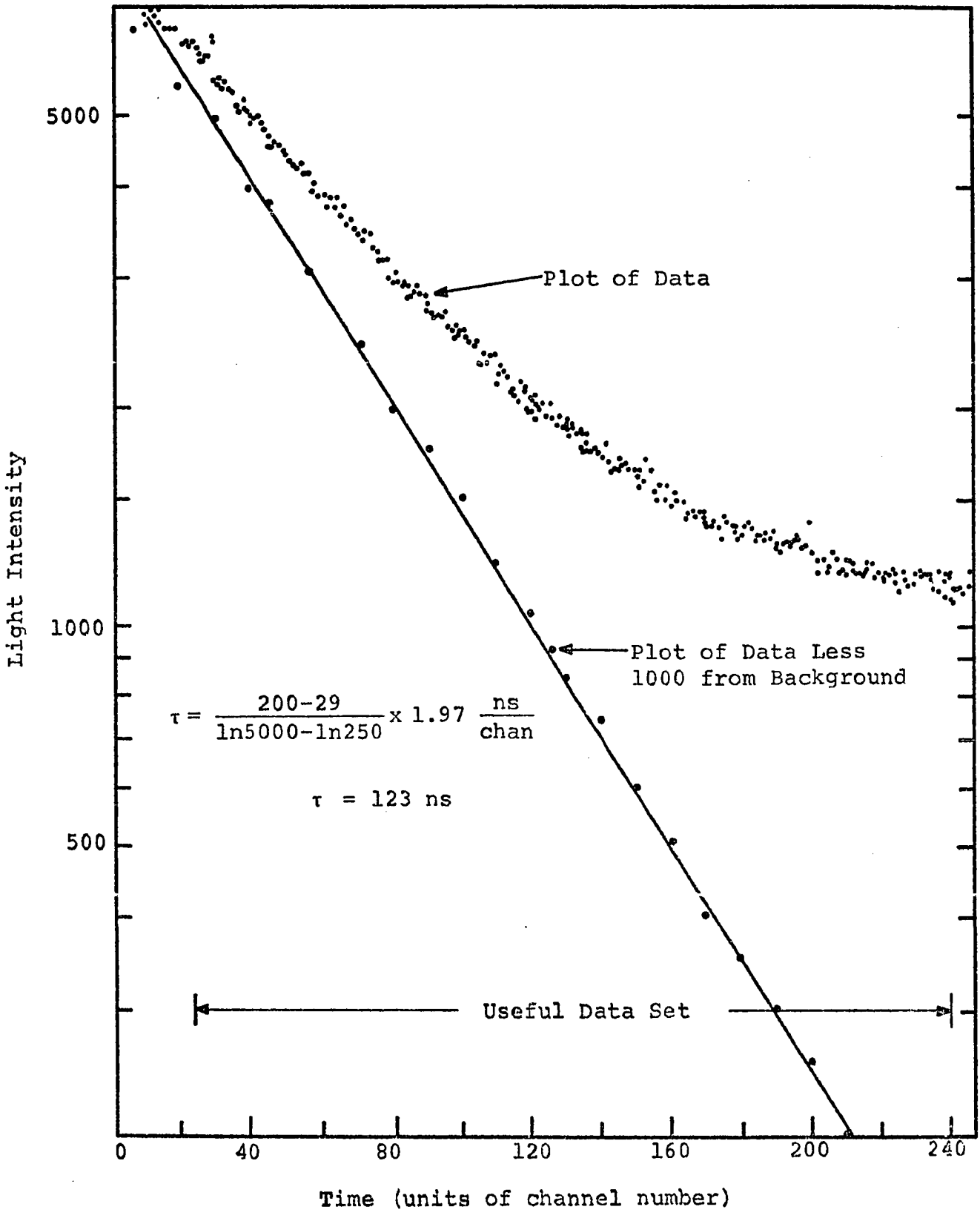

Figure 16. Analysis of light intensity vs. time for a typical case.

than the fast component. It is conceivable that this resulted from a cascade from 6^3S which would be highly populated by transfer at this pressure. Other values for this lifetime are the calculated[4] 138±14 ns and the measured values of 153±2 ns by Heron et al[37] and 145 ns by Bennett et al.[27] It is felt that the result reported here is quite accurate and can be defined more precisely by additional measurements at other pressures below 200 μ-Hg.

The analysis of four measurements made at the 5^3P level indicate a lifetime of 200±100 ns. The data appeared widely scattered apparently due to a limitation of extracting all component exponentials or some non-systematic process occurring in the gas. The calculated[4] value is 225±23 ns and Bennett et al[27] measured 166 ns.

For 6^3P four measurements of lifetime with pressure indicates a zero pressure value of 360±20 ns when the longer component of the two extracted exponentials is used. The shorter component shows more scatter and extrapolates to a zero pressure value of about 80 ns. The calculated[4] lifetime is 350±35 ns. We conclude that we are seeing direct transfer from the 6^1P.

For 7^3P five measurements of lifetime between 73 μ-Hg and 250 μ-Hg each exhibiting two exponential components indicate a lifetime of 83±4 ns for the fast component which exhibits no consistent pressure trend and 550±150 ns for the slow component. The calculated[4] lifetime is 526±53 ns. The fitted coefficient of the slower exponential is about a fourth that of the faster component at high pressure but becomes within a factor of 1.5 at lower pressures. The analysis was highly uncertain due to the large influence caused by adjustment

of the constant term of the data fit equation. It is necessary to obtain more data with much higher accumulation (∿20,000 counts in the first channel) and a longer time scale (800 ns rather than 400 ns) to more completely determine the tail. The data exhibited a weak suggestion of being three exponential rather than two, however, the statistics of the data were not sufficiently good to allow extraction of another component.

Three observations of lifetime for 8^3P indicated a lifetime of 45±10 for the fast component and 400±100 ns for the slow component. These values compare to the calculated[4] value of 714±72 ns. In all three cases the coefficient of the slower exponential was approximately equal to that of the faster one. Each observation appeared to fit two exponentials quite well and contained no constant term.

Two observations for 9^3P suggest values at zero pressure of 110 ns for the fast component and 560 ns for the slow component. No uncertainties were determined because of the small sampling used for the determination. The result obtained from NBS[4] transition probabilities is 1100±110 ns.

Analysis of n^3D Lifetimes (n=3-11)

(See Fig. 17.)

The result of six measurements of lifetime for 3^3D yield a value of 19.4±0.5 ns. The data points were all double exponential. The fast and slow components are shown as a function of pressure in Figs. 18(a) and (b) respectively. The slow component indicates a value of 360±40 which compares quite well with the theoretical[4] value of 339±34 ns for 7F. Other values reported for 3^3D are 13.9±0.2 ns from NBS[4]

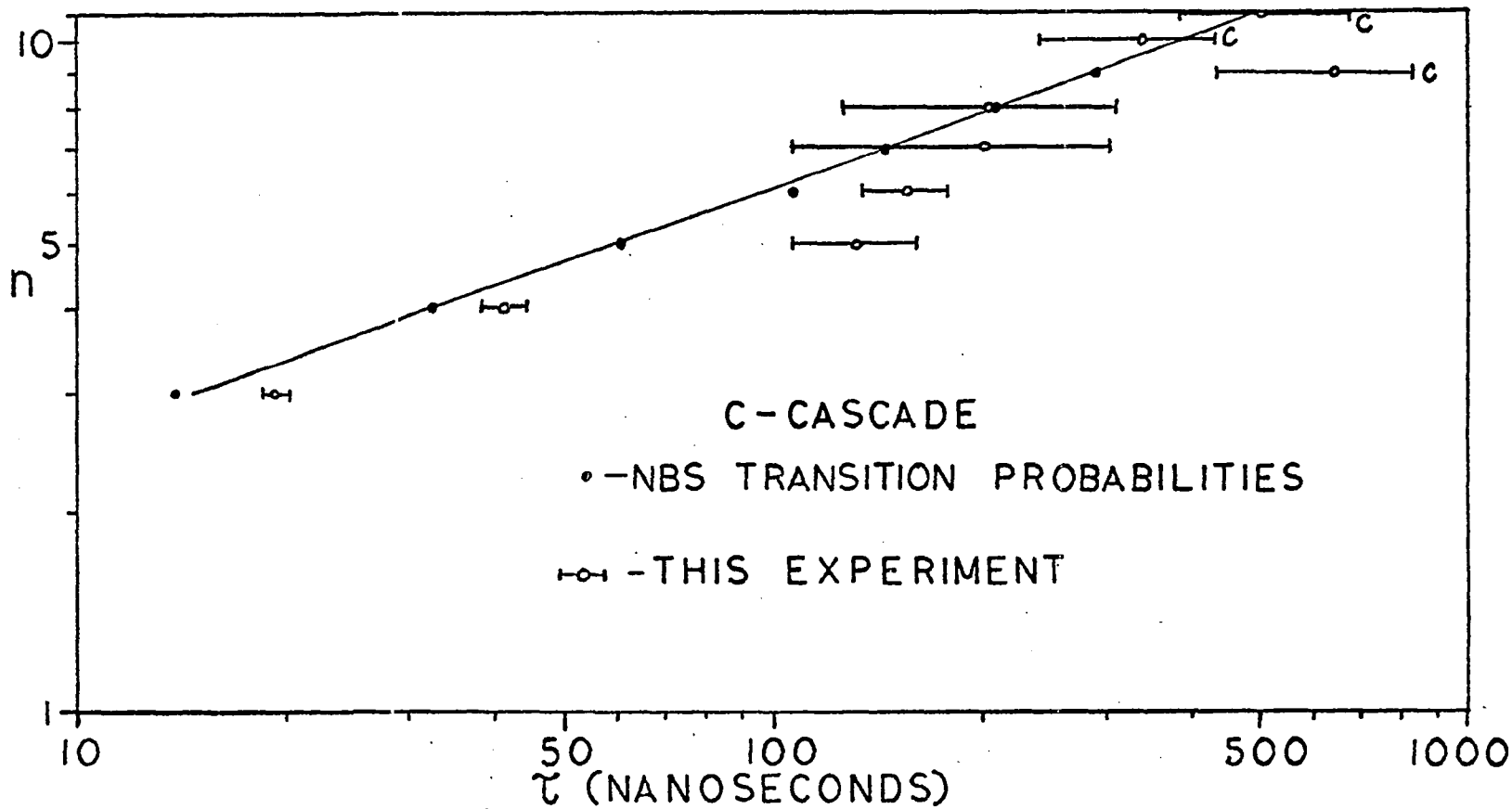

Figure 17. Lifetime vs. Principal Quantum Number for Helium n^3D.

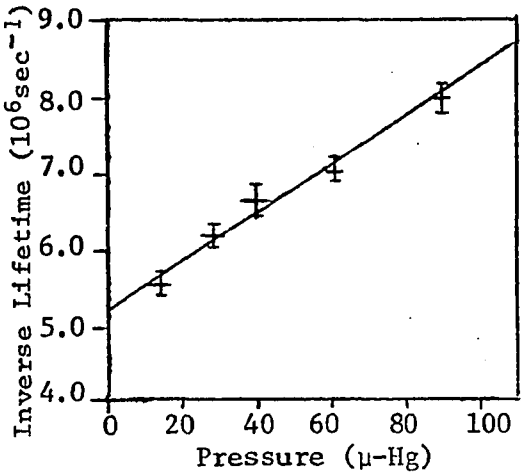

(a) He 3^3D plot of inverse lifetime vs. pressure.

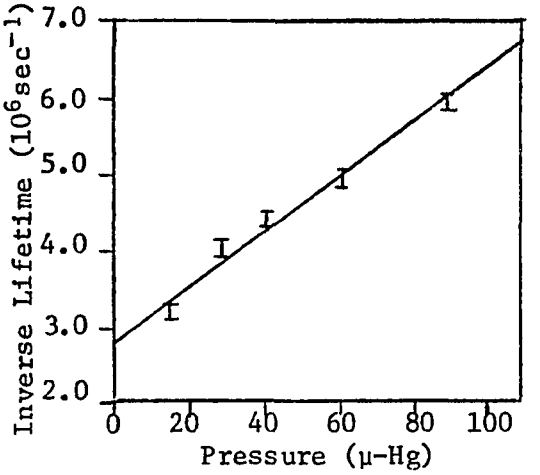

(b) He 3^3D "cascade" plot of inverse lifetime vs. pressure.

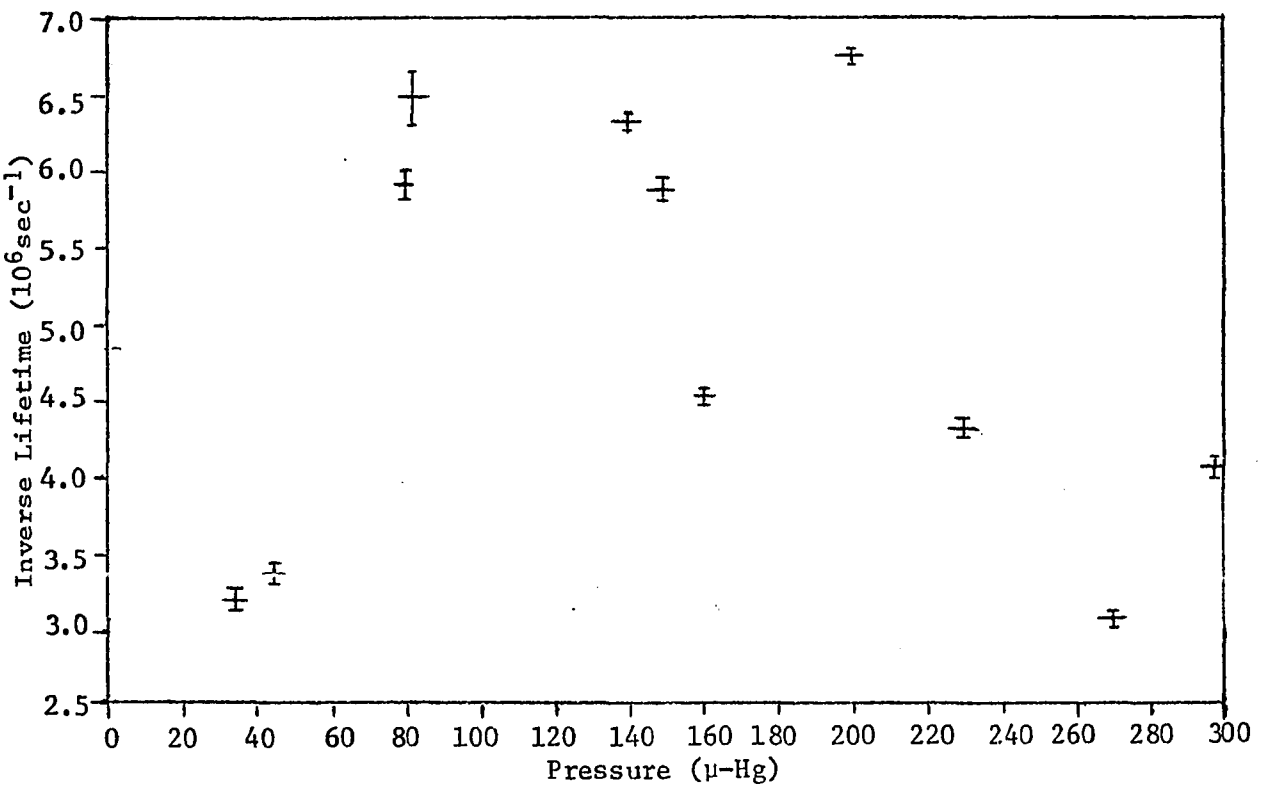

(c) He 7^3D plot of inverse lifetime vs. pressure.

Figure 18. Typical plots of inverse lifetime vs. pressure.

tables, 13±2 ns measured by Osherovich and Verolainen,[26] 15±2 ns measured by Pendleton and Hughes,[29] 14±3 ns measured by Kindlemann and Bennett,[31] 10±5 ns measured by Heron et al,[37] 17 ns by Bennett et al,[27] 14±1 ns measured by Allen et al,[30] 25±5 ns measured by Fowler et al,[33] and 13.4±0.6 measured by Chin-Bing and Head.[35] A recent measurement by Buchhaupt[40] using the Hanle technique yields a value of 22 ns. Buchhaupt also reports a depolarization cross-section of 7×10^{-14} cm^2 which compares to a quenching cross section observed here of 1.3×10^{-14} cm^2.

The lifetime of the 4^3D level is estimated to be about 28±10 ns on the basis of three measurements made at different pressures. By comparison, the transition probabilities of Wiesse[4] yield a lifetime of 32 ns.

For 5^3D and 6^3D only one measurement each was made. Both appeared as single exponentials and were measured at 140 μ-Hg pressure. The constant term assumed to be background noise was less than 1/20 of the coefficient of the exponential. The measured lifetimes were 132±1 ns and 156±1 ns respectively. For comparison the calculated[4] values are 60.2±0.6 ns and 107±11 ns respectively. Other values reported are 35±3 ns by Osherovich and Verolainen,[26] 53 ns by Bennett et al,[27] and 50±2 ns by Chin-Bing and Head[35] for 5^3D.

Eleven measurements of lifetime at various pressures for 7^3D indicate a free atom lifetime of 160±60 ns. Although all lifetimes appeared to be single exponentials and exhibited good statistics, the resultant pressure curve was widely scattered as shown in Fig. 18(c). The calculated[4] lifetime at this state is 145±15 ns.

Eight measurements of lifetime vs. pressure for 8^3D indicates a free atom lifetime for this state of 200±50. This results from assuming the data to be single component only. It appeared that the data fit to a single exponential within the statistical limits although one could force a fit of the data to two exponentials. The two exponential fit resulted in more widely scattered data points. For comparison the value obtainable from NBS[4] tables is 207±21 ns.

For 9^3D thirteen data points were badly scattered. Most of the points were fit to single exponentials and indicated a good fit within scatter of the intensity data obtained. Where two exponential fits were obtained, large uncertainties and bad scatter indicated questionable results. Since no definitive pressure trend was apparent a simple average of single exponential results ranging from 40 to 220 μ-Hg was made yielding a lifetime of 300±100 ns. The lifetime obtained from NBS[4] tables is 300±30 ns.

For 10^3D two of the three data sets were analyzed as double exponentials and the third at higher pressure was analyzed as a single exponential. Using the second exponentials of the two component exponentials a value of 340±60 ns is obtained. Coefficient of the second exponentials indicated they carried the bulk of the population. The value predicted from NBS tables is 380±40 ns.

Two measurements were made for 11^3D at 190 and 300 μ-Hg. Both exhibited two exponential characteristics. The fast components were 63±2 and 109±3 ns respectively whereas the slow components were 494±18 and 722±100 ns respectively. For comparison the NBS[4] table indicates a value of 490±50 ns.

Summary of Helium Measurements

The lifetimes determined to be most probable for each state measured in this effort are summarized in Table 6 along with the number of data samples (normally at different pressures in the range 10-200 μ-Hg) obtained and the calculated "quenching" cross sections.

The results given in Table 6 show poor precision which is most probably due to a thorough balancing of excited states, especially above n=5, through collisional transfers from excited state atom-neutral atom collisions.

Evidence of collisional transfer was observed by Lees and Skinner[41] and postulated to occur in the reaction

$$He(n^1P) + He(1^1S) \rightarrow He(1^1S) + He(n^3D) \ .$$

However this reaction violates the Wigner spin-conservation rule which is expected to hold at low quantum numbers where L-S coupling is strong. Additional experimental[42,43] evidence indicated that the process occurred much too slowly for the predicted lifetimes of the involved states, cascade processes were predictably important and the required cross-section for such a process to be compatable would be much too large for such a reaction. In order to resolve the difficulty St. John and Fowler[44] proposed the process

$$He(n^1P) + He(1^1S) \rightarrow He(nF) + He(1^1S)$$

which then decayed with a large probability to $He(3^3D)$. Theoretical support to this model was delivered by Lin and Fowler[45] when, considering the n^3F and n^1F states totally mixed, they investigated the electrostatic dipole interaction of a $He(n^1P)$ and $He(1^1S)$ collision.

TABLE 6. SUMMARY OF MOST PROBABLE LIFETIMES DETERMINED FROM THESE MEASUREMENTS

Upper Level	No. of Samples	Measured Lifetime (ns)	Quenching X-section (10^{-14} cm^2)	Upper Level	No. of Samples	Measured Lifetime (ns)	Quenching X-section (10^{-14} cm^2)
3^1S	6	56±2	0.71	2^3P	21	125±10	
5^1S	5	110±3	2.5	4^3P	2	125±20	
*6^1S	7	210±4	1.2	5^3P	4	200±100	
*7^1S	1	356	(0.7)	*6^3P	4	360±20	
*8^1S	4	520		*7^3P	5	550±150	
3^1D	20	31±2	0.92	*8^3P	3	400±100	
5^1D	2	56±10		*9^3P	2	560(?)	
6^1D	5	72±3	3.8	3^3D	6	19.4±0.5	3.25
7^1D	4	65±20	-0.63	4^3D	3	28±10	
8^1D	2	?		5^3D	1	132±1	
9^1D	1	?		6^3D	1	156±1	
3^3S	11	57±1	0.97	7^3D	11	145±15	-0.63
5^3S	2	140±20		8^3D	8	200±50	1.3
6^3S	5	75±20	1.0	9^3D	13	300±100	0.67
7^3S	4	?		10^3D	3	340±60	
*8^3S	4	400±170		11^3D	2	?	
9^3S		?					

The results of such an analysis leads to a collisional transfer selection rule of $\Delta L = \pm 2, 0$. Inclusion of higher ordered terms permits smaller contributions at $\Delta L = \pm 1$ and ± 3 which are associated with shorter range interactions and contribute only weakly to the collision cross-section. Recent calculations[46,47] have been made to ascertain the degree of mixing for singlet and triplet states of the same n,ℓ and predict very little mixing except for $\ell=3$ which become strongly mixed. More recent experiments[48-52] have supported this collisional reaction through the F states.

Although the result of this work is somewhat inconclusive because of an unexplicable scatter of the data it does show a definite coupling of the higher n states (n>6) with a faster state. A brief examination of the data (see Appendix C) indicates that for all n at n>6 a fast component is observed which is on the order of that observed at n^1P.

The analysis in Chapter II indicated that in order for a faster state to be observed as a normal decay it must reach the observed state through a collision process. From these observations it is apparent that the transfer process at higher levels is well distributed to all ℓ. The most probable cause of occasional inconsistency of the data is the limitations on resolution of exponential curves containing more than two components, especially when at least two of the component exponentials are within a factor of 2 or one component is too weak to separate but sufficient to perturb the observations of the stronger state.

As a check to ascertain the importance of the highly ionized

central region of the excitation chamber an axial field of 18 gauss was passed through it by means of a D.C. current through a concentric coil. This caused a visible breakup of the central bright region by causing the center bound electrons to rotate about the center, thus spreading out the heavily excited and ionized core. Results of this measurement are given in Appendix C, 3^1D, case identification 1/7/72/4, and shows no significant deviation from results of measurements without the field. It is felt that this measurement would exhibit a marked change if excited state interactions, Stark fields, or alignment effects had been present earlier.

The exceptions to the rule of a single decay component below n=6 are 3^1D and 3^3D which most likely are highly populated by F, G ... which all have a strong probability of decaying through these levels. A complete tabulation of results and selected operating conditions are given in Appendix C.

CHAPTER VI

LIFETIME AND QUENCHING RATES FOR THE H_2 CONTINUUM

Introduction

Utilizing the invertron developed by Holzberlein[23] and the delayed coincidence technique described by Johnson and Fowler[28] the previous measurements of Holzberlein[52] on the continuum in H_2 have been revised. The process of emission of the continuum is found to be more complex than previously envisioned. There are evidently two states in close resonance, and the apparent lifetime at pressures above 1 torr is not the true lifetime of the $^3\Sigma_g$ state. Results of the new experimental data yield a low pressure exchange cross section of $2.0\times10^{-14}cm^2$ between the states and a high pressure quenching cross section of $4.8\times10^{-16}cm^2$ for both states. Application of a magnetic field applied axially to the invertron yielded no change of lifetime for fields up to about 18 gauss (calculated) which was sufficient to disperse the highly visible axial concentration of excited molecules. Linear asymptotic extrapolation of the high pressure data to zero pressure yields a lifetime of 2.6±0.3 ns for the side state whereas linear extrapolation of the low pressure lifetimes indicates a true lifetime for the $v'=0\,^3\Sigma_g^+$ state of 26±2 ns at zero pressure. The new data were obtained by observing emitted light at 2750 Å and

2950 Å which should be due to transitions occurring between the stable $1s\sigma 2s\sigma\ {}^3\Sigma_g$ and the unstable $1s\sigma 2p\sigma\ {}^3\Sigma_u$ vibrational levels. The results were corrected for a small pressure dependent cascade component.

Experimental Observations

The new observations of lifetimes τ in molecular hydrogen were obtained at pressures .034 to .800 torr using a ½-meter Jarrell Ash monochromator and were combined with higher pressure data obtained earlier by Holzberlein[3] to form the plot of $1/\tau$ versus pressure shown in Fig. 19. The significance of the $1/\tau$ plot is that it reveals the dominant processes of a simple exponential state decay linearly according to the relation

$$\frac{1}{\tau} = A + \sigma N_o \bar{v} = \frac{1}{\tau_o} + \frac{\sigma \bar{v} p}{kT} \tag{32}$$

where $N_o \equiv$ population density of neutral molecules,

$\sigma \equiv$ quenching cross section,

$A \equiv$ transition probability out of the excited state,

$\bar{v} \equiv$ mean molecular speed.

The lifetimes at low pressure at the two wavelengths measured 2750 Å and 2950 Å were found to be in the proportion λ^{-3}, showing as is expected that the continuum, in different spectral localities, originates from different upper vibrational states. At 2950 Å the transition is predominantly from v'=0 of the ${}^3\Sigma_g^+$ state, while at 2750 Å it comes predominantly from v'=1. At high pressures there was no such distinction between wavelengths. Data at the lowest pressures have therefore been reduced, by application of the wavelength factor, to equivalent v'=0 values.

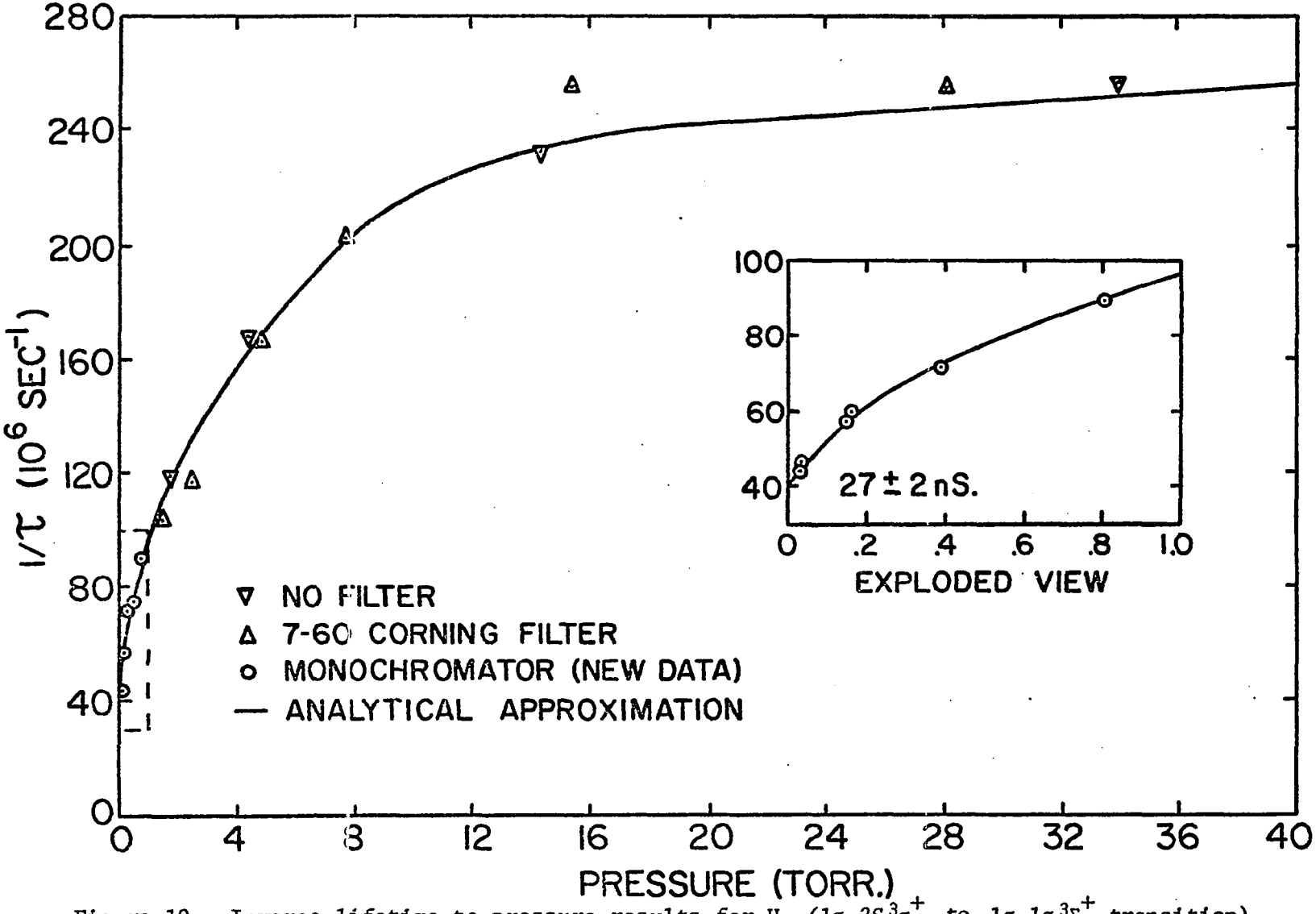

Figure 19. Inverse lifetime to pressure results for H_2 ($1\sigma_g 2s\, {}^3\sigma_g^+$ to $1\sigma_g 1\sigma_u\, {}^3\Sigma_u^+$ transition). Inset shows detail at origin.

The lifetimes plotted in Fig. 19 correspond to the shortest decay observed. In each case our least squares computer program enables us to resolve any complex decays into a sum of exponentials and to identify the two or three fastest decays with reasonable accuracy. In the case of the H_2 continuum only a very weak cascade component was present. Consequently the behavior of the $1/\tau$ plot is strikingly anomalous, having two linear regions, the high pressure data extrapolating to a faster lifetime at zero pressure than the low pressure data, a situation which cannot be explained by a cascade, even if there were a possibility that one had been overlooked.

Theoretical Discussion

The observations plotted in Fig. 19 are characteristic of close coupled systems. Let us consider the expected decay to be observed from two states a and b which decay at rates A_a and A_b from states having the same energy above the ground state so as to allow a collisional resonance, i.e.

$$\dot{N}_a = -\alpha_a N_a + \alpha_{ba} N_b + P_a \tag{33}$$

$$\dot{N}_b = -\alpha_b N_b + \alpha_{ab} N_a + P_b \tag{34}$$

where P_a and P_b are the state production rates in the active period, and

$$\alpha_a = A_a + \sigma_a \bar{v} N + \sigma_{ab} \bar{v} N$$

$$\alpha_b = A_b + \sigma_b \bar{v} N + \sigma_{ba} \bar{v} N$$

$$\alpha_{ab} = \sigma_{ab} \bar{v} N$$

The basic solutions are

$$N_a = Ce^{-\lambda t} \qquad N_b = De^{-\lambda t} \tag{35}$$

with

$$\lambda = \frac{(\alpha_b+\alpha_a) \pm \sqrt{\alpha^2-2\alpha_b\alpha_a+\alpha_a^2+4\alpha_{ab}\alpha_{ba}}}{2} \tag{36}$$

and the general solutions after cutoff, i.e., $P_a = P_b = 0$, are:

$$N_a = C_1e^{-\lambda_1 t} + C_2e^{-\lambda_2 t} \tag{37}$$

and

$$N_b = -\frac{\alpha'+\alpha_b}{\alpha_{ba}} C_1e^{-\lambda_1 t} + \frac{\alpha'-\alpha_b}{\alpha_{ba}} C_2e^{-\lambda_2 t} \tag{38}$$

where

$$\alpha' = \sqrt{\alpha_b^2-2\alpha_b\alpha_a+\alpha_a^2+4\alpha_{ab}\alpha_{ba}} \tag{39}$$

λ_1 and λ_2 are the positively and negatively signed radicals respectively.

Under the experimental conditions used, the on-period will have resulted in exciting the states involved to saturation. Therefore the initial populations at cutoff will be

$$N_{ao} = \frac{\alpha_b P_a+\alpha_{ba} P_b}{\alpha_a\alpha_b-\alpha_{ab}\alpha_{ba}} \tag{40}$$

and

$$N_{bo} = \frac{\alpha_a P_b+\alpha_{ab} P_a}{\alpha_a\alpha_b-\alpha_{ab}\alpha_{ba}} \quad . \tag{41}$$

This leads to an evaluation of the constants C_1 and C_2 as

$$C_1 = \frac{\alpha'-\alpha_b}{2\alpha'} N_{ao} - \frac{\alpha_{ba}}{2\alpha'} N_{bo} \tag{42}$$

$$C_2 = \frac{\alpha'+\alpha_b}{2\alpha'} N_{ao} + \frac{\alpha_{ba}}{2\alpha'} N_{bo} \quad . \tag{43}$$

We are interested only in the final form of Eq. (37) since it represents the state observed in radiation whereas the state represented by Eq. (38) is postulated to be a radiation of another frequency. Eq. (37) becomes

$$N_a = \frac{1}{2\alpha'} \frac{(\alpha_b P_a + \alpha_{ba}\alpha_b P_b + \alpha_a \alpha_{ba} P_b + \alpha_{ab}\alpha_{ba} P_a)}{(\alpha_a\alpha_b - \alpha_{ab}\alpha_{ba})} (e^{-\lambda_2 t} - e^{-\lambda_1 t})$$

$$+ \frac{1}{2} \frac{(\alpha_b P_a + \alpha_{ba} P_b)}{(\alpha_a\alpha_b - \alpha_{ab}\alpha_{ba})} (e^{-\lambda_1 t} + e^{-\lambda_2 t}) \qquad (44)$$

Now $\lambda_1 >> \lambda_2$, and the sum of the coefficients of the exponential in which it occurs is negative also, so that it is an unobservably rapid buildup adjustment of the states involved. The solid line in Fig. 19 is a plot of the decay constant λ_2 of Eq. (44) where from Eq. (36)

$$\lambda_2 = \frac{(A_a + A_b) + (\sigma_a + \sigma_b + \sigma_{ab} + \sigma_{ba})\bar{v}N - \sqrt{|A_a - A_b + (\sigma_a - \sigma_b + \sigma_{ab} - \sigma_{ba})\bar{v}N|^2 + 4\sigma_{ab}\sigma_{ba}\bar{v}^2N^2}}{2} \qquad (45)$$

Values chosen for the parameters to obtain the curve are

$$A_a = 39\times10^6 \text{sec}^{-1} ,$$

$$A_b = 384\times10^6 \text{sec}^{-1} ,$$

$$\sigma_a = \sigma_b = 4.8\times10^{-16} \text{cm}^2 ,$$

$$\sigma_{ab} = 2.0\times10^{-14} \text{cm}^2 ,$$

$$\sigma_{ba} = 2.4\times10^{-14} \text{cm}^2 ,$$

$$\bar{v} = 3.8\times10^5 \text{ cm/sec } (T = 1200^\circ\text{K}) ,$$

$$N = 8.05\times10^{15} \text{ P (torr)} .$$

It is not possible to determine from the decay constant whether the auxiliary state is the $1\sigma_g 1\sigma_u {}^1\Sigma_u$, the $1\sigma_g 2s {}^1\Sigma_g^+$, the $1\sigma_g 2p\pi {}^3\Pi_u$, the $1\sigma_g 2p\pi {}^1\Pi_u$ or all of them put together.[53] Presumably there is enough rotational

overlap for a close resonance with any of these levels. Certainly the potential curves all lie so close together on the small molecular separation side that easy transfer is to be expected. Because of the short lifetime measured for this side state, we would be inclined to identify the $1\sigma_g 2p\pi\,^1\Pi_u$, which radiates as an allowed transition to the ground state as the one whose lifetime was being observed at high pressure.

We can say with certainty that there is a substantial amount of electron excitation directly into the $^3\Sigma_g$ state, because the intensity at low pressures is linearly proportional to the pressure, but it is not possible for us to determine whether there is direct excitation to the side state. We may take the further hint that the side state has a large "allowed" excitation cross section from the feeling of Richardson[54] that the continuum is enhanced at high pressure, and speculate that the 2.6 ns lifetime is an unresolved mixture of two closely similar lifetimes for the $^1\Sigma_u$ and $^1\Pi_u$ states.

The quenching cross section of $6.0\times10^{-16}\,cm^2$ obtained by Center[55] from data taken at pressures above one torr compares favorably with the results reported here, but we would not debate the point in favor of our value. The linear relationship of p/I vs. p observed by Center[55] is also compatible with the system described here. This can be shown by setting $\dot{N}_a = \dot{N}_b = 0$ in Eqs. (33) and (34), solving for N_a and using our parameters plotting p/N_aA_a vs. p.

An additional measurement by Imhoff and Read[56] of 11.0 ns fails to agree with either result reported here, however no pressure dependence is indicated in their report. Such information might show

reason for the discrepancy. Probably they have made an extrapolation from some limited intermediate segment of the true curve.

CHAPTER VII

CONCLUDING REMARKS

It is apparent from the measurements of lifetimes of the helium states reported here that the process of excitation transfer is not restricted to the reaction

$$He(1^1S) + He(n^1P) \rightarrow He(1^1S) + He(nF)$$

but includes transfers to $n^{1,3}D$, n^3P, and $n^{1,3}S$, when n is sufficiently large.

The observed quenching effects at the 3 level are much greater than that observed for Hornbeck-Molnar[57,58] processes of molecular ion association. It is most probable that this process is masked by the effects of blockading or resonance, trapping of the 4^1P level which is considered to be the primary feed to these levels via resonance collisional transfer followed by a decay. Such a mechanism would appear in the $3^{1,3}D$ decay as a fast exponential, would be highly pressure sensitive and would fall sufficiently close in lifetime to cause difficulty in separating it from the D level lifetimes.

Considerable improvement upon the data may be obtained by accumulating data using a double pulse technique with the second pulse turned low so as to excite the desired state at its threshold thus

minimizing populations to higher state. Such an approach was used for several data points in this work but occasionally the voltage was set too high because of impatience developed at accumulating data at a low count rate. In addition it is necessary to obtain data at lower pressures, say 1 to 50 μ-Hg, which for higher levels poses a problem of excitation. Apparently the bulk of their population arises from transfer which is very pressure dependent and essentially disappears at low pressures. Direct electron excitation must be enhanced. This can be accomplished by operating at higher temperatures, which decreases cathode lifetime and rapidly coats window surfaces with carbon, or developing the triode structure so as to obtain electrons from the cathode at high voltage then reducing the electron energy for selective excitation.

The measurements made on molecular hydrogen were consistent and fit the close coupled system theory developed very well.

During the course of this experiment the following improvements have been developed or conceived. Spectra signal to noise has been enhanced by operating with long pulses at high pulse repetition frequency. Additional improvement is obtained by operating the TPHC on the 50 ns scale, using the ORTEC 271 PMT amplifier output as a TPHC start signal, delaying this same pulse through 20 ns (or less) to the TPHC stop gate and using the excitation pulse monitor to operate the TPHC coincidence gate using a cable delay selected to maximize the count rate. The normal procedure for spectra acquisition then calls for using the TPHC output to pulse the multichannel analyzer operating in the multiscaling mode at its slowest scan rate as the

monochromator is swept through the spectrum.

A method of accurately determining errors due to double photon events has been considered. This technique involves using a second TPHC in parallel to the first TPHC using a logic circuit between them so as to ignore the first stop pulse (detected photon) but pass on the second stop pulse to the second TPHC. The logic circuit must be cleared by the start pulse which is common to both TPHC's. The output of the second TPHC can be monitored at a ratemeter to determine the validity of assuming no two photon events or delayed and entered into the multichannel analyzer. It has the obvious limitation of not being able to resolve two photons if the second one occurs within the switching time of the logic circuit used. In principle one could stack more TPHC's and logic circuits to improve statistics, however, the aforementioned limitation on resolution would limit this procedure. The limitation is compounded by the high probability of seeing a second photon early in a decay exponential rather than towards the tail of the exponential.

Another technique that offers possibility of improving data usefulness is one of accumulating first on a relatively long time scale ($\sim$1000 ns) so as to determine well the constant level and long exponential then accumulate on a short time scale ($\sim$200 ns) and use the analyzed results of the long time scale to eliminate some of the degrees of freedom for its analysis. Conceivably one could use two TPHC's and two analyzers to acquire both sets of data simultaneously.

BIBLIOGRAPHY

1. I. D. Latimer, J. I. Mills and R. A. Day, J. Quant. Spectrosc. Radiat. Transfer 10, 692 (1970).

2. R. G. Fowler, "Radiation from Low Pressure Discharges," Handbuch der Physik, Gas Discharges II, XXII (1956).

3. L. Marton (editor), Advances in Electronics and Electron Physics (New York: Academic Press, Inc., 1970), p. 115.

4. W. L. Wiese, M. W. Smith and B. M. Glennon, Atomic Transition Probabilities, Vol. I, NSRDS-NBS4, 1966.

5. W. L. Wiese, M. W. Smith and B. M. Miles, Atomic Transition Probabilities, Vol. 2, NSRDS-NBS22, 1969.

6. B. M. Miles and W. L. Wiese, Bibliography on Atomic Transition Probabilities, NBS Special Publication 320, 1970.

7. T. M. Holzberlein, Ph.D. Dissertation, University of Oklahoma (1963).

8. A. W. Johnson, Ph.D. Dissertation, University of Oklahoma (1968).

9. G. E. Copeland, Ph.D. Dissertation, University of Oklahoma (1970).

10. A. R. Schaefer, Ph.D. Dissertation, University of Oklahoma (1970).

11. R. A. Mickish, Master's Thesis, University of Oklahoma (1970).

12. P. R. Skwerski, Jr., Master's Thesis, University of Oklahoma (1969).

13. W. Kaplan, Advanced Calculus (Reading: Addison-Wesley Publishing Company, Inc., 1952).

14. A. von Engel, Ionized Gases (Oxford University Press, 1965).

15. R. K. L. L. van den Eynde, Th. Niemeyer and G. Wiebes, FOM-No. 31.249, Amalf-No. 140, July 1970, FOM-Instituut voor Atoom-- en Molecuulfysica, Amsterdam.

16. R. M. St. John and T. W. Nee, J. Opt. Soc. Am. 55, 426 (1965).

17. J. D. Jobe and R. M. St. John, Phys. Rev. A5, 295 (1972).

18. Mrs. Jan Norris, private communication, University of California, Los Alamos Scientific Laboratory, Los Alamos, New Mexico.

19. H. Margenau and G. M. Murphy, The Mathematics of Physics and Chemistry, 2nd ed. (Princeton, N.J.: D. Van Nostrand Co., Inc., 1956), pp. 504-519.

20. W. E. Deming, Statistical Adjustment of Data (New York: Dover Publications, Inc., 1964).

21. P. R. Bevington, Data Reduction and Error Analysis for the Physical Sciences (New York: McGraw-Hill Book Co., 1969).

22. D. W. Marquardt, J. Soc. Indust. Appl. Math. 11, 2 (1963).

23. T. M. Holzberlein, Rev. Sci. Instr. 35, 1041 (1964).

24. G. Russell and T. M. Holzberlein, Jour. App. Phys. 40, 3071 (1969).

25. RCA Tunnel Diode Manual, RCA Semiconductor and Materials Division, Somerville, New Jersey (1963).

26. A. L. Osherovich and Ya. F. Verolainen, Optics and Spectroscopy (U.S.S.R.) 24, 81 (1968).

27. W. R. Bennett, Jr., P. J. Kindlemann and G. N. Mercer, Appl. Opt. Suppl. 2 Chem. Lasers, 34 (1965).

28. A. Wayne Johnson and R. G. Fowler, J. Chem. Phys. 53, 65 (1970).

29. W. R. Pendleton, Jr., and R. H. Hughes, Phys. Rev. 138, A683 (1965).

30. L. Allen, D. G. Jones and D. G. Schofield, J. Opt. Soc. Amer. 59, 842 (1969).

31. P. J. Kindlemann and W. R. Bennett, Bull. Am. Phys. Soc. 8, 87 (1963).

32. A. H. Gabriel and D. W. O. Heddle, Proc. Roy. Soc. (London) 258, 24 (1960).

33. R. G. Fowler, T. M. Holzberlein, C. H. Jacobson and S. J. B. Corrigan, Proc. Phys. Soc. (London) 84, 539 (1964).

34. W. Drtil, Z. Naturforsch. 24a, 350 (1969).

35. S. A. Chin-Bing and C. E. Head, Bull. Am. Phys. Soc. 15, 1375 (1970).

36. L. L. Nichols and W. E. Wilson, Appl. Optics 7, 167 (1968).

37. S. Heron, R. W. P. McWhirter and E. H. Rhoderick, Proc. Roy. Soc. (London) Ser. A, 234 (1956).

38. R. G. Bennett and F. W. Dalby, J. Chem. Phys. 31, 434 (1959).

39. A. L. Osherovich and I. G. Savich, Opt. Spektrosk. 4, 715 (1958).

40. K. Buchhaupt, Z. Naturforsch. 24a, 1058 (1969).

41. J. H. Lees and H. W. B. Skinner, Proc. Roy. Sco. (London) A137, 186 (1932).

42. S. Heron, R. W. P. McWhirter and E. H. Rhoderick, Proc. Roy. Soc. (London) A234, 565 (1956).

43. A. H. Gabriel and D. W. O. Heddle, Proc. Roy. Soc. (London) A258, 124 (1960).

44. R. M. St. John and R. G. Fowler, Phys. Rev. 122, 1813 (1961).

45. C. C. Lin and R. G. Fowler, Ann. Phys. (New York) 15, 461 (1961).

46. R. M. Parish and R. W. Mires, Phys. Rev. A4, 6, 2145 (1971).

47. R. K. L. L. van den Eynde, Th. Niemeyer and G. Wieves, FOM-No. 31.249, Amolf-No. 140, juli 1971, FOM-Instituut voor Atoom-- en Molocuulfysica, Kruislaan 407 Amsterdam.

48. C. C. Lin and R. M. St. John, Phys. Rev. 128, 1749 (1962).

49. W. R. Pendleton, Jr., and R. H. Hughes, Phys. Rev. 138, A683 (1965).

50. R. L. Abrams and G. J. Wolga, Phys. Rev. Letters 19, 1411 (1962).

51. J. D. Jobe and R. M. St. John, J. Opt. Soc. Am. 57, 1449 (1967).

52. R. G. Fowler and T. M. Holzberlein, J. Chem. Phys. 45, 1123 (1966).

53. A. J. Merer and R. S. Mulliken, Laboratory of Molecular Structure and Spectra, Department of Physics, University of Chicago, Tech. Report, 1968, P200.

54. O. W. Richardson, Molecular Hydrogen and its Spectrum (New Haven: Yale University Press, 1934), p. 293.

55. R. E. Center, private communication.

56. R. E. Imhof and F. H. Read, "Lifetime Measurements by an Electron Photon Coincidence Method," Second International Conference on Beam-Foil Spectroscopy (Lysekil, Sweden, June 1970).

57. F. H. Wellenstein and W. W. Robertson, J. Chem. Phys. 56, 1077 (1972).

58. M. P. Teter, F. E. Niles and W. W. Robertson, J. Chem. Phys. 44, 3018 (1966).

APPENDIX A

LISTING OF COMPUTER PROGRAMS AND SUBROUTINES

FPLOT 20:08 THU. FEB 05,1970

```
      DIMENSION Y(512),A(5),YP(512)
      DIMENSION CHAN(10),TIM(10)
      REAL INCR,L1,L2
      DATA A/"X","+",".","  ","*"/
C DATA INPUT
      CALL INPAK(N,NTC,CHAN,TIM,TIME,Y)
      PRINT1234,
 1234 FORMAT(1H ,"ENTER PLOT INCREMENT")
    1 INPUT ,K
      IF (K)2,2,3
    2 PRINT999
      CALL EXIT
C HEADING
    3 CONTINUE
C Y VALUES TO BE PLOTTED
 9201 FORMAT(1H ,2A6,3X,"DATE-",A2,A3,A4,3X,"RUN #",I2)
C SEARCH FOR MAXIMUM AND MINIMUM VALUES
      B=Y(1)
      S=10000.
      DO 20 I=2,N
      IF (Y(I)-B)15,15,11
   11 B=Y(I)
      GO TO 20
   15 IF (Y(I)-S)16,20,20
   16 IF(Y(I).EQ.0.0)GO TO20
      S=Y(I)
   20 CONTINUE
C CALCULATION OF SCALING FACTOR AND RANGE
      PRINT 910,S,B
      INPUT,S,B
      PRINT 201,S,B
      B=ALOG(B)
      S =ALOG(S)
      SC=(B-S)/63.0
C SET UP BORDER AND PRINT SCALE
      PRINT903
      PRINT 902,(A(5),I=1,65)
C PLOTTING OF DATA
      DO 30 I=1,N,K
      I1=I-1
      NY=1
      IF(Y(I)-S.LE.0.0)GO TO 30
      NY=(ALOG(Y(I))-S)/SC+1
      DO 21 J=1,NY
   21 YP(J)=A(4)
```

```
 FPLOT    20:08   THU.   FEB 05,1970

      YP(NY)=A(2)
   30 PRINT 293,I1,(YP(J),J=1,NY)
C FINAL BORDER
      PRINT 902,(A(5),I=1,65)
      PRINT 202,SC
      GO TO 1
  902 FORMAT(1H ,3X,65A1)
  201 FORMAT(1H1,F8.0,52X,F8.0)
  202 FORMAT(1HO,"SCALE=",F8.5,"LN(COUNTS)/PRINT CHANNEL")
  293 FORMAT(I4,"*",64A1)
  903 FORMAT(1H ,3X,"*",63X,"*")
  910 FORMAT("ENTER SCALE LIMITS,DEFAULT VALUES ARE ",I6,I8)
  999 FORMAT(1HO,"END OF JOB")
      END


 INPAK    20:08   THU.   FEB 05,1970

      SUBROUTINE INPAK(N1,NTC,CHAN,TIM,TIME,Y)
      DIMENSION CHAN(10),TIM(10),Y(256)
     1,DATE(3)
      INTEGER CHAN
      REAL L1,L2
      CALL DATIME(TIMED,TIMEB,DATE)
      CALL OPENF(1,"INPUT")
      READ(1,9101)L1,L2,DA,XMO,YR,RN,SA,VL,P
      READ(1,9102)N1,NTC,(CHAN(I),I=1,NTC)
      READ(1,9103)(TIM(I),I=1,NTC)
 9101 FORMAT(2A6,A2,A3,A4,I2,A6,F5.0,F5.1)
 9102 FORMAT(I3,I1,8I3)
 9103 FORMAT(8F7.2)
      N=N1
      READ(1,7000)TIME,(Y(I),I=1,N)
 4000 FORMAT(15F4.0)
 5000 FORMAT(14F5.0)
 6000 FORMAT(10F7.0)
 7000 FORMAT(I6,9I7)
      CALL CLOSEF(1,"INPUT")
      PRINT9201,L1,L2,DA,XMO,YR,RN
      PRINT9202,SA,VL,P,TIMED,DATE
 9201 FORMAT(1HO,/////,2A6,3X,"DATE-",A2,A3,A4,3X,"RUN #",I2)
 9202 FORMAT(1H ,"SAMPLE-",A6,3X,"WAVELENGTH=",F5.0," A",
     13X,"PRESSURE=",F5.1," MICRONS"//" CALCULATED AT",
     21X,A6,1X,3A6/)
      RETURN
      END
```

```
RICH    20:08  THU.  FEB 05,1970

      COMMON N,K,KK,NFIRST,N1DEL,IAM,IN1,NN2,NF2,N1A,R2DEL,BM
     1,IPLU,AC,AFCTR,KK2,CHKZ,KK2KK,IFSS4,INTEG,Y(300),X(300,1)
      COMMON U(300),CHAN(10),B(10),PG(10),TIM(10),V(300)
      COMMON DY(300),ICH(5),BLT(10),XBM(10,14)
      REAL INCR
      INTEGER CHAN
  531 FORMAT("LIFETIMES (NS)   ",5F12.5)
  535 FORMAT("COEFFICIENTS     ",5F12.5)
  540 FORMAT(10X,"THE UNWEIGHTED SIGMA IS ",1PE12.5)
      CLBRTR=0.0
      CALL INPAK(N1,NTC,CHAN,TIM,TIME,DY)
      PRINT,"PRINT REGRES. RESULTS? ,TABULATE Y? (0-NO  1-YES)"
      SWTCH=0;K=0
      INPUT,SWTCH,K
      IF(K.EQ.0)GO TO 1
      PRINT 11,(DY(I),I=1,N1)
   11 FORMAT(1X,10F7.0)
    1 PRINT,"ENTER NO. OF PARAMETERS,FIRST POINT,LAST POINT,"
      PRINT," REP RATE,BREAK POINT,CONST(IF KNOWN)"
      K=5;IN1=1;NN2=255;REPR=10000.;N1A=1
      DO 38 I=1,10
   38 B(I)=0.
      INPUT,K,IN1,NN2,REPR,N1A,B(K)
      DO 6 I=1,NTC
      U(I)=CHAN(I)
    6 V(I)=TIM(I)
      IF (TIM(1)) 350,355,360
  350 CLBRTR=-TIM(1)
      RMSER=TIM(2)
      GO TO 370
  355 IF(CLBRTR) 1,356,370
  356 CLBRTR=1.0
      RMSER=0.0
      GO TO 370
  360 CONTINUE
  425 FORMAT(1H ,"COUNT RATE=",F5.1,"%")
      SA0=2.0
      CALL RGRES(V,U,A0,A1,1,NTC,SA1,SA0)
      PRINT 450,A0,SA0
  450 FORMAT("TIME AXIS INTERCEPT = ",F10.5," NS.,  STD DEV = ",
     1F10.5," NS")
      CLBRTR=A1
      RMSER=SA1
  370 CONTINUE
      SFRR=0.0
      DO 415 I=1,N1
  415 SFRR=SFRR+DY(I)
      SFRR=((SFRR/TIME)/REPR)*100.
      PRINT 425,SFRR
```

RICH 20:08 THU. FEB 05,1970

```
      YQ=0.
      N=NN2-IN1+1
      DO 5 I=1,N
      U(I)=I-1
      X(I,1)=I
      IN1M1=I+IN1-1
      YQ=AMAX1(YQ,DY(IN1M1))
    5 Y(I)=DY(IN1M1)
      KK=(K-1)/2
      BM=0
      AC=0
    3 AFCTR=1.0
      NFIRST=1
      SCALE=63./ALOG(1000.)
      CHKZ=0.0
      N2DEL=50
      INCR=.1
      INTEG=0
      IAM=1
      KK1=KK
      I=N
    9 N2SAV=I
      N1=N2SAV
   10 N2=N1
      R2DEL=R2
      N1=N1-N2DEL
      NF2=N2
      IF(N1-N1A)14,14,15
   14 AFCTR=10.
      R2DEL=R2
      NF2=N1A
      N1=N1A
      N1A=1
      IAM=3
   15 DO 50 I=N1,N2
      KK2=KK1
      V(I)=Y(I)-B(K)
   30 IF (KK2-KK)35,45,45
   35 KK2=KK2+1
      KK2KK=KK2+KK
      V(I)=V(I)-B(KK2KK)*EXP(-U(I)/B(KK2))
      GO TO 30
   45 IF(V(I)-CHKZ)46,46,50
   46 CONTINUE
      I=I-1
      IF(N2-N1A-5)150,150,9
   50 V(I)=ALOG(V(I))
      BMSAV=BM
      ACSAV=AC
   55 CALL RGRES(V,U,AC,BM,N1,N2SAV,R2,SWTCH)
```

```
RICH     20:08   THU.   FEB 05,1970

      GO TO (60,70,80,100),IAM
   60 R2Z1=R2
      IAM=IAM+1
      N2DEL=20
      GO TO 10
   70 IAM=IAM+1
      N2=N1
      IF(KK1.EQ.1)GO TO 14
      N2=N2+20
      GO TO 10
   80 R3DEL=R2Z1-R2
   84 IF(R2-AFCTR*R2DEL)85,10,10
   85 IF(KK1-KK)140,86,86
   86 IAM=IAM+1
      AFCTR=1.
      IF(N1-N1A)88,88,87
   87 N1=NF2
   88 N2=N2SAV
   90 R2Z1=R2
      BKSAV=B(K)
   96 B(K)=B(K)+INCR*EXP(AC+BM*U(N2))
      GO TO 15
  100 IF(R2-R2Z1)101,101,104
  101 GO TO (102,102,105),NFIRST
  102 NFIRST=NFIRST+1
      INCR=INCR/10.
      B(K)=BKSAV
      BM=BMSAV
      AC=ACSAV
      GO TO 96
  104 NFIRST=3
      GO TO 90
  105 INCR=-INCR/10
      BM=BMSAV
      AC=ACSAV
      INTEG=INTEG+1
      IF(INTEG-4.0)96,96,120
  120 B(K)=BKSAV
      R2DEL=R2Z1
      CHKZ=YQ/1000.*EXP(20./SCALE)
  140 IF(N1-N1A)141,141,142
  141 BMSAV=BM
      ACSAV=AC
  142 CONTINUE
      AFCTR=1.
      B(KK1)=-1/BMSAV
      KK1KK=KK1+KK
      B(KK1KK)=EXP(ACSAV)
      IAM=1
      KK1=KK1-1
```

```
RICH    20:08  THU.  FEB 05,1970

      PRINT 7777,N1,N2SAV,R2DEL
7777  FORMAT(" EXP FIT FROM",I4," TO",I4,"LINEARITY(R2) IS"
     1,1PE15.9)
      IF(N1-1)145,150,145
 145  CONTINUE
      N2SAV=N1
      IF(KK1-0)150,150,10
 150  IF(KK1-0)155,166,155
 155  KK=KK-KK1
      K=2*KK+1
      DO 160 I=1,KK
      IPK=I+KK1
 160  B(I)=B(IPK)
      DO 165 I=1,KK
      IPLU=I+KK1*2+KK
      IPKK=I+KK
 165  B(IPKK)=B(IPLU)
      IPLU=K+KK1*2
      B(K)=B(IPLU)
 166  SIG=0.;SIGM=0.
      DO 210 I=1,N
      YT=B(K)
      DO 200 J=1,KK
      KJ=KK+J
 200  YT=YT+B(KJ)*EXP(-X(I,1)/B(J))
 210  SIG=SIG+Y(I)/YT;SIGM=SIGM+(Y(I)-YT)**2
      SIG=SIG/N;SIGM=SQRT(SIGM/N)
      IF(KK1.LT.0)GO TO 168
      KK1=-1
      DO 167 I=1,KK
      PG(2*I)=B(I);KK3=KK+I;B(KK3)=B(KK3)*SIG
      PG(2*I-1)=B(KK3)
 167  BLT(I)=CLBRTR*B(I)
      GO TO 166
 168  PRINT 540,SIGM
      PG(K)=B(K)
      PRINT 531,(BLT(I),I=1,KK)
      KK1=KK+1;IFSS4=0
      PRINT 535,(B(I),I=KK1,K)
      PRINT 1111,CLBRTR,RMSER
1111  FORMAT("CALIBRATION IS ",F8.5," NS/CHAN  WITH STD DEV OF",
     1F8.6,"  NS/CHAN")
      K=K+1
      PRINT,"PLOT?(0-NO,PLOT INCR-YES)"
      INPUT,IFSS4
      IF(IFSS4.EQ.0)GO TO 1
      CALL DSPAK
      GO TO 1
9000  CALL EXIT
      END
```

```
RGRES   20:08  THU.  FEB 05,1970

      SUBROUTINE RGRES (V,U,A,B,N1,N2,R2,SWTCH)
      DIMENSION U(512),V(512)
      REAL M1,M2
  120 FORMAT("ZERO   (STD ERROR OF ESTIMATE EXCEEDS STD DEV
     10F Y ")
      N=N2-N1+1
  100 FORMAT(1X,"SIMPLE LINEAR REGRESSION
     1 EQUATION: LOG(Y-F(X))=A+B*X",//1X,"INDX R*R VALUE    95%
     2CONF LIMITS BEGIN END DIFF")
  150 FORMAT (1H1)
  200 FORMAT(F9.5,4H  A=,3F12.8,I4,I6,I6/,9X,4
     1H  B=,3F12.8)
      IF(SWTCH.E0.2.)GO TO 11
      IF(A) 8,10,8
    8 IF (ICNT-25) 11,11,9
    9 PRINT 150
   10 ICNT=1
      IF(SWTCH.EQ.1)GO TO 101
  102 PRINT110,
  110 FORMAT(1H ,"ITERATIONS NOT DISPLAYED")
      GO TO 11
  101 PRINT 100,
   11 CONTINUE
      S1=0
      S2=0
      S3=0
      S4=0
      S5=0
      DO 20 I=N1,N2
      S1=S1+U(I)
      S2=S2+U(I)*U(I)
      S3=S3+V(I)
      S4=S4+V(I)*V(I)
   20 S5=S5+U(I)*V(I)
      M1=S1/N
      M2=S3/N
      D1=S2/N-M1*M1
      D2=S4/N-M2*M2
      D3=S5/N-M1*M2
      C1=N*D1
      R8=0
      B=D3/D1
      A=M2-B*M1
      D4=D2-B*D3
      D44=D4
      IF(D4-D2) 2070,2040,2040
```

```
RGRES   20:08  THU.  FEB 05,1970

2040 R8=1
     R2=0
     GO TO 2080
2070 R2=1-(D4/D2)
2080 CONTINUE
     IF(R8) 2110,2130,2110
2110 PRINT 120
     GO TO 2160
2130 D2M4=D2-D4
     D4SQR=SQRT(D4)
2160 D4=N*D4/(N-2)
     T=1.95996+2.37226/(N-2)+2.82250/(N-2)*(N-2)
     D5=SQRT(D4/C1)
     D6=SQRT(D4/N)
     B1=B-T*D5
     B2=B+T*D5
     A1=A-T*D6
     A2=A+T*D6
     IF(SWTCH.NE.1)GO TO 56
     PRINT 200,R2,A,A1,A2,N1,N2,N,B,B1,B2
  56 CONTINUE
     IF(SW TCH.NE.2.0)GO TO 57
     R2=D5
     SW TCH=D6
  57 CONTINUE
     RETURN
     END
```

```
 DSPAK    20:08   THU.   FEB 05,1970

      SUBROUTINE DSPAK
C PLOT ROUTINE
      COMMON N,IK,IW,M,IB,ITEST,IDUM,NDUM,IPR,IFG,IM,YT,TEST,
     1WVAR,SSQ,IDF,DET,ISW,IPLT,ISC,Y(300),X(1,300),W(300),IX(10),
     2PG(10),P(10),SP(10),YC(300),DY(300),BM(10,11),ALAB(10),INTT,
     3PART(10),NSETS
      EQUIVALENCE (IDUM,IN1),(NDUM,NN2)
      DIMENSION ICH(10),APLT(65)
      INTEGER APLT
      DATA IBCH,ISCH,ICH/" ","*","A","B","C","D","E","T","U","V"
     1,"W","X"/
      DATA IOCH/"0"/
  500 FORMAT (1X,I3,65A1)
  901 FORMAT(1H0)
  905 FORMAT (2X,F7.3,53X,F7.0)
      K=IK-1
      KK=IK/2-1
      YQ=Y(1)
      DO 5 I=1,N
    5 YQ=AMAX1(YQ,Y(I))
      SCALE=63./ALOG(1000.)
      CHKZ=EXP(1./SCALE)*YQ/1000.
      J=  -IPLT
      PRINT 901
      YQLN1=(YQ/1000.)
      PRINT 905,YQLN1,YQ
  170 IXPLT=0
      N1=65
  200 DO 210 I=1,65
  210 APLT(I)=ISCH
      APLT(32)=IOCH
      J=J+1
      GO TO 250
  215 J=J+IPLT
      IF(J-N) 216,216,170
  216 CONTINUE
      IXPLT=IN1+J-1
      DO 220 I=2,64
  220 APLT(I)=IBCH
      DO 240 I=1,KK
      DUM=Y(J)-P(K)
      DO 230 IJ=1,KK
      IF(IJ-I)225,230,225
  225 DUM=DUM-P(2*IJ-1)*EXP(-X(1,J)/P(2*IJ))
  230 CONTINUE
      IF(DUM-CHKZ)237,237,235
  235 NMBR =(ALOG(DUM)-ALOG(YQ/1000.))*SCALE+1.
      IF(NMBR-64)238,238,236
  236 NMBR=64
      GO TO 238
```

```
DSPAK    20:08  THU.  FEB 05,1970

  237 NMBR = 2
  238 APLT(NMBR) = ICH(I)
      IF (N1.LT.NMBR) N1=NMBR
  240 CONTINUE
      NMBR=(DUM-P(K-2)*EXP(-X(1,J)/P(2*KK)))/(Y(J)**.5)*2.+32.
      IF(NMBR-1       )247,247,245
  245 CONTINUE
      IF(NMBR-64)248,248,246
  246 NMBR=64
      GO TO 248
  247 NMBR = 2
  248 APLT(NMBR) = ICH(KK+1)
      IF(N1.LT.NMBR)N1=NMBR
  250 PRINT 500,IXPLT,(APLT(I),I=1,N1)
      N1=2
      IF (J-N)215,170,251
  251 CONTINUE
      RETURN
      END


LASL     20:08  THU.  FEB 05,1970

      $LIB,MINV,,,***
      $LIB,GMPRD,,,***
      $SAV
      $NDM
C MAIN PROGRAM FOR NONLINEAR LEAST SQ. EXP. FIT.  FROM LASL
      DIMENSION Z(1)
      COMMON N,IK,IW,M,IB,ITEST,IDUM,NDUM,IPR,IFG,IM,YT,TEST,
     1WVAR,SSQ,IDF,DET,ISW,IPLT,ISC,Y(300),X(1,300),W(300),IX(10),
     2PG(10),P(10),SP(10),YC(300),DY(300),BM(10,11),ALAB(10),INTT,
     3PART(10),NSETS,DUM(1)
     4,Z
      EQUIVALENCE (IDUM,IN1),(NDUM,NN2)
C CLEAR DUM, PART
    1 DUM(1)=0.
      DO 20 K=1,10
   20 PART(K)=0.0
C CALL INPUT ROUTINE
      IN1=0
      NN2=5
      CALL ISPAK
C CALL CALCULATION ROUTINE
      CALL QSPAK
C CALL OUTPUT ROUTINE
      CALL RSPAK
C CALL PLOT ROUTINE
      IPLT=0
      PRINT,"ENTER PLOT INCR IF PLOT IS DESIRED."
```

```
LASL     20:08  THU.  FEB 05,1970

      INPUT,IPLT
      IF(IPLT.GT.0)CALL DSPAK
      GOTO 1
      END


ISPAK    20:08  THU.  FEB 05,1970

      SUBROUTINE ISPAK
C INPUT ROUTINE
      DIMENSION Z(1)
      COMMON N,IK,IW,M,IB,ITEST,IDUM,NDUM,IPR,IFG,IM,YT,TEST,
     1WVAR,SSQ,IDF,DET,ISW,IPLT,ISC,Y(300),X(1,300),W(300),IX(10),
     2PG(10),P(10),SP(10),YC(300),DY(300),BM(10,11),ALAB(10),INTT,
     3PART(10),NSETS,DUM(1)
     4,Z
      EQUIVALENCE (IDUM,IN1),(NDUM,NN2)
      CALL INPAK(N,IB,IX,P,TIME,Y)
      PRINT,"ENTER NO. OF PARAMS,FIRST PT., LAST PT., WEIGHT POWER"
      PRINT,",IPR=0,1,2,OR 3 FOR INCR. OUTPUT,IM=2 HOLD CONST."
      IF(P(1)) 350,355,360
  350 CLBRTR=-P(1)
      GO TO 2
  355 CLBRTR=1.0
      GO TO 2
  360 DET=2.0
      DO 3 I=1,IB
      DY(I)=P(I)
    3 W(I)=IX(I)
      CALL RGRES(DY,W,TEST,CLBRTR,1,IB,AI,DET)
    2 IK=5;IN1=1;NN2=255;WEIT=0;IPR=0
      IM=1
      INPUT,IK,IN1,NN2,WEIT,IPR,IM
      IX(2)=IK
      NSETS=0;IB=0;ITEST=0;IK=IK+1
      ISW =0
  201 FORMAT(1X,11I3,8F3.0,3I3)
      IX(1)=IK;IFG=2;M=1;KK=IK-2;KI=IK-1
      PRINT,"ENTER TAU(SHORT,LONG),COEFF(SHORT,LONG),CONSTANT"
      INPUT,(PG(K),K=2,KK,2),(PG(J),J=1,KI,2)
      PG(IK)=0.0
      PG(IK-1)=PG(IK-1)+.5
      PRINT,"CALIBRATION IS",CLBRTR," NS/CHAN"
      DO 11 I=1,N
      AI=I-1
   11 X(1,I)=AI*CLBRTR
C SET UP WEIGHTS
      IF(WEIT.NE.0.0) GO TO 6
      DO 40 I=1,N
   40 W(I)=1.0
```

```
ISPAK    20:08   THU.   FEB 05,1970

      GOTO8
    6 W(1)=1.0
      YCONST=0.0
      DO 45 J=2,IK,2
   45 YCONST=YCONST+PG(J-1)*EXP(-X(1,1)/PG(J))
      DO50I=2,N
      W(I)=0.0
      DO 47 J=2,IK,2
   47 W(I)=W(I)+PG(J-1)*EXP(-X(1,I)/PG(J))
   50 W(I)=W(I)/YCONST
      IF(WEIT.EQ.1.0)GO TO 8
  405 FORMAT("WEIGHT RANGES FROM 1.0 TO ",F7.3," FOR CHAN ",I3)
    7 DO 60 I=2,N
   60 W(I)=W(I)**WEIT
    8 TEST=1.0E-08
      N=NN2-IN1+1
      PRINT 405,W(N),NN2
      DO 55 I=1,N
      IN1M1=I+IN1-1
   55 Y(I)=Y(IN1M1)
      RETURN
    1 CALL EXIT
      END


QSPAK    20:08   THU.   FEB 05,1970

      SUBROUTINE QSPAK
C CALCULATION ROUTINE
      DIMENSION AM(100),DP(10),PC(10),AN(10)
      DIMENSION Z(1),MA(10),MB(10)
      COMMONN,IK,IW,M,IB,ITEST,IDUM,NDUM,IPR,IFG,IM,YT,TEST,
     1WVAR,SSQ,IDF,DET,ISW,IPLT,ISC,Y(300),X(1,300),W(300),IX(10),
     2PG(10),P(10),SP(10),YC(300),DY(300),BM(110),ALAB(10),INTT,
     3PART(10),NSETS,DUM(1)
     4,Z
      REAL LBDA
      EQUIVALENCE (ITEST,LASTIT)
C INITIAL OUTPUT OPTION
      IF(IPR.EQ.0)GOTO1
      PRINT 400,TEST
  400 FORMAT(/8H TEST = ,1PE15.7/)
C INITIALIZATION FOR MAIN ITERATION LOOP
    1 KFREE=IK-IM
      KP=KFREE+1
      IDF=N-KFREE
      DF=IDF
      IT=0;IFG=1
      LBDA=.0001
      DO10K=1,IK
```

```
 QSPAK   20:08  THU.  FEB 05,1970

      DP(K)=0.0
      SP(K)=0.0
      PC(K)=PG(K)
   10 P(K)=PG(K)
      LASTIT=0
      M25C=0
      IF(KFREE.EQ.0)GOTO3
C MAIN ITERATION LOOP
    2 IT=IT+1
      H=1
      DO30K=1,KFREE
      DO20KK=1,KFREE
      JJ=K+(KK-1)*KFREE
      AM(JJ)=0.
   20 BM(JJ)=0.
      JJ=K+(KP-1)*KFREE
      BM(JJ)=0.
      JJ=K+K*KFREE
   30 BM(JJ)=0.
    3 VAR=0.0
      SSQ=0.0
C LOOP TO SET UP NORMAL EQUATIONS
      DO90I=1,N
C CALL YP ROUTINE, CALCULATE SUM OF SQUARES
      DO40J=1,M
   40 Z(J)=X(J,I)
      CALLYPS(I)
      YC(I)=YT
      DY(I)=Y(I)-YC(I)
      VAR=VAR+W(I)*DY(I)**2
      SSQ=SSQ+DY(I)**2
      IF(KFREE.EQ.0)GOTO90
C SET UP AN AS VECTOR OF PARTIAL DERIVATIVES
      K1=0
      DO60K=1,IK
      IF(IM.EQ.0)GOTO4
      DO50KK=1,IM
      IF(K.EQ.IX(KK))GOTO5
   50 CONTINUE
    4 K2=K-K1
      AN(K2)=PART(K)
      GOTO60
    5 K1=K1+1
   60 CONTINUE
C FORM A AND B MATRICES
      DO80K=1,KFREE
      DO70KK=1,KFREE
      JJ=K+(KK-1)*KFREE
      AM(JJ)=AM(JJ)+AN(K)*AN(KK)*W(I)
      IJ=JJ+KFREE
```

```
 OSPAK   20:08  THU.  FEB 05,1970

   70 BM(IJ)=AM(JJ)
   80 BM(K)=BM(K)+AN(K)*DY(I)*W(I)
   90 CONTINUE
      WVAR=VAR
      IF(KFREE.EQ.0)GO TO 23
      IF(LASTIT.EQ.1)LBDA=0
      CALL LAMBDA(1,PC,LBDA,DP,IT,AM)
      NM=2
C OPTIONAL PRINTOUT OF A AND B MATRICES ON LAST ITERATION
      IF(LASTIT.EQ.0)GOTO6
      IF(IPR.LT.3)GO TO6
      PRINT 500
  500 FORMAT(///,3X,1HK,19X,6HA(K,L),28X,4HB(K)//)
      DO110K=1,KFREE
      PRINT 600,BM(K)
  600 FORMAT(//1H+,1P1E67.5)
      JJ=(K-1)*KFREE+1
      IJ=K*KFREE
  110 PRINT 700,K,(AM(II),II=JJ,IJ)
  700 FORMAT(I5,1P4E12.4/(4X,4E12.4))
C SOLVE THE NORMAL EQUATIONS
    6 IF(KFREE.GT.1)GOTO7
      DET=AM(1)
      BM(2)=1.0/AM(1)
      GO TO 8
    7 CONTINUE
      CALL MINV(BM(KP),KFREE,DET,MA,MB)
      IF(DET.EQ.0.)LASTIT=1
      IF(DET.EQ.0.)PRINT,"SINGULAR STSTEM ITER NO  ",IT
      CALL GMPRD(BM(KP),BM,DP,KFREE,KFREE,1)
      DO 115 I=1,KFREE
      IJ=(I-1)*KFREE+I
      SP(I)=DP(I);DP(I)=DP(I)/SQRT(AM(IJ))
  115 PC(I)=P(I)+DP(I)
C WRITE THE VALUE OF THE DETERMINANT, A INVERSE, AND
C  NO. OF ITERATIONS
      CALL LAMBDA(NM,PC,LBDA,DP,IT,AM)
      IF(NM.EQ.2) GO TO 7
    8 IF(LASTIT.EQ.0)GOTO11
      PRINT 800,IT,DET
  800 FORMAT(I6," ITERATIONS, DET. OF PART. DERIV. MATRIX ="
     1,1PE14.6)
C CALCULATE NEW PARAMETER VALUES AND CHECK FOR SIGN CHANGES
C   IF NECESSARY
   11 K1=0
      DO140K=1,IK
      IF(IM.EQ.0)GOTO12
      DO130KK=1,IM
      IF(K.EQ.IX(KK))GOTO16
  130 CONTINUE
```

```
OSPAK   20:08  THU.  FEB 05,1970

   12 K2=K-K1
   13 PC(K)=P(K)+H*DP(K)
      IF(LASTIT.NE.0)GOTO140
      IF(IFG-1)14,140,15
   14 IF(IT.GT.5)GOTO140
   15 IF(P(K)*PC(K).GE.0)GOTO140
      H=H/2
      IF(H.GE.1.0E-10)GOTO11
      PRINT,"PROG. QUIT ITERATING DUE TO PARAMETER",K," CHANGED SIGN"
      H=0.
      LASTIT=1
      GO TO 8
   16 K1=K1+1
  140 CONTINUE
C OPTIONAL PRINTOUT FOR EACH ITERATION
      IF(LASTIT.NE.0)GOTO19
      IF(IPR.LT.1)GO TO 17
      PRINT 1300,IT,H,VAR
 1300 FORMAT(1HO,I3,1P2E17.7)
 1400 FORMAT (1P6E11.3)
      IF(IPR.LT.2)GO TO 17
      PRINT 1400,(PC(K),K=1,IK)
C TEST FOR CONVERGENCE
   17 KK=0
      DO160K=1,IK
      IF(P(K).EQ.0)GOTO18
      IF(ABS((PC(K)-P(K))/P(K))-TEST)160,160,19
   18 KK=KK+1
  160 CONTINUE
      IF(KK.EQ.IK)GOTO19
      M25C=1
C SET PARAMETER VALUES FOR THE NEXT ITERATION
   19 DO170K=1,IK
  170 P(K)=PC(K)
C AFTER LAST ITERATION GO BACK FOR FINAL CALCULATION OF YC,
C   DY,ETC.
      IF(LASTIT.EQ.0)GOTO21
      KFREE=0
      GOTO3
C TEST WHETHER 25 ITERATIONS HAVE BEEN TAKEN
   21 IF(M25C.EQ.1)GOTO22
      IF(IT.LT.25)GOTO2
C GO BACK FOR LAST ITERATION
   22 LASTIT=1
      GOTO2
C CALCULATE WEIGHTED VARIANCE, STANDARD DEV. OF THE PARAMS.
   23 WVAR=VAR/DF
      TEST=SQRT(SSQ/DF)
      K1=0
      DO190K=1,IK
```

```
QSPAK    20:08   THU.   FEB 05,1970

      IF(IM.EQ.0)GOTO24
      DO180KK=1,IM
      IF(K.EQ.IX(KK))GOTO25
  180 CONTINUE
   24 K2=K-K1
      K3=K2+K2*(IK-IM)
      K4=K3-IK+IM
      SP(K)=SQRT(BM(K3)*WVAR/AM(K4))
      GOTO190
   25 K1=K1+1
  190 CONTINUE
      RETURN
      END


RSPAK    20:08   THU.   FEB 05,1970

      SUBROUTINE RSPAK
C OUTPUT ROUTINE
      DIMENSION Z(1)
      COMMON N,IK,IW,M,IB,ITEST,IDUM,NDUM,IPR,IFG,IM,YT,TEST,
     1WVAR,SSQ,IDF,DET,ISW,IPLT,ISC,Y(300),X(1,300),W(300),IX(10),
     2PG(10),P(10),SP(10),YC(300),DY(300),BM(110),ALAB(10),INTT,
     3PART(10),NSETS,DUM(1)
      DIMENSION TS(40)
C PAGE 1 OF THE STANDARD OUTPUT
      I=-1
      CALL YPS(I)
      PRINT 200,WVAR,TEST,SSQ
  200 FORMAT(/26H THE WEIGHTED VARIANCE IS 1PE14.7,
     1/" THE UNWEIGHTED SIGMA IS ",1PE14.7,
     2/49HAND THE UNWEIGHTED SUM OF SQUARES OF THE DEVS IS 1PE14.7)
  300 FORMAT("      GUESS OF  FINAL VAL OF   S.D. OF
     1       EXACT LST SQRS EQNS"/" K  K-TH PARAM  K-TH
     2PARAM  K-TH PARAM      FITTED FCTN  INPUT DATA")
      PRINT 300
      KFREE=IK-IM
      DO 40 K=1,KFREE
    2 A=0.0
      B=0.0
      DO 30 I=1,N
      Z(1)=X(1,I)
      CALL YPS(I)
      A=A+W(I)*YC(I)*PART(K)
   30 B=B+W(I)*Y(I)*PART(K)
      PRINT 500,K,PG(K),P(K),SP(K),A,B
  500 FORMAT(I3,1P3E12.4,3X,1P2E12.4)
   40 CONTINUE
C           CAL AND RITE  CORR MATRIX
      IF(IPR.LT.1)GO TO 70
```

```
RSPAK    20:08   THU.   FEB 05,1970

      PRINT 700
  700 FORMAT(/////43H MATRIX OF CORRELATIONS BETWEEN FREE PARAMS,
     1)
      DO 60 K1=1,KFREE
      DO 50 K2=1,KFREE
      IJ=K2*KFREE+K1
      JJ=K1*KFREE+K1
      KJ=K2*KFREE+K2
   50 TS(K2)=BM(IJ)/SQRT(BM(JJ)*BM(KJ))
  851 FORMAT(I3,8F8.3/(F11.3,F8.3))
   56 PRINT 851,K1,(TS(K),K=1,KFREE)
   60 CONTINUE
   70 RETURN
      END


YPS      20:08   THU.   FEB 05,1970

      SUBROUTINE YPS(I)
C FUNCTION AND PARTIAL DERIVATIVE ROUTINE
      DIMENSION Z(1)
      COMMON N,IK,IW,M,IB,ITEST,IDUM,NDUM,IPR,IFG,IM,YT,TEST,
     1WVAR,SSQ,IDF,DET,ISW,IPLT,ISC,Y(300),X(1,300),W(300),IX(10),
     2PG(10),P(10),SP(10),YC(300),DY(300),BM(10,11),ALAB(10),INTT,
     3PART(10),NSETS,DUM(1)
     4,Z
      K=IK-1
      IF(I)1,3,3
  900 FORMAT(//8X,"SUM OF EXPONENTIALS: Y(I)=P(1)*EXP(-X(I)"
     1,"/P(2))+...+P(",I1,").")
    1 PRINT 900,K
      GOTO4
    3 YT=0.0
      DO 10 K=2,IK,2
      PART(K-1)=EXP(-Z(1)/P(K))
      PART(K)=P(K-1)*PART(K-1)
      YT=YT+PART(K)
   10 PART(K)=PART(K)*Z(1)/P(K)**2
    4 RETURN
      END
```

```
LAMBDA  20:08  THU.  FEB 05,1970

      SUBROUTINE LAMBDA (NM,PC,LBDA,DP,IT,AN)
      DIMENSION PC(10),AM(110),DP(10)
      REAL LBDA,NU
      DIMENSION AN(100)
      COMMONN,IK,IW,M,IB,ITEST,IDUM,NDUM,IPR,IFG,IM,YT,TEST,
     1WVAR,SSQ,IDF,DET,ISW,IPLT,ISC,Y(300),X(1,300),W(300),IX(10),
     2PG(10),P(10),SP(10),YC(300),DY(300),BM(110),ALAB(10),INTT,
     3PART(10),NSETS,DUM(1)
      KFREE=IK-IM;NU=10;NI=KFREE*(KFREE+1)
      H=1.0;NU=10.
      GO TO (10,100) NM
   10 DO 20 K=1,KFREE
      IJ=(K-1)*KFREE+K
      BM(K)=BM(K)/SQRT(AN(IJ))
      DO 20 KK=1,KFREE
      KJ=(KK-1)*KFREE+KK
      I=K*KFREE+KK
      BM(I)=BM(I)/SQRT(AN(IJ)*AN(KJ))
   20 AM(I)=BM(I)
      GO TO 500
  100 D=0.;GD=0.;G=0.
      DO 120 J=1,KFREE
      G=BM(J)**2+G;D=SP(J)**2+D
  120 GD=BM(J)*SP(J)+GD
      GD=GD/SQRT(D*G)
      IF(IPR.NE.0)PRINT,"  COS(GAMMA)= ",GD
  160 PHI=0.
      DO 200 J=1,N
      YT=0.
      IN=IK-1
      DO 150 K=1,IN,2
  150 YT=YT+PC(K)*EXP(-X(1,J)/PC(K+1))
  200 PHI=W(J)*(Y(J)-YT)**2+PHI
      IF(PHI.LE.WVAR)GO TO 600
      IF(GD.LT..707.AND.LBDA.GT.0.)GO TO 400
      H=H/2.0;K=0
      IF(IPR.NE.0)PRINT 920,H,PHI
      DO 220 I=1,KFREE
      DP(I)=H*DP(I);PC(I)=P(I)+DP(I);CHK=ABS(DP(I)/PC(I))
      IF(CHK.LT.TEST)K=K+1
  220 CONTINUE
      IF(KFREE-K)600,600,160
  400 LBDA=LBDA*NU
      IF(IPR.NE.0)PRINT 910,LBDA,IT,PHI
      IJ=KFREE+1
      DO 300 K=IJ,NI
  300 BM(K)=AM(K)
      GO TO 520
  500 IF(LBDA.GT..0001)LBDA=LBDA/NU
  520 IJ=KFREE+1
```

```
LAMBDA  20:08  THU.  FEB 05,1970

      DO 530 K=IJ,NI,IJ
  530 BM(K)=AM(K)+LBDA
      RETURN
  600 NM=1
      IF(IPR.NE.0)PRINT," PHI= ",PHI
      RETURN
  900 FORMAT(1P3E11.4)
  910 FORMAT("LAMBDA= ",1PE7.1,"  ITER NO. ",I2," PHI= ",
     11PE15.9)
  920 FORMAT(" H= ",1PE8.2," PHI= ",1PE15.9)
      END


JERK1   20:08  THU.  FEB 05,1970

      $NDM
      DIMENSION Y(512),ICHAN(1),TIM(1),A(10)
      REAL L1,L2
      PRINT,"READ ID TAPE"
      READ 101,L1,L2,DA,XMO,YR,RN,SA,V,P
      PRINT 200
      NTC=1;ICHAN(1)=1
      INPUT,N,TIM(1),AM
      IF(TIM(1).GT.0.)TIM(1)=-TIM(1)
      PRINT,"NUMBER OF EXPTL. PARAMS.,1 ST COEF. ,1 ST LIFETIME,"
      PRINT,"2 ND COEF., ... , CONSTANT"
      INPUT,IK,(A(I),I=1,IK)
      IK=IK+1
      A(IK)=0.0
      B=1.0
      ASUM=0.0
      DO 1 I=1,N
      Y(I)=0.
      DO 3 J=1,IK,2
    3 Y(I)=Y(I)+A(J)*EXP(TIM(1)*(I-1)/A(J+1))
      ANOISE=AM*(RNDM(B)-0.5)*SQRT(Y(I))
      ASUM=ASUM+ANOISE**2
    1 Y(I)=Y(I)+ANOISE
      PRINT,"SUM OF NOISE FOR DATA IS ",ASUM
      ASUM=SQRT(ASUM/(N-IK+1))
      PRINT,"SIGMA FOR DATA IS  ",ASUM
      TIME=2000.
      CALL OPENF(1,"INPUT")
      WRITE(1,101)L1,L2,DA,XMO,YR,RN,SA,V,P
      WRITE(1,102)N,NTC,(ICHAN(I),I=1,NTC)
      WRITE(1,103)(TIM(I),I=1,NTC)
      WRITE(1,104)TIME,(Y(I),I=1,N)
      CALL CLOSEF(1,"INPUT")
  101 FORMAT(2A6,A2,A3,A4,I2,A6,F5.0,F5.1)
  102 FORMAT(I3,I1,8I3)
```

```
JERK1    20:08  THU.  FEB 05,1970

 103 FORMAT(8F7.2)
 104 FORMAT(I6,9I7)
 200 FORMAT("ENTER NUMBER OF CHANNELS(N), CALIBRATION (NS/CHAN"
    1,"), MULTIPLIER FOR NOISE")
     END
```

APPENDIX B

EXAMPLES OF INPUT DATA FILE AND EXECUTIONS FOR FPLOT, RICH, LASL AND JERK1.

```
INPUT      22:13  ACC WED.  MAR 11,1970


R T THOMPSONSEP  1,68 3HELIUM3867.   6.5
2554 11 19 67103
  63.25  90.90 256.50 380.35
  3411   5019   4988   4930   4970   5124   4903   5049   5030   4866
  4961   4415   4202   4101   3861   3801   3691   3456   3277   3232
  2958   2889   2761   2677   2514   2385   2294   2279   2232   2128
  2030   1896   1832   1760   1707   1661   1556   1460   1453   1442
  1401   1433   1356   1302   1178   1175   1161   1088   1125   1094
  1074    986    953   1030    966    959    877    895    826    828
   848    816    817    769    788    755    735    740    725    714
   719    703    697    684    689    669    596    632    645    639
   590    570    596    605    610    568    586    594    544    557
   530    541    544    574    549    531    550    489    519    509
   534    495    491    507    516    495    479    491    507    508
   473    479    448    466    486    497    452    451    435    457
   400    500    403    443    438    448    435    442    427    400
   437    423    411    467    437    398    383    430    421    374
   425    394    428    433    415    428    362    409    395    411
   393    364    384    394    418    372    379    382    398    414
   404    406    377    365    374    367    385    416    352    361
   371    336    371    355    348    373    377    384    358    366
   357    359    355    362    375    385    371    313    380    334
   318    324    328    349    304    338    360    364    350    300
   318    354    321    355    366    358    339    376    307    336
   333    308    323    343    358    326    319    311    329    318
   324    338    291    308    315    340    331    298    318    305
   335    330    325    280    317    278    316    303    313    305
   294    263    302    307    315    303    311    305    283    289
   275    278    306    273    286    411


RAN:    01.3 SECS
```

```
FPLOT        21:04    ACC WED.  MAR 11,1970


R T THOMPSON    DATE-SEP  1,68    RUN # 3
 SAMPLE-HELIUM    WAVELENGTH=3867. A    PRESSURE=   6.5 MICRONS

 CALCULATED AT 21:04  WED.  MAR 11,1970

 ENTER PLOT INCREMENT
? 3

ENTER SCALE LIMITS,DEFAULT VALUES ARE     263     5124
?
```

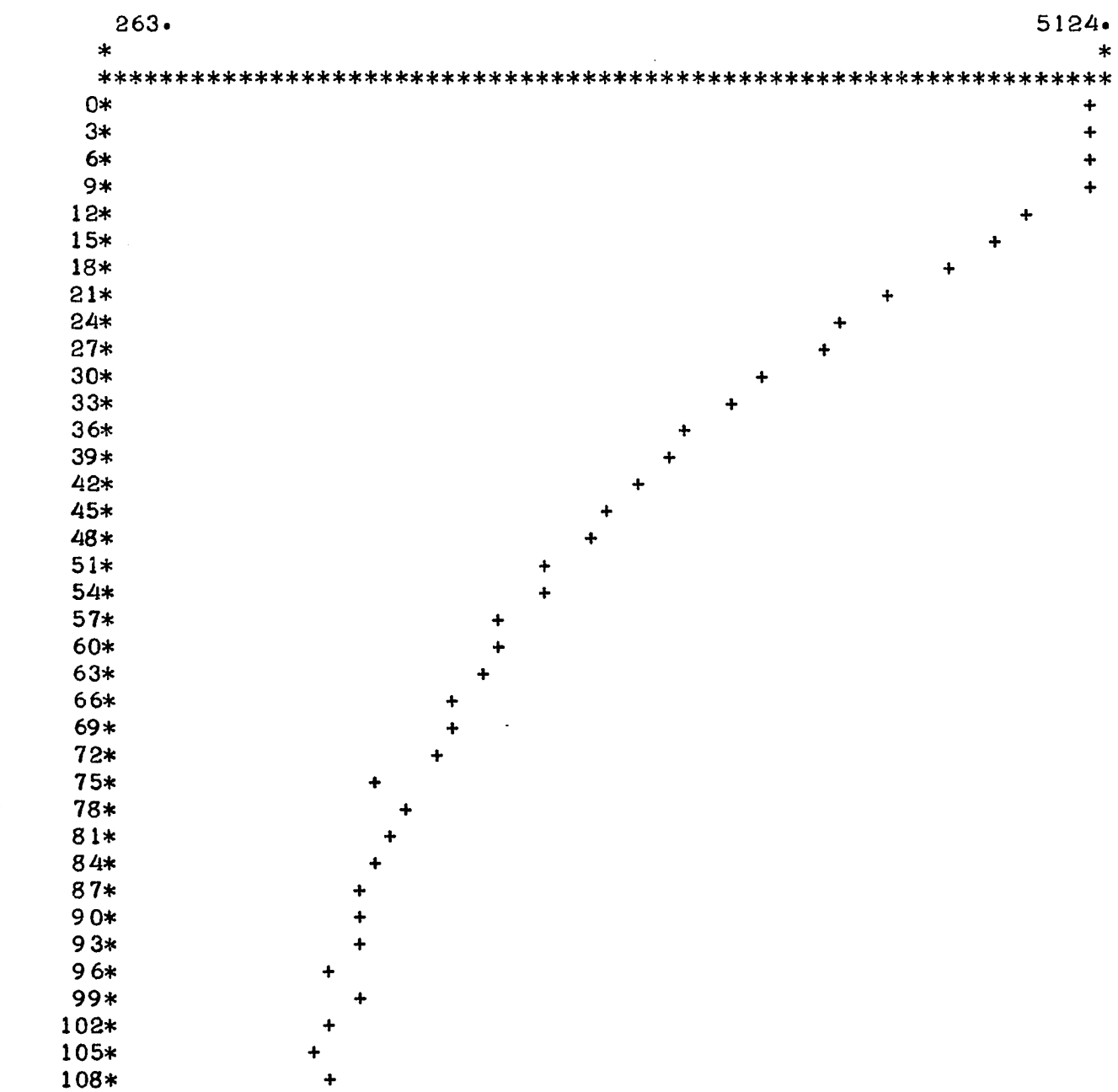

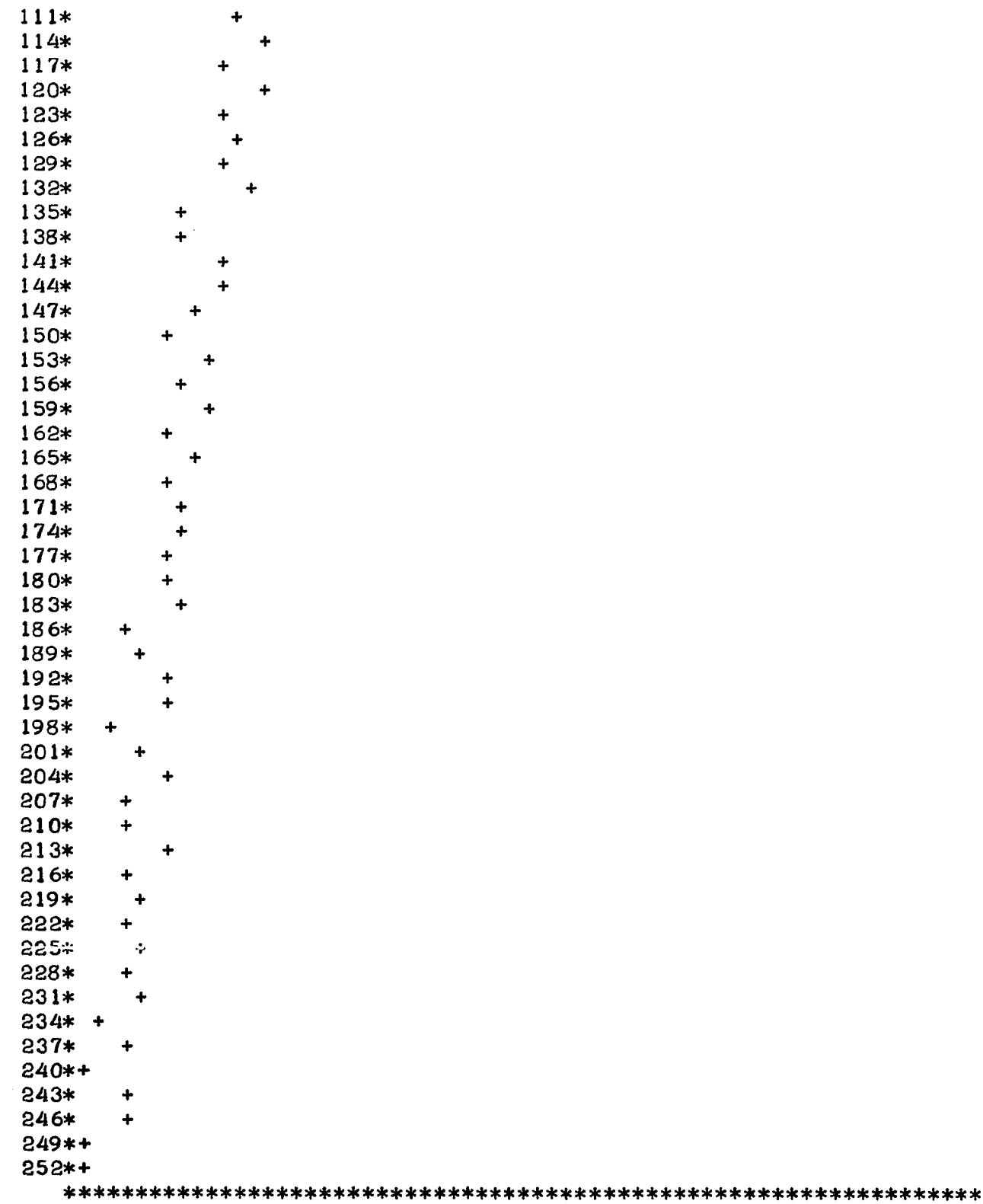
111*
114*
117*
120*
123*
126*
129*
132*
135*
138*
141*
144*
147*
150*
153*
156*
159*
162*
165*
168*
171*
174*
177*
180*
183*
186*
189*
192*
195*
198*
201*
204*
207*
210*
213*
216*
219*
222*
225*
228*
231*
234*
237*
240*
243*
246*
249*
252*

RAN: 07.7 SECS

```
RICH          21:45    ACC WED.  MAR 11,1970



R T THOMPSON    DATE-SEP  1,68    RUN # 3
 SAMPLE-HELIUM    WAVELENGTH=3867. A    PRESSURE=   6.5 MICRONS

 CALCULATED AT 21:45  WED.  MAR 11,1970

PRINT REGRES. RESULTS? ,TABULATE Y? (0-NO  1-YES)
?

ENTER NO. OF PARAMETERS,FIRST POINT,LAST POINT,
 REP RATE,BREAK POINT,CONST(IF KNOWN)
? 5,9,249,1100

TIME AXIS INTERCEPT =    25.39875 NS.,  STD DEV =     0.06672 NS
 COUNT RATE=  6.2%
 ITERATIONS NOT DISPLAYED
 EXP FIT FROM  71 TO 241LINEARITY(R2) IS 9.05383143E-01
 EXP FIT FROM   1 TO  67LINEARITY(R2) IS 9.85460981E-01
          THE UNWEIGHTED SIGMA IS   5.5275E+01
          THE WEIGHTED SIGMA IS   9.5978E+01
LIFETIMES (NS)       60.53005   521.59458
COEFFICIENTS       4231.36769   624.43014   162.02452
CALIBRATION IS  3.44703 NS/CHAN  WITH STD DEV OF0.001786  NS/CHAN
PLOT?(0-NO,PLOT INCR-YES)
? 5
```

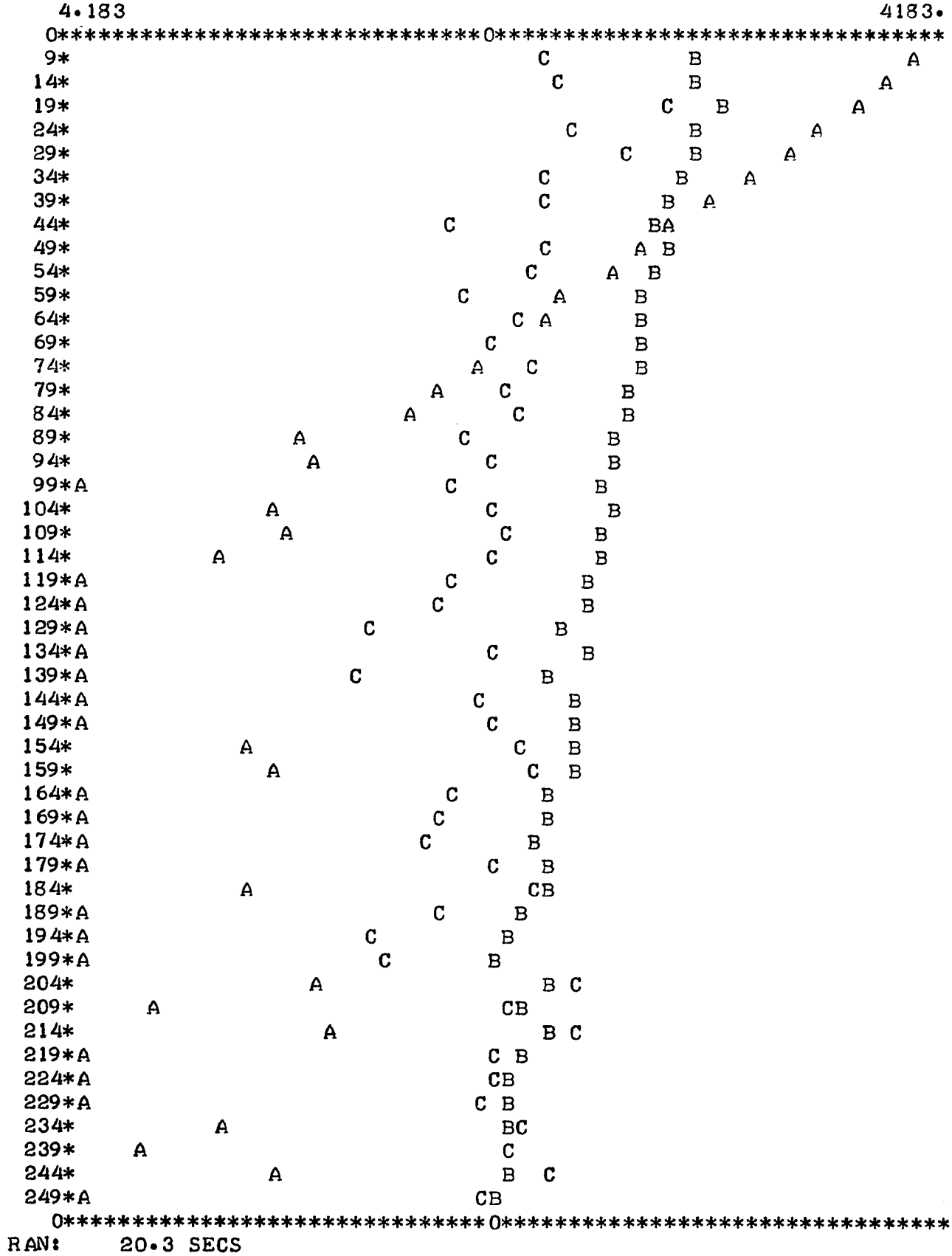
4.183
4183.
RAN: 20.3 SECS

```
LASL          21:58    ACC WED.  MAR 11,1970

R T THOMPSON    DATE-SEP  1,68    RUN # 3
 SAMPLE-HELIUM    WAVELENGTH=3867. A    PRESSURE=   6.5 MICRONS

 CALCULATED AT 21:58  WED.  MAR 11,1970

ENTER NO. OF PARAMS,FIRST PT.,  LAST PT.,  WEIGHT POWER
,IPR=0,1,2,OR 3 FOR INCR. OUTPUT,IM=2 HOLD CONST.
? 5,9,249,-1,0

ENTER TAU(SHORT,LONG),COEFF(SHORT,LONG),CONSTANT
? 60,522,4231,624,162

CALIBRATION IS   3.447025090E+00 NS/CHAN
WEIGHT RANGES FROM 1.0 TO  16.837 FOR CHAN 249
     6 ITERATIONS, DET. OF PART. DERIV. MATRIX =    6.71629E-05


         SUM OF EXPONENTIALS: Y(I)=P(1)*EXP(-X(I)/P(2))+...+P(5).


 THE WEIGHTED VARIANCE IS    5.160564E+03
 THE UNWEIGHTED SIGMA IS    3.214420E+01
AND THE UNWEIGHTED SUM OF SQUARES OF THE DEVS IS    2.438469E+05
     GUESS OF  FINAL VAL OF    S.D. OF          EXACT LST SQRS EQNS
 K  K-TH PARAM  K-TH PARAM  K-TH PARAM      FITTED FCTN  INPUT DATA
  1   4.231E+03   4.188E+03   4.519E+01       1.871E+00   1.871E+00
  2   6.000E+01   6.198E+01   1.117E+00       1.687E+03   1.687E+03
  3   6.240E+02   5.562E+02   2.882E+01       1.559E+05   1.559E+05
  4   5.220E+02   4.099E+02   6.460E+01       4.268E+05   4.268E+05
  5   1.625E+02   2.249E+02   2.334E+01       1.172E+06   1.172E+06
ENTER PLOT INCR IF PLOT IS DESIRED.
? 5
```

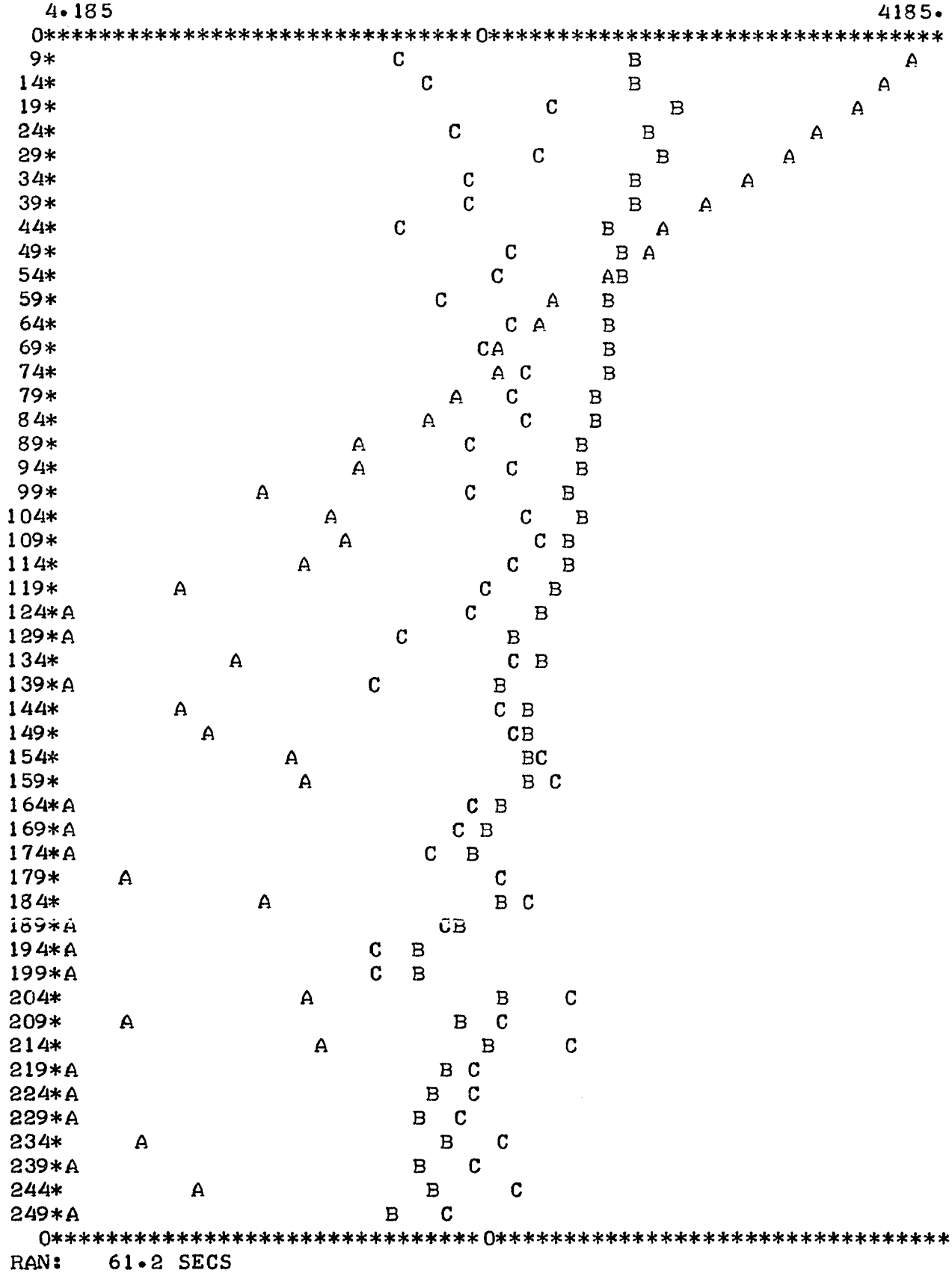
4.185
4185.
0
9*
14*
19*
24*
29*
34*
39*
44*
49*
54*
59*
64*
69*
74*
79*
84*
89*
94*
99*
104*
109*
114*
119*
124*A
129*A
134*
139*A
144*
149*
154*
159*
164*A
169*A
174*A
179*
184*
189*A
194*A
199*A
204*
209*
214*
219*A
224*A
229*A
234*
239*A
244*
249*A

RAN: 61.2 SECS

```
JERK1        22:24   ACC WED.  MAR 11,1970


READ ID TAPE
? R T THOMPSONMAR 11,70 3HE SIM3867.000.0

ENTER NUMBER OF CHANNELS(N), CALIBRATION (NS/CHAN), MULTIPLIER FOR NOISE
?  241,3.447,4.03

NUMBER OF EXPTL. PARAMS.,1 ST COEF. ,1 ST LIFETIME,
2 ND COEF., ... , CONSTANT
? 5,4188,61.98,556.2,409.9,224.9

SUM OF NOISE FOR DATA IS     2.436121065E+05
SIGMA FOR DATA IS      3.212872062E+01

RAN:   04.0 SECS

DATA FILE "INPUT" GENERATED BY JERK1


R T THOMPSONMAR 11,70 3HE SIM3867.  0.0
2411  1
  -3.45
  2000   4979   4769   4621   4375   4129   3973   3643   3533   3351
  3288   3183   2974   2966   2687   2708   2501   2466   2429   2306
  2087   2041   2034   1894   1877   1821   1706   1739   1540   1597
  1541   1434   1385   1375   1268   1269   1183   1214   1166   1156
  1099   1131   1030   1070    934    926    974    987    916    898
   849    870    885    837    803    732    767    767    728    769
   765    761    718    668    702    675    699    622    632    621
   640    618    585    649    606    543    616    613    601    527
   553    582    599    516    505    498    539    547    490    524
   485    479    500    485    462    536    451    528    476    447
   457    502    490    449    466    494    497    426    485    420
   451    426    420    425    415    479    424    447    479    460
   468    424    412    401    425    415    463    420    385    390
   393    447    406    404    422    384    397    402    384    390
   425    406    374    432    416    429    412    424    407    347
   372    422    412    372    373    340    362    398    406    359
   393    394    394    385    397    393    330    378    370    353
   322    354    357    323    382    358    363    379    345    373
   314    380    329    320    350    309    314    330    374    349
   316    341    336    301    354    319    368    306    302    321
   311    307    360    352    328    332    344    310    350    317
   335    305    321    315    284    290    319    283    312    303
   344    315    334    278    333    321    310    282    285    332
   308    301    334    310    285    274    298    323    326    323
   278    318
```

APPENDIX C

EXPERIMENTAL OBSERVATIONS FOR HELIUM LIFETIME MEASUREMENTS[a]

Upper State	1st Pulse Energy (ev)	2nd Pulse Energy (ev)	2nd Pulse Duration (ns)	Pulse Fall Time (ns)	Data Acquisition Rate (% of pulse rate)	Pressure (μ-Hg)	1st Lifetime (ns)	2nd Lifetime (ns)	1st Exponential Amplitude	2nd Exponential Amplitude	Constant	Identification
3^1S		90	500		2.9	19	57.1±0.7		12320±37		1485±38	11/30/69/2
		90	500		2.5	27	64.0 2.2		2253 25		4219 27	11/30/69/3
		97±2	500		2.3	90	60.4 0.6		8746 27		1480 23	11/28/69/4
		75 5	500			98	60.0 3.0		4749 47		1325 44	11/28/69/5
		70	500			100	61.4 0.5		12880 31		97 31	11/30/69/1
		92 4	500		2.7	200	69.3 0.6		10000 26		327 26	11/28/69/3
5^1S					3.7	25	133.8±0.9		2154±13		58±2	9/1/68/6
					10.4	55	105.0 0.6		3472 22		75 2	8/27/68/6
					10.9	60	112.4 0.9		2938 11		57 5	9/2/68/3
					11.9	120	85.6 0.6		4044 17		64 4	9/2/68/2
					8.3	325	39.6 0.8	140±6	3482 5	556±45	10 0.9	9/2/68/1
6^1S						25	184.0±1.2		3700±16		197±4	9/1/68/5
					9.1	44	88.0 19	181±19	1099 530	1957±536	105 7	8/29/68/13
					4 4	55	64.0 3.0	209 45	1697 78	257 81	122 5	8/27/68/7
					9.8	80	39.9 0.7	177 7	5269 52	888 47	82 3	8/26/68/5
					9.2	120	129.0 2.3	489 160	3465 49	112 56	107 400	8/29/68/9
					9.3	200	93.0 3.0	388 224	3297 86	193 77	74 21	8/29/68/5
					9.4	300	20.2 1.6	209 4	676 29	1017 14	40 3	8/29/68/1
					8.8	350	44.0 1.0	193 12	3407 42	518 40	70 3	8/29/68/4
7^1S			500	25	1.8	140	44.2±4.0	192±24	2050±174	1925±136	477±53	6/23/70/2
8^1S		145	500	50	5.7	76	59.4±0.7	431±27	5887±41	982±47	5	7/27/70/1
		140-120	500	25		110	55.0 1.0	551 201	3621 45	761 130	0±150	9/17/70/2
		81±4	500	25		140	26.2 0.8	119 4	7217 150	5005 148	281 17	8/24/70/1
		81±4	500	25		140	16.4 2.0	98 8	3352 208	5605 112	45 132	8/24/70/2
9^1S		275-80	500	15		145	46.8±0.4		7584±27		462±13	8/24/70/4

[a]Stastical uncertainties are given for the fitted exponential parameters. Where none are given the parameter was held constant.

APPENDIX C (continued)

Upper State	1st Pulse Energy (ev)	2nd Pulse Energy (ev)	2nd Pulse Duration (ns)	Pulse Fall Time (ns)	Data Acquisition Rate (% of pulse rate)	Pressure (μ-Hg)	1st Lifetime (ns)	2nd Lifetime (ns)	1st Exponential Amplitude	2nd Exponential Amplitude	Constant	Identification
6^1P					5.8	40	33.8±0.6	293±25	3978±43	408±18	183±8	8/29/68/12
					9.3	120	23.4 0.4	200 7	3754 45	574 18	78 3	8/29/68/10
		90/80	500	25		135	20.2 0.2	153 5	17890 80	5905 74	0	8/25/70/4
					8.9	200	18.0 0.3	214 4	4671 54	1241 17	197 4	8/29/68/6
					8.8	300	17.7 0.5	196 4	2743 65	811 14	43 2	8/29/68/2
7^1P		90/80	500	25		125	16.8±0.3	146±3	6044±55	3259±44	0	8/25/70/3
					4.6	150	24.1 1.0	280 24	677 19	162 7	63±3	8/27/68/8
					9.2	150	49.2 1.4	355 40	2284 36	433 22	128 11	8/27/68/10
8^1P		140	500	25	7.3	78	30.5±2.0	4731(>10^5)	16820±655	3700(>10^5)	572(>10^5)	7/27/70/2
		95/82	500	30		120	17.4 0.5	152±4	4989 62	3020±54	0	8/25/70/2
		110/80	500	30		145	41.9 1.0	67	2241 16		626±15	8/24/70/6
		96/80	500	25		145	8.5 0.8	67 3	5402 263	12150 176	10	8/19/70/4[b]
		225/80	500	15		150	45.8 0.7		2656 15		333 12	8/24/70/5
		62	500	30		500	15.1 0.8	120 11	3326 102	3331 42	447 110	8/25/70/1
9^1P		96/80	500	25		140	36.0±2.0	259±7	1826±30	1362±31	10	8/19/70/3
10^1P		96/80	500	25		130	37.7±2.0	255±10	1657±35	1158±38	10	8/19/70/2
3^1P		100	500		2.6	23	13.3±0.2		12630±78		1006±20	11/30/69/5
4^1P		124/95	500	20		100	29.7±0.6	83±5	7792±196	1734±211	0	8/26/70/2
5^1P		124/95	500	20		100	27.9±0.3	114±4	13850±120	3385±136	0	8/26/70/1
		90/80	500	25		140	23.1 0.4	108 4	3850 44	1169 50	0	8/25/70/5
3^1D		125	30	15	0.7	25	20.0±1.0		582±20		727±2	1/28/72/2
	140	150	30	15	2.0	26	21.4 0.5	281±24	5443 64	2148±39	906 24	1/28/72/1
	90	85	90	10	8.0	26	19.2 0.3	385 35	8672 46	1864 47	100	10/20/71/4
	380	60	120	30	4.0	30	22.8 0.5	256 17	5054 50	1944 22	423 46	1/7/72/3
	380	60	120	30	5.6	31	25.6 0.6	191 9	6444 83	2282 51	0 55	1/7/72/4[c]
	135	85	110	15	6.7	41	31.3 0.5	235 17	8213 68	2078 34	74 45	1/7/72/1
	140	270	40	15	7.6	56	27.8 0.4	124 7	15309 146	2859 147	687 22	1/26/72/1

[b] Third exponential observed having 356±33 ns lifetime and 2711±270 amplitude.

[c] Third exponential observed having 1644±372 ns lifetime and 648±67 amplitude.

APPENDIX C (continued)

Upper State	1st Pulse Energy (ev)	2nd Pulse Energy (ev)	2nd Pulse Duration (ns)	Pulse Fall Time (ns)	Data Acquisition Rate (% of pulse rate)	Pressure (μ-Hg)	1st Lifetime (ns)	2nd Lifetime (ns)	1st Exponential Amplitude	2nd Exponential Amplitude	Constant	Identification
3^1D	125	60	110	15	5.6	58	25.6±0.8	107±4	4993±100	2497±103	298±8	1/7/72/2
(cont.)	80	50	90	10	8.0	58	18.0 0.3	141 4	10750 66	3671 74	100	10/20/70/3
	170	50	20	15	8.6	60	27.7 0.5	418 57	5707 48	2072 110	269 150	1/25/72/1
	150	100	40	15	2.1	61	19.7 0.7	158 12	2848 53	1299 35	1295 24	1/26/72/2
	95	300	110	5	4.4	70	49.8 2.0	183 38	7556 206	1050 190	100 36	1/8/72/1
		320	100	10	6.0	77	44.9 4.0	92 14	5736 107	2773 1075	137 17	12/16/71/3
	125	52	120	20	4.6	80	26.2 0.5	153 6	5648 57	1794 47	191 13	1/7/72/6[d]
	125	52	120	20	6.9	82	28.7 0.4	192 8	13373 109	4358 74	149 42	1/7/72/5
	60	40	90	10	8.0	90	17.4 0.7	99 3	6361 69	2932 77	100	10/20/72/2
		250	110	25	1.1	110	33.3 3.0	89 10	2258 206	1113 214	80 7	12/15/71/3
		220	120	25	4.9	110	31.0 2.0	76 5	6135	4185 508	331 10	12/15/71/2
		280	100	10	5.3	195	20.9 0.6	89 4	5224 100	2317 102	461 9	12/16/71/2
		160	100	10	2.9	195	56.4 0.6	372 215	8999 78	458 60	0	12/16/71/1
5^1D					11.3	55	51.2±1.0	272±32	5163±55	499±47	189±9	8/27/68/5
					10.7	120	47.4±3.0	158 39	4783 358	1378 332	128 49	9/2/68/6
6^1D					8.1	15	71.4±4.0	1882±652	450±11	315±76	0±80	8/27/68/11
					9.0	40	53.2 2.0	323 30	3828 51	623 35	93 12	8/29/68/11
					8.3	110	45.9 2.0	297 19	2256 39	790 30	162 10	8/29/68/8
					29.5	200	28.7 1.0	240 6	2531 45	1730 27	235 7	8/29/68/7
					8.9	325	23.7 1.0	196 3	1750 42	1910 24	103 3	8/29/68/3
7^1D					20.0	80	41.0±2.0	501±72	3404±69	1662±53	352±101	8/26/68/3
					8.7	80	41.0 2.0	625 100	1119 24	524 23	120 37	8/26/68/4
					14.4	150	50.0 2.0	376 40	2819 35	532 20	55 15	8/27/68/9
						450	19.0 3.0	200 4	487 32	1173 16	111 3	8/26/68/1
8^1D		100-90	500	20	7.1	100	27.0±1.0	286±2	8514±67	5667±36	0	8/26/70/5
		103±3	500	30	4.1	110	33.0 0.6	577 13	3220 29	2100 20	0	9/17/70/1
9^1D		100-84	500	20	7.1	110	55.5±0.7	298±6	11140±78	4021±90	0	8/26/70/4
10^1D		100-84	500	20	3.5	110	69.5±1.0	405±16	14940±141	4649±162	0	8/16/70/3

[d] This measurement was made with ∿15 gauss axial magnetic field applied.

APPENDIX C (continued)

Upper State	1st Pulse Energy (ev)	2nd Pulse Energy (ev)	2nd Pulse Duration (ns)	Pulse Fall Time (ns)	Data Acquisition Rate (% of pulse rate)	Pressure (μ-Hg)	1st Lifetime (ns)	2nd Lifetime (ns)	1st Exponential Amplitude	2nd Exponential Amplitude	Constant	Identification
3^3S		84/76	500		1.3	33	55.8±0.7		5659±27		1179±21	11/20/69/5
						38	60.7 2.0		2796 19		1719 18	11/28/69/2
						45	49.4 0.5		4512 16		958 11	11/20/69/4
						80	51.4 0.4		7926 25		604 17	11/20/69/3
			500		6.4	100	42.1 0.5	202±22	41200 340	5547±297	552 140	6/18/70/2
		150-100	500		10.1	110	43.2 1.0		18030 41		855 10	6/22/70/2
	100	100	90			125	52.0 1.0		9779 42		215 4	10/20/70/1
			500		12.6	130	29.3 3.0	145 273	3898 547	730 103	0 520	6/23/70/1
		95-70	500		4.0	180	52.9 0.6		10670 38		2014 36	11/28/69/1
						200	42.6 0.4		3650 15		306 8	11/20/69/1
		150-50	500		7.6	200	47.0 0.4		13870 34		561 43	6/22/70/1
						240	41.4 0.3		7792 28		831 11	11/20/69/2
5^3S					9.7	35	108.5±1.0		4134±23		185±2	8/28/68/7
		90-70	500	20		170	59.0 1.0		13220 36		1207 36	9/2/70/3
6^3S					0.7	65	62.2±2 0	412±72	4189±48	556±29	224±27	9/1/68/3
					7.1	10	72.0 2.0	289 72	2788 64	273 64	122 10	8/28/ 8/3[a]
					7.4	10	72.0 2.0	359 85	4512 63	378 57	180 18	8/28/68/3[b]
					9.8	35	77.0 6.0	208 31	1726 173	660 179	105 6	8/28/68/6
					8.9	55			2677 16		116 2	8/28/68/6
7^3S					13.4	10	129.0±13	494±324	1308±190	396±40	28±60	8/28/68/2
					5.7	13	63.0 4.0	602 154	933 35	537 25	272 57	8/28/68/4
					6.4	35	112.0 13	563 261	2173 342	1903 225	0 356	9/1/68/2
					9.7	110	84.0 4.0	356 44	2446 131	1409 109	68 35	9/1/68/1
8^3S		140-120	500	25		115	33.0±1.0	577±13	3220±29	2100±20	0	9/17/70/3
		90-70	500	20		145	84.5 3.0	463 38	8980 307	4964 332	100	9/10/70/1
		90-70	500	20		155	87.0 2.0		7703 30		587±39	9/2/70/1
						170	50.0 2.0	203 5	6956 156	6001 174	10	9/2/70/2
9^3S		115-80	500	20		105	26.0±2.0	171±26	950±55	841±29	127±39	8/26/70/6
		80-70	500	20		170	36.0 2.0	238 5	2234 46	2591 49	10	9/2/70/4

APPENDIX C (continued)

Upper State	1st Pulse Energy (ev)	2nd Pulse Energy (ev)	2nd Pulse Duration (ns)	Pulse Fall Time (ns)	Data Acquisition Rate (% of pulse rate)	Pressure (μ-Hg)	1st Lifetime (ns)	2nd Lifetime (ns)	1st Exponential Amplitude	2nd Exponential Amplitude	Constant	Identification
2^3P	40	30	500	<20	16.5	25	124±9		727±40		1067±8	6/20/69/3
	46	30	500		5.6	33	134 2		5183 22		2214 14	2/27/69/3[b]
	46	30	500		11.1	33	136 0.3		2716 19		1114 11	2/27/69/3
	40	22	500		10.0	43	124 1		4004 20		520 6	12/28/67/2
		95	500			60	126 2		3511 21		2763 13	9/13/69/6
		110	500		9.4	60	114 2		3579 22		2091 12	9/13/69/5
	50	22	500		7.9	74	118 3		992 11		373 5	2/25/69/3
	38	26	500		10.2	74	143 2		3199 17		771 9	2/25/69/4
		100	500		5.4	92	126 1		3739 3		3362 1	1/6/69/1
	53	30	500		17.0	100	133 3		1633 13		422 7	2/25/69/1
	51	30	500		10.8	100	135 3		1739 18		393 6	2/25/69/2
		90	500		13.6	115	130 2		4579 23		1065 10	9/13/69/1
		135	500		10.6	115	132 2		8483 51		706 13	9/11/69/4
		120	500		9.7	115	133 1		6650 28		740 10	9/13/69/4
		150	500		9.8	115	136 2		3711 24		263 8	9/13/69/3
		90	500		9.0	115	138 2		7354 38		2209 17	9/11/69/2
	41	28	500		16.5	150	120 2		5861 30		1873 14	6/20/69/2
	44	26	500		17.5	150	132 4		4929 63		1798 33	6/20/69/1
	36	24	500		13.8	330	122 1		5274 17		1543 12	2/27/69/16
	36	24	500		13.5	330	123 2		4652 20		1081 9	2/27/69/1
	33	26	500	↓	14.8	625	123 2		6429 42		951 12	6/20/69/4
4^3P		150	500	30	5.5	74	105.1±0.5		9046±26		204±8	7/30/70/8
		90-74	500	20	6.6	200	76.7 3.0	167±10	10200 676	4156±700	0	8/12/70/2
5^3P		120	500	30	3.6	67	148±2		6473±18		547±15	7/11/70/2
		150	500	30	4.2	74	116 1		7751 21		367 11	7/30/70/7
		100-80	500	20	6.5	135	73 4	164±6	6709 568	6297±588	0	8/18/70/5
		90-74	500	20	6.6	200	72 4	158 5	7046 685	8953 708	0	8/12/70/3
							111 1		15230 33		423 13	
6^3P		115	500	30	2.3	70	75±4	577±67	2318±82	1323±92	0	7/11/70/3
		150	500	30	6.4	75	78 18	254 134	3506 1713	3919 1254	73±490	7/30/70/6
		100-80	500	20	7.3	135	76 3	193 5	12520 525	9394 265	100	8/18/70/4
		90-74	500	20	6.6	210	67 10	159 16	5809 2031	12040 1942	227 121	8/12/70/4

APPENDIX C (continued)

Upper State	1st Pulse Energy (ev)	2nd Pulse Energy (ev)	2nd Pulse Duration (ns)	Pulse Fall Time (ns)	Data Acquisition Rate (% of pulse rate)	Pressure (μ-Hg)	1st Lifetime (ns)	2nd Lifetime (ns)	1st Exponential Amplitude	2nd Exponential Amplitude	Constant	Identification
7^3P		150	500	30	5.9	73	86±5	414±38	3769±219	2715±234	0	7/30/70/5
		70	500	30	3.6	100	41 1	528 26	3098 28	780 21	5	7/11/70/4
		100-80	500	20	6.5	135	79 3	278 17	5713 243	3007 260	0	8/18/70/3
		90-74	500	20	6.6	210	86 4	237 11	6848 396	4803 415	0	8/12/70/5
			500		4.0	250	84 2	733 80	3540 56	1069 64	0	6/18/70/1
8^3P		150	500	30	3.4	78	42±2	291±11	1507±46	1654±51	0	7/30/70/4
		100-80	500	20	2.3	135	43 2	241 4	4043 74	4822 84	0	8/18/70/2
		90-74	500	20	6.6	210	54 2	229 5	4774 105	4332 118	0	8/12/70/6
9^3P		100-80	500	20	1.2	135	56±3	309±18	2339±85	1731±95	0	8/18/70/1
		90-74	500	20	6.6	210	44 2	248 8	3788 60	1957 67	0	8/12/70/7
3^3D	70	125	90	10	4.9	15	18±1	312±5	4442±51	2257±20	500	10/21/70/5
	70	120	90	10	5.8	29	16 1	246 2	4971 58	3590 23	500	10/21/70/4
	70	120	90	10	5.8	40	15 1	249 2	4062 78	4582 27	500	10/21/70/3
	70	60	90	10	7.8	61	14 1	203 2	10460 168	5911 30	500	10/21/70/2
	60	48	90	10	11.0	90	13 1	168 1	8495 172	4601 27	500	/21/70/1
	40	70	90	10	10.5	180	5 2	168 1	649 110	5384 25	100	10/20/70/5
4^3D	125	80		15	9.2	65	40±2	301±6	4000±71	5250±52	803±18	1/25/72/2
	170	50		15	2.0	86	24 1	200 13	1902 47	1566 25	220 29	1/25/72/3
				30	7.8	92	24 1	200 3	4190 80	4600 48	1098 8	1/30/72/1
5^3D		132-100	500	25	8.1	140	132±1		13650±24		544±20	6/23/70/3
6^3D		132-100	500	25	7.0	140	156±1		12550±26		723±26	6/23/70/4
7^3D	150	145	90	15	11.0	37	310±5		5423±24		1458±29	10/16/70/6
	150	80	90	15		45	297 6		2368 13		494 16	10/16/70/5
		150	500	25	7.7	80	168 2		7559 21		814 25	7/27/70/3
		150	500	25	7.5	82	154 4	772±314	14300 427	2510±212	0 370	7/27/70/4
		132-100	500	25	6.2	140	158 1		11050 22		822 22	6/23/70/5
		100-80	90	20	6.8	150	170 2		11080 25		478 28	8/11/70/3
	80	60	90	15	7.2	160	220 2		9277		459 13	10/16/70/1
		90-74	500	20	6.6	200	148 1		10960 20		441 17	8/12/70/1
	90	60	500	15	7.1	230	232 2		10520 21		936 15	10/16/70/3

APPENDIX C (continued)

Upper State	1st Pulse Energy (ev)	2nd Pulse Energy (ev)	2nd Pulse Duration (ns)	Pulse Fall Time (ns)	Data Acquisition Rate (% of pulse rate)	Pressure (μ-Hg)	1st Lifetime (ns)	2nd Lifetime (ns)	1st Exponential Amplitude	2nd Exponential Amplitude	Constant	Identification
7^3D	48	29	500	25	8.5	270	325±4		6022±21		548±26	10/16/70/2
(cont.)	50	30	500	50	11.5	300	246 2		4933 15		286 12	10/16/70/1
8^3D		190	500	30	5.3	30	57±7	624±29	745±49	2562±56	0	6/27/70/3
		125	500	50	6.3	33	52 2	798 34	2670 41	2704 43	50	6/27/70/4
		125	500	30	8.0	36	49 2	675 24	3162 46	3224 49	0	6/27/70/5
		150	500	30	5.6	76	241 6		4127 37		887±46	7/27/70/5
		150	500	30	6.6	76	172 10	542 23	3957 286	4413 301	500	7/27/70/6
		132-88	500	25	7.5	140	87 7	266 12	5345 572	7934 594	100	6/23/70/6
		100-80	500	20	6.8	150	184 2		10540 27		539 34	8/11/70/2
9^3D		200	500	30	5.8	24	125±16	1707±505	1419±177	2303±187	0	6/27/70/1
		200	500	30	7.3	28	56 3	951 70	2165 56	2881 64	0	6/27/70/2
			90	15	5.0	40	60 4	1492 697	2124 71	3677 1185	0±1261	10/16/70/7
		150	500	30	2.5	70	333 6		2313 11		489 12	7/30/70/2
		150	500	30	8.2	77	73 11	287 11	1762 275	7941 254	1320 44	7/27/70/7
		115	500	30	7.3	80	520 9		4659 31		714 38	7/30/70/1
	85	85	90	15	6.7	85	368 9		5385 42		1469 53	10/16/70/10
		104-84	500	20	6.6	125	182 2		10500 32		602 40	8/19/70/1
		112-80	500	25	7.7	140	53 6	275 44	3674 551	8350 156	500 471	6/23/70/7
		100-80	500	20	7.1	150	189 2		9227 29		420 37	8/11/70/1
		100-80	500	20	6.5	150	79 3	261 11	8189 390	6380 415	0	8/18/70/7
	65	55	90	15	6.8	160	302 4		7078 24		1621 28	10/16/70/9
		100-80	500	20	6.9	190	159 1		21060 33		1127 35	8/10/70/3
		96	500		4.4	194	24 2	75 4	7962 481	6698 509	1286	11/30/69/4
	60	55	90	15	6.8	220	283 3		8778 21		1017 22	10/16/70/8
10^3D		150	500	30	7.5	74	56±11	287±8	1014±132	7114±124	1376±32	7/30/70/3
		100-80	500	20	4.8	135	64 3	251 6	6839 188	6573 222	0	8/18/70/6
		100-80	500	20	6.4	190	169 1		20770 36		957 43	8/10/70/2
11^3D	80	85	90	15	2.2	190	63±2	494±18	1805±29	929±29	100	10/17/70/2
	60	55	90	20	1.9	300	109 3	722 102	2899 50	903 56	0±54	10/17/70/1